Cross-Channel Similarity Analysis and Application Using a Multidimensional Structural Measure

Journal:	*Transactions on Antennas and Propagation*
Manuscript ID	AP2408-2128
Manuscript Type:	Paper
Date Submitted by the Author:	04-Aug-2024
Complete List of Authors:	Yi, Cheng; Southeast University; Purple Mountain Laboratories Zhang, Peize; Southeast University; Oulun yliopisto Wang, Haiming; Southeast University; Purple Mountain Laboratories Wang, Cheng-Xiang; Southeast University; Purple Mountain Laboratories You, Xiaohu; Southeast University; Purple Mountain Laboratories
Keywords:	Communication channels, Fading channels, Microwave radio propagation, Millimeter wave propagation, Multipath channels, Propagation measurements, Radio propagation

AUTHOR RESPONSES TO SUBMISSION QUESTIONS

What is the problem being addressed by the manuscript and why is it important to the Antennas & Propagation community? (limited to 100 words)	To explore and exploit the channel correlation across multiple frequency bands and scenarios, knowledge of frequency- and environment-dependent propagation characteristics is of great importance for reducing the system complexity. However, there is a dearth of research focusing on experimental characterization of the multidimensional channel similarities simultaneously. This work will favor the community by providing channel similarity analysis across the centimeter-wave and millimeter-wave bands in two typical environments using a multidimensional structural channel similarity index measure, as well as an investigation of the feasibility of out-of-band information-assisted beam search.
What is the novelty of your work over the existing work? (limited to 100 words)	1) To evaluate the similarities of different channels in the form of numerical values, an objective CSIM is proposed, which accounts for the multidimensional structural information of the effective rays, including the complex amplitude, delay, AoA, and AoD. 2) The CSIM can be used to measure channel similarity under different transceiver configurations, considering the effects of delay resolution and angular resolution. Its statistical characteristics can reflect channel similarity across different bands or environments. 3) Channel similarity is related to beam direction differences to investigate the feasibility of out-of-band information-assisted beam search strategies.
Provide up to three references, published or under review, (journal papers, conference papers, technical reports, etc.) done by the authors/coauthors that are closest to the present work. Upload them as supporting documents if they are under review or not available in the public domain. Enter “N.A.” if it is not applicable.	[1] C. Yi et al., â€œMultipath similarity index measure across multiple frequency bands,â€ IEEE WCL, 2021. [2] J. Huang et al., â€œMulti-frequency multi-scenario millimeter wave MIMO channel measurements and modeling for B5G wireless communication systems,â€ IEEE JSAC, 2020. [3] P. Zhang, et al., â€œIndoor small-scale spatiotemporal propagation characteristics at multiple millimeter-wave bands,â€ IEEE AWPL, 2018.
Provide at least three references (journal papers, conference papers, technical reports, etc.) done by other authors that are most important to the present work. These references should also be discussed in the submitted manuscript	[1] D. Dupleich et al., â€œMulti-band propagation and radio channel characterization in street canyon scenarios for 5G and beyond,â€ IEEE Access, vol. 7, pp. 160385â€“160396, 2019. [2]Â N. G. Prelcic et al., â€œMillimeter-wave communication with out-of-band

and listed among its references. Please include the citation numbers used in the manuscript for easy reference.	information,â€ IEEE Commun. Mag., vol. 55, no. 12, pp. 140â€“146, 2017. [3] T. Jiang et al., â€œThe comparative study of S-V model between 3.5 and 28 GHz in indoor and outdoor scenarios,â€ IEEE TVT, vol. 69, no. 3, pp. 2351â€“2364, 2020.

Four Questions and Answers for the Manuscript "Cross-Channel Similarity Analysis and Application Using a Multidimensional Structural Measure"

Q1. What is the problem being addressed by the manuscript and why is it important to the Antennas & Propagation community? (limited to 100 words).

Re:

To explore and exploit the channel correlation across multiple frequency bands and scenarios, knowledge of frequency- and environment-dependent propagation characteristics is of great importance for reducing the system complexity. However, there is a dearth of research focusing on experimental characterization of the multidimensional channel similarities simultaneously. This work will favor the community by providing channel similarity analysis across the centimeter-wave and millimeter-wave bands in two typical environments using a multidimensional structural channel similarity index measure, as well as an investigation of the feasibility of out-of-band information-assisted beam search.

Q2. What is the novelty of your work over the existing work? (limited to 100 words).

Re:

1) To evaluate the similarities of different channels in the form of numerical values, an objective CSIM is proposed, which accounts for the multidimensional structural information of the effective rays, including the complex amplitude, delay, AoA, and AoD.

2) The CSIM can be used to measure channel similarity under different transceiver configurations, considering the effects of delay resolution and angular resolution. Its statistical characteristics can reflect channel similarity across different bands or environments.

3) Channel similarity is related to beam direction differences to investigate the feasibility of out-of-band information-assisted beam search strategies.

Q3. Provide up to three references, published or under review, (journal papers, conference papers, technical reports, etc.) done by the authors/coauthors that are closest to the present work. Upload them as supporting documents if they are under review or not available in the public domain. Enter "N.A." if it is not applicable.

Re:

[1] C. Yi *et al.*, "Multipath similarity index measure across multiple frequency bands," *IEEE WCL, vol*. 10, no. 8, pp. 1677–1681, 2021.

[2] J. Huang *et al.*, "Multi-frequency multi-scenario millimeter wave MIMO channel measurements and modeling for B5G wireless communication systems," *IEEE JSAC*, vol. 38, no. 9, pp. 2010–2025, 2020.

[3] P. Zhang, *et al.*, "Indoor small-scale spatiotemporal propagation characteristics at multiple millimeter-wave bands," *IEEE AWPL*, vol. 17, no. 12, pp. 2250–2254, 2018.

Q4. Provide up to three references (journal papers, conference papers, technical reports, etc.) done by other authors that are most important to the present work. Enter "N.A." if it is not applicable.

Re:

[1] N. G. Prelcic *et al.*, "Millimeter-wave communication with out-of-band information," *IEEE Commun. Mag.*, vol. 55, no. 12, pp. 140–146, 2017.

[2] T. Jiang *et al.*, "The comparative study of S-V model between 3.5 and 28 GHz in indoor and outdoor scenarios," *IEEE TVT*, vol. 69, no. 3, pp. 2351–2364, 2020.

[3] D. Dupleich *et al.*, "Multi-band propagation and radio channel characterization in street canyon scenarios for 5G and beyond," *IEEE Access*, vol. 7, pp. 160385–160396, 2019.

Cross-Channel Similarity Analysis and Application Using a Multidimensional Structural Measure

Cheng Yi, *Graduate Student Member, IEEE*, Peize Zhang, *Member, IEEE*, Haiming Wang, *Member, IEEE*, Cheng-Xiang Wang, *Fellow, IEEE*, and Xiaohu You, *Fellow, IEEE*

***Abstract*—To meet the required full coverage and ultrahigh data rate demands of next-generation mobile communications, the coexistence of multiple radio frequency systems operating in well-separated frequency bands in precisely identified scenarios must be exploited. In this context, an investigation of frequency-dependent and environment-dependent channel characteristics by exploring the spatial and temporal correlations of multi-path channels across different frequency bands and different environments is imperative. In this paper, a structural channel similarity index measure (CSIM) is proposed, which comprehensively considers several multipath parameters of two different channels, including amplitude, phase, delay, angle of arrival (AoA), and angle of departure (AoD). Based on extensive field measurement campaigns and ray tracing simulations conducted across both centimeter wave (cmWave) and millimeter wave (mmWave) bands in typical indoor and outdoor scenarios, the proposed CSIM is proven to effectively measure similarity from specific dimensions as well as the statistical distributions, and the similarities between channels across different frequencies and different environments are presented. Moreover, the feasibility of out-of-band information-assisted beam search based on cross-band channel similarity is also validated.**

***Index Terms*—Channel similarity index measure (CSIM), channel characteristics, channel simulations and measurements, multi-band and multi-environment, beam search**

I. Introduction

THE saturation of the spectrum in sub-6 GHz band has made it impossible to meet the exploding demands for communication capacity and high transmission rates [1], [2]. The development and utilization of higher frequency bands is considered an effective solution to this dilemma. The abundant unplanned spectrum resources in millimeter wave (mmWave) bands have attracted the enthusiastic attention of researchers worldwide [3]. On the one hand, by combining the capabilities of high-frequency and low-frequency systems, multiband communication systems show great promise for achieving both a breadth and depth of coverage compared with traditional single-frequency systems [4]. The wide range of frequencies spanned leads to different propagation mechanisms and gives rise to differences in channel characteristics. Radio waves in sub-6 GHz band can achieve wider coverage because of their high diffraction and penetration performance, whereas mmWave signals suffer from more serious path loss and blockage and can only be used for short-range coverage. Large-scale antenna arrays have thus been introduced to focus the energy in the desired directions, although they greatly increase the system's hardware complexity as well as the computational overhead of signal processing. To reduce the training overhead of angle of arrival (AoA) estimation, several algorithms have been proposed that explore sub-6 GHz channel state information (CSI) to assist mmWave spatial correlation matrix estimation [5]–[8]. On the other hand, wireless communication system design and coverage performance are strongly related to deployment environments. The mmWave channel characteristics are sensitive to the propagation environment, which requires accurate scenario recognition to meet the dedicated communication demands in specific propagation environments. Therefore, we must fully clarify how the propagation characteristics change with the carrier frequency in the different propagation environments.

The radio propagation characteristics in the sub-6 GHz band have been extensively studied, and the corresponding systems have been widely used in the current commercial communication systems. At present, many studies have focused on the channel characteristics of the popular mmWave frequency bands, and many accurate or universal channel models have been proposed on the basis of both measured and simulated data [9]. Based on extensive measured channel data from typical indoor and outdoor scenarios in the 28 GHz and 39 GHz bands, the frequency dependence of the path loss and the root mean square (RMS) angular spread were discussed in [10] and [11]. In [3], a measurement-based mmWave propagation channel model from 28 GHz to 73 GHz was presented. The propagation characteristics were modeled in multiple dimensions, which included directional and omnidirectional channel models, temporal and spatial channel models, and outage probabilities. In addition, side-by-side comparisons of propagation characteristics over a

Manuscript received ; revised ; accepted . Date of publication ; date of current . This work was supported in part by the National Natural Science Foundation of China under Grants 62271133 and 61960206006 and the Fundamental Research Funds for the Central Universities of China under Grant 2242022k60006. *(Corresponding author: Haiming Wang.)*

Cheng Yi and Haiming Wang are with the State Key Laboratory of Millimeter Waves, Southeast University, Nanjing 211189, China, and with the Pervasive Communication Research Center, Purple Mountain Laboratories, Nanjing 211111, China (e-mail: chengyi@seu.edu.cn, hmwang@seu.edu.cn).

Peize Zhang was with the State Key Laboratory of Millimeter Waves, Southeast University, Nanjing 211189, China, and is now with the Centre for Wireless Communications, University of Oulu, 90570 Oulu, Finland (e-mail: peize.zhang@oulu.fi).

Cheng-Xiang Wang and Xiaohu You are with the National Mobile Communications Research Laboratory, Southeast University, Nanjing 211189, China, and with the Pervasive Communication Research Center, Purple Mountain Laboratories, Nanjing 211111, China (e-mail: chxwang@seu.edu.cn, xhyu@seu.edu.cn).

Color versions of one or more of the figures in this paper are available online at http://ieeexplore.ieee.org.

Digital Object Identifier

wide range of mmWave bands were provided. Many works have focused on channel simulations and measurements across multiple frequency bands and environments. However, they have derived channel correlations based on visual observations or statistical comparisons of the channel parameters [12], [13]. For example, channel measurements were conducted in the 3.5 GHz and 28 GHz bands in indoor and outdoor scenarios to study the channel property differences between the microwave band and the mmWave band [14]. The Saleh–Valenzuela (S-V) model was chosen to analyze the statistical parameters of the clusters, such as the number of clusters, the intercluster interval, and the ray decay factor. The effects of the frequency and bandwidth on the decay factor are discussed in detail. In [15], the authors carried out channel measurements in an indoor cubicle office and a conference room, using seven frequency bands ranging from 2.4–61 GHz. Based on the multipath parameter estimation results, frequency-dependent modeling of path loss, shadow fading, the cross-polarization ratio, delay spread and angular spread was presented. However, these channel parameters can represent only the characteristics of a certain dimension of a particular channel but cannot establish a connection between two channels.

Intuitively, a high level of channel similarity between the mmWave and sub-6 GHz channels can be observed when the environment and the transceiver configurations are the same. Therefore, the question arises of exactly how similar they are, and to what degree of similarity can we use out-of-band information. A specific index is needed to measure this similarity. The correlation coefficient, which reflects the degree of linear correlation between two variables, is a common index for evaluating the correlation between signals received at adjacent antenna units in MIMO systems [16]. However, the correlation coefficient is only evaluated from a mathematical perspective, which is easily affected by noise, and cannot be measured comprehensively across multiple dimensions. Power profiles with similar correlation coefficients do not necessarily show similar differences. The same deficiency is found in similarity evaluations of time series or images. When measuring the correlation of two time series, the trend of the series is introduced to compensate for the information lost by judging only by the Euclidean distance [17]–[19]. Compared with the mean square error (MSE) and the peak signal-to-noise ratio (PSNR), the structural similarity (SSIM) calculated based on the brightness and contrast of local patterns can better reflect the similarity between images from the structural perspective, which is more in line with the human perception of images [20], [21]. Consequently, inspired by this structural similarity, more physical characteristics of the propagation channels should also be considered when evaluating two power profiles. The clustered delay line (CDL) channel model of the 3rd Generation Partnership Project (3GPP) [22], which is mainly used for link-level channel simulations, specifies a series of parameters, including the delays of clusters, the angles of departure (AoDs), the AoAs, the phases, and the amplitudes. These parameters determine the propagation characteristics with respect to the transceiver. The multipath component distance (MCD) [23] is one of the indices widely used in automatic multipath clustering algorithms [23]–[26] to quantify the separation between multipath components (MPCs). Furthermore, a channel similarity index measure was proposed in [27], in which the power delay profile is regarded as a time series, and cluster properties, such as the arrival time and decay rate, are considered. Two spatial channel similarity metrics focused on exploring the feasibility of using sub-6 GHz channel information for coarse estimation of mmWave beam directions were proposed in [28], [29]. However, these metrics can be used only for channel similarity measurements in either the time domain or angular domain, and not for all dimensions.

More importantly, how can channel cross-band similarity be used as prior knowledge to guide the design of the out-of-band spatial information-assisted beam search strategy, and at what level of channel similarity can the beam search algorithm obtain a stable prediction performance? The relationship between channel similarity and the availability of out-of-band information needs to be explored, as well as the influence of various factors, such as the antenna array pattern, the propagation environment complexity, and whether the direct path is obstructed.

In this work, a structural channel similarity index measure (CSIM) is proposed on the basis of multidimensional structural information. Not only can it be used to compare the similarity between two specific channels, but its statistical characteristics can also reflect the similarity between different frequency bands and different propagation environments. Based on the proposed CSIM, the feasibility of out-of-band information-assisted beam search is also investigated. The main contributions of this work are summarized as follows.

1) To reasonably and effectively evaluate the similarities of different channels in the form of numerical values, an objective CSIM is proposed, which accounts for the multidimensional structural information of the effective rays, including the complex amplitude, delay, AoA, and AoD. The proposed structural CSIM can evaluate channel similarity from one or more dimensions.
2) The CSIM can be used to measure channel similarity under different transceiver configurations, considering the effects of delay resolution and angular resolution. Its statistical characteristics can reflect channel similarity across different bands or environments.
3) Channel similarity is related to beam direction differences to investigate the feasibility of out-of-band information-assisted beam search strategies. The availability of out-of-band information depends on the complexity of the propagation environment, which is related to the K factor.

The remainder of this paper is organized as follows. Section II presents extensive channel measurements and simulations conducted at multiple bands in two environments that collected a large amount of channel data to use for analyzing the channel similarity. The proposed multidimensional CSIM is introduced in Section II. In Section IV, the statistical distributions of the CSIM across multiple frequency bands and two environments are presented, as well as the feasibility of out-of-band information-assisted beam search. Finally, Section V concludes the paper.

II. Channel Measurement and Simulation Campaigns

Channel measurements and simulations were conducted in multiple frequency bands in typical indoor and outdoor scenarios, i.e., a conference room and an office campus. The test frequencies ranged from the microwave band to the mmWave band, including 3 GHz, 5 GHz, 28 GHz, and 37.5 GHz. A large amount of channel data was obtained from the measurements and simulations for channel similarity analyses. In this section, the propagation environments and the measurement and simulation configurations are described in detail, followed by data preprocessing and a channel characteristic analysis.

A. Channel Measurements

Using a commercial off-the-shelf (COTS) instrument-based flexible channel sounder [30], channel measurements were conducted in multiple frequency bands by changing the corresponding radio frequency (RF) device. Considering the limitations of the hardware configuration and the measurement cost, only channel state information (CSI) in the time domain and the AoA domain was detected and analyzed. For the mmWave channel measurements, high-gain horn antennas were used to receive spatial MPCs by rotating in the azimuth and elevation planes. The angle resolution was 10°, which is related to the half-power beam width (HPBW) of the receiving antennas and the rotary step size of the rotator. An open-ended waveguide antenna with an HPBW greater than 80° was employed for wide coverage on the transmitter (TX) side. For the sub-6 GHz channel measurements, dipole antennas were used on both the TX and receiver (RX) sides. To obtain the AoA, a virtual planar array of 8×8 elements was used by translating the dipole antenna at the RX. The TX and RX antennas were placed in both vertically and horizontally polarized configurations during the channel measurements. The detailed specifications can be found in Table I. GPS-disciplined rubidium standard references were used for precise clock synchronization. Before the measurements, the system impulse response was calculated by physically connecting the RF ports of the TX and RX.

TABLE I
Multifrequency Channel Measurement Specifications

Parameter		Value			
Carrier Frequency (GHz)		3	5	28	37.5
Bandwidth (MHz)		100		100 300	
TX Antenna	Gain (dBi)	2.0		6.0	6.5
	E-plane HPBW (°)	60		102	80
	H-plane HPBW (°)	360		63	55
RX Antenna	Gain (dBi)	2.0		26.2	27.5
	E-plane HPBW (°)	60		10	
	H-plane HPBW (°)	360		10	
RX Rotation Range in Azimuth (°)		/		$0 \sim 350$	
RX Rotation Range in Elevation (°)		/		$50 \sim 120$	
RX Rotation Step (°)		/		10	

Fig. 1 depicts the layouts of the TX and RX locations in the typical indoor and outdoor scenarios. The dimensions of the

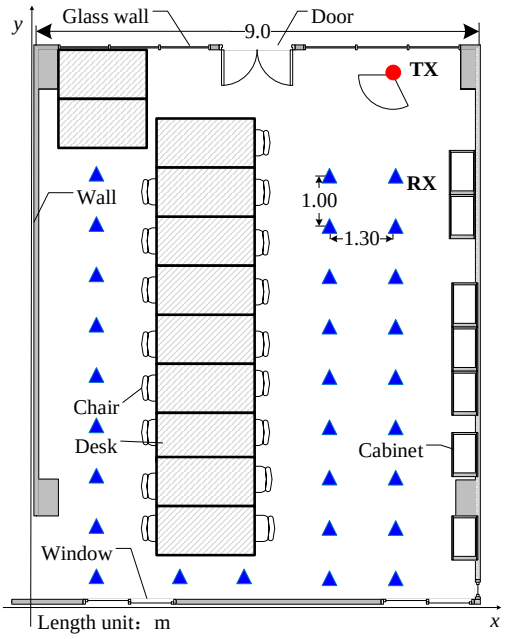

(a)

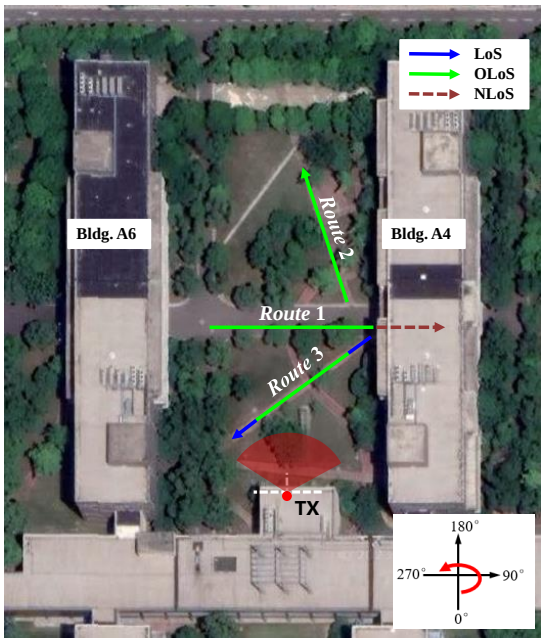

(b)

Fig. 1. Layouts of (a) the conference room scenario and (b) the outdoor office campus scenario.

conference room are $11.7 \times 9.0 \times 3.0$ m^3. In the conference room, there are several pieces of typical office furniture, such as metal cabinets, wooden desks, and leather chairs. The height of the desks is approximately 0.8 m. On the desktops, there are some office supplies and experimental equipment. The walls are made of concrete, glass, and wood. The metal cabinets and railings next to the floor-to-ceiling windows are the main scatterers. In this scenario, the TXs were fixed in the northwest corner of the conference room at a height of 2.6 m. Twenty-nine RX locations were selected, with fixed spacings of 1 m and 1.3 m. The height of the RX antennas was set to

1.8 m, which is slightly greater than the desktop height, so all the measured TX–RX location pairs corresponded to the line-of-sight (LoS) scenario. The outdoor scenario is a typical office campus surrounded by buildings 9–18 m in height. The roads on the office campus are lined with evergreen camphor trees with thick branches and leaves. The average tree height is approximately 8 m. There are several winding paths and bushes in the roadside flower beds. In this scenario, the TX antennas were deployed on the roof of the building at a height of 12.3 m, with the beam pointing into the middle of the canyon. Dozens of typical RX locations were selected along the three routes, including 8 LoS TX–RX pairs, 45 obstacle-LoS (OLoS) TX–RX pairs obstructed by foliage, and 6 non-LoS (NLoS) TX–RX pairs blocked by the building. The TX–RX separation distances varied from 20 m to 85 m, and the spacing of the RX locations along each route was 2 m.

Measurements were carried out at the 3 GHz, 5 GHz (specifically, 5.4 GHz in the indoor scenario and 4.8 GHz in the outdoor scenario due to the interference signals encountered during the measurements), 28 GHz and 37.5 GHz bands. A simplified peak detection algorithm [11] is proposed here to estimate MPCs. For the direction-scan measurement method, the angular power spectrum (APS) can be obtained in accordance with the received power of the directional channel. For simplicity, the angular resolution of the MPCs is considered 10° since standard gain horn antennas with an HPBW of 10° were adopted. For the sub-6 GHz channel measurements, the SAGE algorithm [31], [32] is used to accurately estimate the MPCs.

B. Channel Simulations

To compensate for the resolution limitations in the channel measurements, the commercial ray-tracing-based simulator Wireless InSite was applied to obtain higher-resolution CIRs in multiple frequency bands. All the simulation configurations are consistent with the measurement settings. The dimensions of the scenarios, and the placement of the scatterers, were recreated as much as possible in the simulator. In the conference room, the TXs were placed in the same location in the northwest corner in the multifrequency channel simulations at a height of 2.6 m. A total of 2240 RXs were distributed uniformly over a rectangular area with a spacing of 0.2 m to simulate the channel conditions throughout the space. The RX height was 1.8 m, which is consistent with the height of the channel sounder used in the field measurements. In the office campus, the TX antenna was deployed on top of the southern building. Three RX sets along the roads (*Route 1*, *Route 2* and *Route 3*) were selected, including 3168 RX locations with a spacing of 0.5 m. Due to the shading of the vegetation, most communication links are OLoS links, which are distributed mainly along *Route 1* and *Route 2* and in the middle of *Route 3*. The remaining links are LoS links at both ends of *Route 3* and NLoS links along *Route 1* extending to the corridor in the building.

The antennas used in the simulations are horn/dipole antennas with the same HPBWs as the measurement antennas used in the corresponding frequency band. Note that the material properties, including the relative permittivity and conductivity, were updated with the carrier frequency in accordance with the ITU recommendations [33]. The transmit power was uniformly set to 0 dBm, and the receiver sensitivity was set to -250 dBm to ensure that sufficient paths could be received. Based on previous research on the simulation depth, the orders of three propagation mechanisms, i.e., reflection, transmission, and diffraction, were set to $[6, 2, 2]$ for a trade-off between the accuracy of the simulation results and the time consumption. In addition, the machine learning-assisted calibration method was introduced to further fine-tune the simulation parameters to make the simulation channels more consistent with the measured channels [34]. Using the ray-tracing-based simulator, more simulation results at multiple frequency bands, different delay/angular resolutions, and polarization configurations can be obtained directly for more in-depth comparative investigations. The detailed simulation configurations are listed in Table II.

TABLE II
MULTIFREQUENCY CHANNEL SIMULATION CONFIGURATIONS

Parameter	Value
Carrier Frequency (GHz)	3, 5, 28, 37.5
Bandwidth (MHz)	100, 300, 1000
Angular resolution (°)	1, 10, 20, 30, 40, 50, 60
Polarization	co- and cross-polarization
Reflection order	6
Transmission order	2
Diffraction order	2

C. Channel Characteristic Analysis

The RMS delay spread and RMS angular spread are channel characteristic parameters used to measure the dispersion of the signal in the time domain or the angle domain. The RMS delay spread and RMS angular spread measured at the specific RX position across multiple frequency bands are depicted in Fig. 2. An obvious trend is that the channel dispersion characteristics decrease with increasing carrier frequency. A comparison of the results of these two scenarios reveals that the RMS delay spread measured in the conference room scenario is smaller than that measured in the office campus scenario, but the conclusion of the RMS angular spread is the opposite. This is mainly due to the distinctive propagation environments. In the conference room scenario, the signals pass through the surrounding walls or internal objects to reach the receiver. The incoming directions of the scattering paths are rich, and their powers are relatively strong, so the signal energy is concentrated in the time domain and dispersed in the angle domain. In addition, these dispersion parameters do not vary dramatically because of the similar propagation environments in the conference room scenario. The office campus scenario is wide open, and the internal environment varies, showing different channel characteristics at different RX positions. The scattering paths take longer to travel to the RXs, and they tend to be weaker in power. The channels are relatively sparse

TABLE III
PARAMETERS OF THE THREE EXAMPLE CHANNELS

Channel	$\mathcal{C}_{\mathrm{A}}$	$\mathcal{C}_{\mathrm{B}}$	$\mathcal{C}_{\mathrm{C}}$
Distance (m)	8.3	8.3	5.1
Frequency (GHz)	3	37.5	37.5
Number of MPCs	24	8	7
Average Delay (ns)	34.3	30.1	18.9
RMS Delay Spread (ns)	8.6	6.6	8.3
Average AAoA (°)	48.5	54.2	0.6
RMS AAoA Spread (°)	49.3	44.1	51.2

both in the time domain and the angle domain. For the LoS channels, the RMS delay spread and RMS angular spread are small, but the RMS delay spread is still larger than that in the conference room scenarios. Owing to the blockage effect, the degree of dispersion in both the time domain and the angle domain also increases. For the channels measured along *Route 2*, the strong reflection paths from the backward glass curtain wall result in a greater delay and angular spread.

However, channel parameters characterize the characteristics of a particular channel rather than the connection between two channels. On the one hand, these parameters only show the frequency dependence of the propagation characteristics, and we still cannot explore the detailed characteristics of the channels across different frequencies on the basis of these parameters alone. On the other hand, channels in different propagation environments may have similar channel parameters, and more parameters are needed to characterize and distinguish them. For example, the normalized power delay profiles (PDPs) and power angle profiles (PAPs) of three simulated channels in the conference room scenario are presented in Fig. 3, as are the channel parameters listed in Table III. $\mathcal{C}_{\mathrm{A}}$ and $\mathcal{C}_{\mathrm{B}}$ are simulated channels obtained at the same RX location at 3 GHz and 37.5 GHz, respectively. The TX-RX distance is 8.3 m. $\mathcal{C}_{\mathrm{C}}$ is another mmWave channel simulated at a relatively close distance of 5.1 m. The MPCs of the mmWave channels are sparser than those of the sub-6 GHz channel in both the time domain and the spatial domain, with the number of MPCs being approximately one-third of that of the sub-6 GHz channel, and there are fewer MPCs in the clusters. However, the incoming directions of the reflected rays are still abundant in the indoor scenario. Note that $\mathcal{C}_{\mathrm{A}}$ and $\mathcal{C}_{\mathrm{C}}$ have similar delay/angular spreads, but they do have obvious differences. Thus, more parameters, such as the average delay and average AoA, are needed for further characterization. In a comparison between $\mathcal{C}_{\mathrm{A}}$ and $\mathcal{C}_{\mathrm{B}}$, whose propagation environments are exactly the same, almost all of the rays in $\mathcal{C}_{\mathrm{B}}$ can be found to have corresponding rays in $\mathcal{C}_{\mathrm{A}}$, except they have a difference in the normalized power. However, these channel parameters do not intuitively reflect this similarity.

III. CHANNEL SIMILARITY ANALYSIS

Based on the analysis in subsection II-C, a single channel parameter is not enough to represent a specific channel, let alone reflect the connection between two channels. Therefore, if one wants to use the known channel information to infer an unknown channel, a novel measure is needed to associate these two channels. In this section, a channel similarity index named the CSIM is proposed according to the improved multipath parameter distance. The similarity of any two channels in one or more dimensions can be measured by a numerical value, and the time/angular resolutions are also accounted for.

A. Channel Similarity Index Measure (CSIM)

The channel similarity can be decomposed into the similarities of several MPC pairs, which are defined in terms of the parameter distance in different dimensions. The CIR $h(t)$ can be represented as a multidimensional function of the channel parameters, including the complex amplitude α, the delay τ, the AoA Φ_{R} (including the azimuth AoA φ_{R} and the elevation AoA θ_{R}), and the AoD Φ_{T} (including the azimuth AoD φ_{T} and the elevation AoD θ_{T}):

$$h(t) = \sum_{i}^{L} \alpha_i \delta(\tau - \tau_i)\delta(\Phi_{\mathrm{R}} - \Phi_{\mathrm{R},i})\delta(\Phi_{\mathrm{T}} - \Phi_{\mathrm{T},i}), \quad (1)$$

where L is the number of MPCs. These parameters set each specific MPC apart from the others and eventually give rise to a unique channel. The parametric multipath channel can be represented by $\mathcal{C} = \{\Theta_1, ..., \Theta_L\}$, where $\Theta_i = \{\alpha_i, \tau_i, \Phi_{\mathrm{R},i}, \Phi_{\mathrm{T},i}\}$ $(1 \le i \le L$ and where $i \in \mathbb{Z})$ represents the parameters of the ith MPC. Suppose that $\mathcal{C}_{\mathrm{X}}$ and $\mathcal{C}_{\mathrm{Y}}$ are two channels to be compared, with the detected MPCs of L_{X} and L_{Y}, respectively. $\Theta_{i,\mathrm{X}}$ and $\Theta_{j,\mathrm{Y}}$ represent the parameter sets of the ith MPC in $\mathcal{C}_{\mathrm{X}}$ and the jth MPC in $\mathcal{C}_{\mathrm{Y}}$. The multidimensional MPC parameter distance $d(\Theta_{i,\mathrm{X}}, \Theta_{j,\mathrm{Y}})$ can be synthesized as a Euclidean distance on the candidate dimensions as follows:

$$d(\Theta_{i,\mathrm{X}}, \Theta_{j,\mathrm{Y}}) = \sqrt{\frac{1}{N}(d_{\alpha_{ij}}{}^2 + d_{\tau_{ij}}{}^2 + d_{\Phi_{\mathrm{R}},ij}{}^2 + d_{\Phi_{\mathrm{T}},ij}{}^2 + \ldots)}, \quad (2)$$

where N is the number of selected dimensions. The multidimensional MPC parameter distance is extensible, and the candidate dimensions include, but are not limited to, the complex amplitude, delay, AoA, and AoD dimensions, corresponding to distances $d_{\alpha_{ij}}$, $d_{\tau_{ij}}$, $d_{\Phi_{\mathrm{R},ij}}$ and $d_{\Phi_{\mathrm{T},ij}}$.

Before comparison, power normalization and a unified coordinate system are required to exclude the system gain and facilitate fair comparisons. To simplify the calculation, a reasonable threshold should be set to extract only MPCs with power levels greater than this threshold while ignoring small signals. Then, the total power of all effective MPCs is normalized to 0 dBm. An improved MCD is proposed to calculate the multidimensional channel parameter distances. Coherence parameter distances are introduced on the basis of the angular resolution and the delay resolution of the communication system, which also eliminate the dimensional differences in different dimensions, scaling the distance measure to within the range of 0 to 1. Specifically, the distances $d_{\alpha_{ij}}$, $d_{\tau_{ij}}$ and $d_{\Phi_{\mathrm{R(T)},ij}}$ are defined as:

$$d_{\alpha_{ij}} = \frac{1}{2}\left\|\alpha_i - \alpha_j\right\|_2, \quad (3)$$

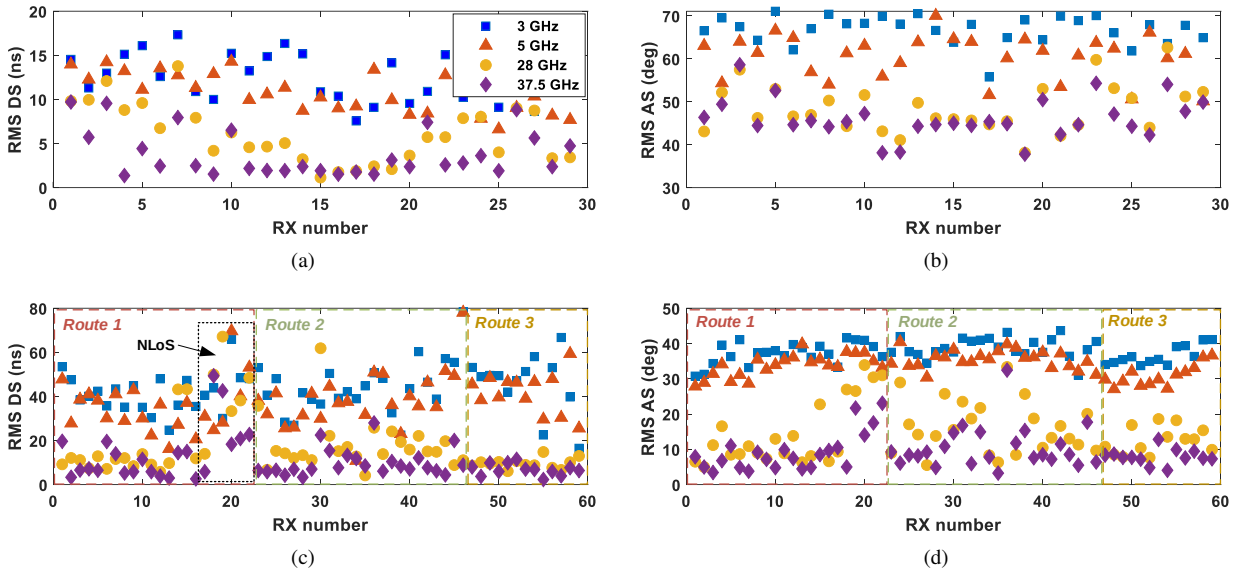

Fig. 2. Measured (a) RMS delay spread and (b) RMS AAoA spread in the conference room scenario and measured (c) RMS delay spread and (d) RMS AAoA spread in the office campus scenario.

$$d_{\tau_{ij}} = \begin{cases} \frac{|\tau_i - \tau_j|}{\widetilde{\tau}}, & |\tau_i - \tau_j| \le \widetilde{\tau}, \\ 1, & \text{otherwise}, \end{cases} \tag{4}$$

$$d_{\Phi_{\mathrm{R(T)},ij}} = \begin{cases} \frac{\Delta_{\mathrm{R(T)}}}{\min\left(\widetilde{\vartheta}_{\mathrm{R(T)}}, \pi\right)}, & \Delta_{\mathrm{R(T)}} \le \min\left(\widetilde{\vartheta}_{\mathrm{R(T)}}, \pi\right), \\ 1, & \text{otherwise}, \end{cases} \tag{5}$$

where $\|\cdot\|_2$ represents the Euclidean norm and $\Delta_{\mathrm{R(T)}} = \left\langle \Phi_{\mathrm{R(T)},i}, \Phi_{\mathrm{R(T)},j} \right\rangle$ is the space angle formed by $\Phi_{\mathrm{R(T)},i}$ and $\Phi_{\mathrm{R(T)},j}$. $\widetilde{\tau}$ represents the least distinguishable delay, which is related to the signal bandwidth, and is set to the average delay resolution of the channels to be compared. $\widetilde{\vartheta}_{\mathrm{R(T)}}$ is the average angular resolution on the RX/TX side, representing the least distinguishable angle. Intuitively, under a unified coordinate system, two MPCs are considered similar if the beams formed by them overlap in the space-time range, and the degree of similarity is linearly related to the parameter distance.

The smaller the value of $d(\Theta_{i,\mathrm{X}}, \Theta_{j,\mathrm{Y}})$ is, the more similar the two MPCs are. The value of $d(\Theta_{i,\mathrm{X}}, \Theta_{j,\mathrm{Y}})$ is equal to 0 only if the two MPCs are exactly the same on the target dimensions. Conversely, the MPC similarity is defined as:

$$s_{ij} = 1 - d(\Theta_{i,\mathrm{X}}, \Theta_{j,\mathrm{Y}}) \in [0, 1]. \tag{6}$$

According to the maximum s_{ij}, the MPCs in $\mathcal{C}_{\mathrm{X}}$ and $\mathcal{C}_{\mathrm{Y}}$ are pairwise matched into L_{match} pairs, which form a set $\mathbb{M}$. Considering the contribution of the MPC power to the total channel power, the channel similarity CSIM is finally derived as the power-weighted average similarity, that is:

$$\mathrm{CSIM}(\mathcal{C}_{\mathrm{X}}, \mathcal{C}_{\mathrm{Y}}) = \left(\sum_{i,j \in \mathbb{M}} \frac{|\alpha_i|^2 + |\alpha_j|^2}{2} s_{ij} \right) \times 100\%. \tag{7}$$

B. Cross-Channel Similarity Assessment

Based on the proposed CSIM in subsection III-A, the CSIMs between the example channels are summarized in Table IV. The CSIM is site-specific since the frame of reference is unified in all the comparisons. Channels under the same propagation environment have strong similarity. The similarity between $\mathcal{C}_{\mathrm{A}}$ and $\mathcal{C}_{\mathrm{B}}$ is more than 70% in any dimension, which is significantly greater than the similarities of the channels under different propagation environments. A comparison of $\mathrm{CSIM}(\mathcal{C}_{\mathrm{A}}, \mathcal{C}_{\mathrm{B}})$ and $\mathrm{CSIM}(\mathcal{C}_{\mathrm{B}}, \mathcal{C}_{\mathrm{C}})$ reveals that the channel difference caused by the location change is greater than that caused by the frequency change. The differences between the site-specific channel characteristics are caused mainly by the propagation mechanism changing with increasing carrier frequency, since the propagation environment is relatively static. The frequency-dependent electrical parameters of the scatterers affect the multipath powers, which further results in a difference in the MPC distribution. The full-dimensional CSIMs are generally smaller than the single-dimensional CSIMs because the differences in more dimensions are taken into account. Unlike the conventional channel parameters, the proposed CSIM can effectively evaluate the degree of the similarity between MPCs in various dimensions.

The reconstructed power spectra can be computed on the basis of the discrete MPCs and with the antenna pattern and system responses embedded [29], [32]. In Fig. 4, the continuous power spectra filtered with standard beam patterns of certain beam widths in different frequency bands are shown in the time domain and the angular domain. Taking the angular power spectrum as an example, an MPC with a larger beam width will have an impact on a wider range of the power spectrum. Ray #1 and Ray #2 are the direct path and the primary reflection path of $\mathcal{C}_{\mathrm{A}}$, respectively, with their AAoA values being 18.4° apart. These two MPCs do not interfere with each other if the sub-6 GHz system has an angular resolution of 10° because the two reconstructed beams are separated, whereas the two beams overlap if the angular resolution is 30°.

We assume that the bandwidth of the mmWave channels

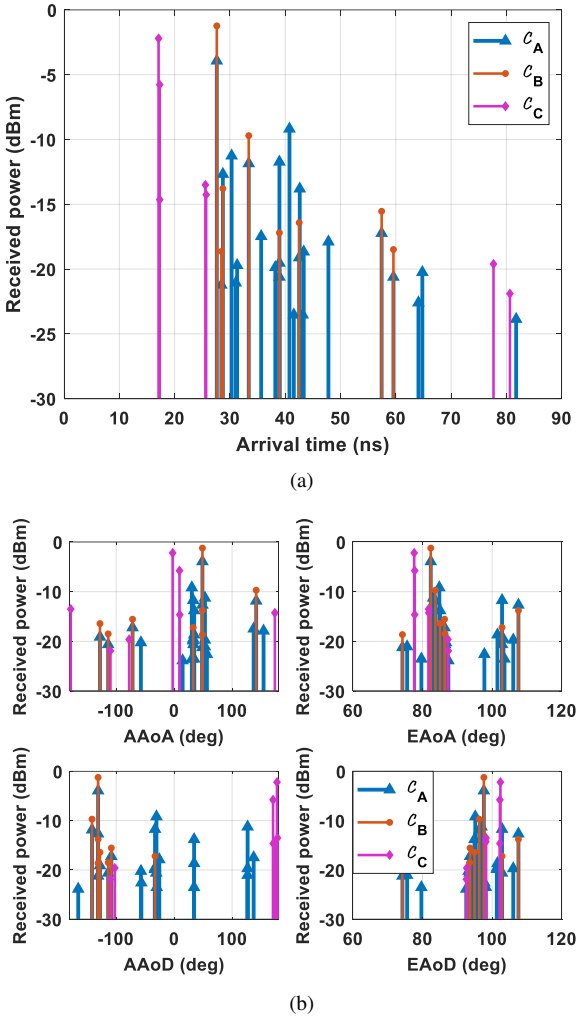

Fig. 3. Simulated PDPs and PAPs. (a) PDPs; (b) PAPs. Here, $\mathcal{C}_{\mathrm{A}}$ and $\mathcal{C}_{\mathrm{B}}$ are obtained from the same RX location in different frequency bands, and $\mathcal{C}_{\mathrm{B}}$ and $\mathcal{C}_{\mathrm{C}}$ are obtained from different RX locations at 37.5 GHz.

B_{HF} is 300 MHz, and that the angular resolution $\widetilde{\vartheta}_{\mathrm{HF}}$ is 10° due to the generally greater bandwidth and better beam pointing accuracy of mmWave systems, and those of the sub-6 GHz channel are set to B_{LF}=100 MHz and $\widetilde{\vartheta}_{\mathrm{LF}}$=30°. To explore the effects of delay resolution and angular resolution on channel similarity, CSIMs with different resolutions of the sub-6 GHz system are also calculated for comparison. The delay and AAoA dimensional similarity between $\mathcal{C}_{\mathrm{A}}$ and $\mathcal{C}_{\mathrm{B}}$ are 85.8% and 87.2%, respectively, which are slightly greater than those without considering delay or angular resolution. With increasing delay resolution or angular resolution, the similarity between the channels decreases. This is because in the CSIM evaluation system, beam overlap is regarded as a prerequisite for similarity between two MPCs. Consequently, a higher resolution increases the requirements for channel similarity.

IV. Results and Discussion

Based on the large amount of multiband channel data measured and simulated in the two typical environments, the channel similarities across frequency bands or environments

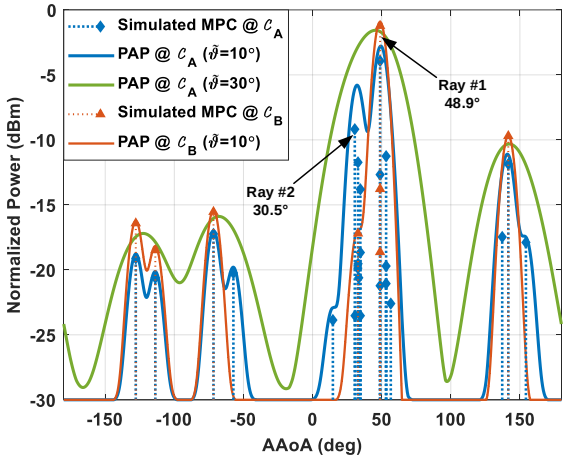

Fig. 4. Angular power spectra filtered with standard beam patterns.

TABLE IV
CSIM Results for the Three Simulated Channels

CSIM (%)	w/o considering delay/angular resolution			w/ considering delay/angular resolution		
	Full	Delay	AAoA	Full	Delay	AAoA
$\mathcal{C}_{\mathrm{A}}$ vs. $\mathcal{C}_{\mathrm{B}}$	73.1	81.8	83.3	78.0	85.8	87.2
$\mathcal{C}_{\mathrm{A}}$ vs. $\mathcal{C}_{\mathrm{C}}$	13.6	29.3	29.3	16.3	36.2	34.6
$\mathcal{C}_{\mathrm{B}}$ vs. $\mathcal{C}_{\mathrm{C}}$	23.8	41.2	40.4	26.4	47.7	46.0

are presented, as are the influences of the blockage and polarization configurations. Moreover, as an application example, the feasibility of out-of-band information-assisted beam search by using the CSIM as prior knowledge is also presented.

A. Frequency Similarity Analysis

The similarities of channels across multiple frequency bands obtained at the same location are calculated, which provides a comparison of the site-specific channel characteristics across different frequencies. The complementary cumulative distribution functions (CCDFs) of the CSIM are depicted in Fig. 5, and their statistics are provided in Table V. Figs. 5(a) and 5(d) show the empirical CCDFs of the CSIM measured in the conference room environment and the office campus environment. Obviously, there is a clear distinction in the similarities between cross-band channels. The similarities between mmWave channels and between sub-6 GHz channels both tend to be high, up to an average of more than 90%. The similarities between well-separated frequency bands seem to be related to the frequency interval and the frequency ratio between the mmWave bands and the sub-6 GHz bands; however, the complexity of the propagation environment and the characteristics of the scatterers are more important. In general, the smaller the frequency span and the frequency ratio are, the greater the similarity. A comparison of Fig. 5(a) and Fig. 5(d) reveals that the cross-band similarities in the office campus environment are slightly greater than those in the conference room environment, and the corresponding similarities between the mmWave channels and sub-6 GHz channels are approximately 5% greater. According to the distributions of

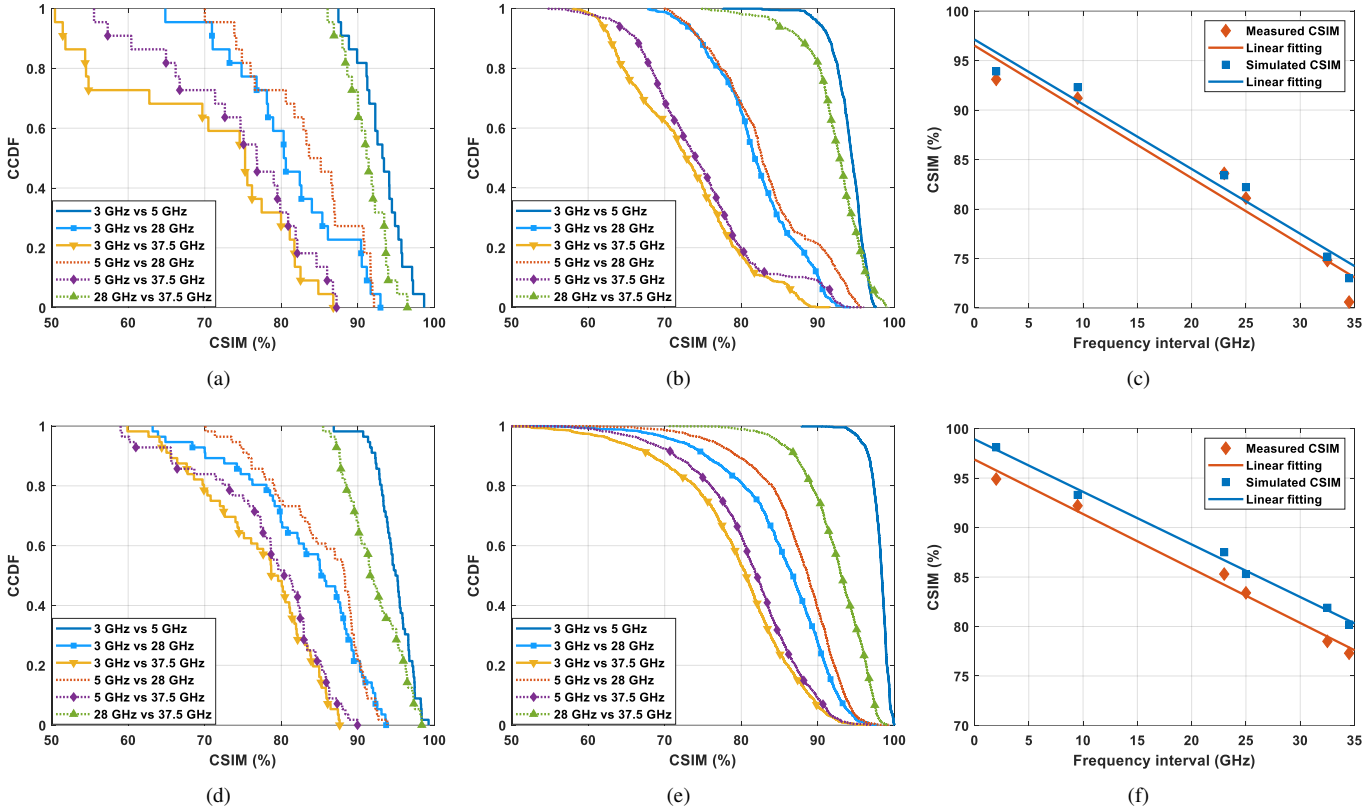

Fig. 5. Simulated and measured CCDFs of the CSIM across different frequency bands. (a) Measured and (b) simulated CSIMs in the conference room scenario, and (c) linear fitting of the CSIM with frequency interval; (d) Measured and (e) simulated CSIMs in the office campus scenario, and (f) linear fitting of the CSIM with frequency interval.

the measured MPCs, there are more strong reflection/scattering MPCs in the indoor environment, whereas there is usually only one direct path, and few reflection/scattering MPCs in the outdoor environment; thus, the indoor propagation environment is more complex with more strong multipaths, weakening the similarity between the channels.

The simulation results provide extensive channel data with higher delay/angular resolution and include more candidate dimensions. The CCDFs of the multidimensional CSIM are shown in Figs. 5(b) and 5(e). The statistical distributions of the simulated CSIMs are consistent with the trends of the measured results. Since the MPCs are relatively sparse in the angular domain in the office campus environment, the degrees of channel similarity among all frequency bands are high, and are greater than those in the conference room environment, which is consistent with the previous conclusion. Figs. 5(c) and 5(f) present the linear fitting of the mean CSIMs with the frequency interval between the two frequency bands. As the frequency interval increases, the mean CSIM decrease with slopes of -0.65 and -0.55 in the conference room environment and the office campus environment, respectively. The simulation results have the same variation trend as the measured results, with a slight overestimation of 1–2 percentage points.

Note that the simulated results are slightly larger than the corresponding measured results; this is because of the changes in the real measurement environment, and the differences in the measurement system configuration, which weaken the measured channel similarities. The different measurement schemes applied for the mmWave channel measurements and sub-6 GHz channel measurements inevitably affect the extraction of effective paths. The interference signals that often appear during the sub-6 GHz channel measurements are an important cause of angle estimation deviation. There will always be interference in a practical application environment, especially in an outdoor environment. Nevertheless, the simulation results match the actual channels well. In addition, when attempting to use out-of-band angle information to assist in beam search on the basis of channel similarity, a sufficient error margin must be considered.

Furthermore, the channel similarity under different propagation scenarios (i.e., the LoS, OLoS and NLoS scenarios) is discussed based on the channel data from the office campus environment. As shown in Fig. 6, the channel similarity between any two frequency bands under the LoS scenario is greater than that under the OLoS/NLoS scenario. When a direct path is missing, the signals must penetrate or bypass the scatterers in the environment or reflect off their surfaces to reach the RX, resulting in lower received power levels. The electromagnetic properties of the scatterers in different frequency bands increase the uncertainty of the reflected rays, and thus reduce the degree of channel similarity. The similarity gain increases with increasing frequency difference. For the sub-6 GHz channels, the statistical results for the channel similarity under the OLoS and NLoS scenarios are almost the same because of the strong penetration and diffraction capa-

TABLE V
CSIM STATISTICS ACROSS MULTIPLE FREQUENCIES

Freq. (GHz)	Conference Room				Office Campus									
	meas.		simu.		meas.		simu.		simu. (LoS)		simu. (OLoS)		simu. (NLoS)	
	mean	std	mean	std	mean	std	mean	std	mean	std	mean	std	mean	std
3 vs 5	93.1	3.0	93.9	2.3	94.9	2.3	98.1	1.2	99.1	0.9	98.1	1.3	97.7	1.1
3 vs 28	81.1	7.6	82.2	5.7	83.4	7.9	85.3	6.9	90.8	3.1	87.0	4.6	78.4	7.6
3 vs 37.5	70.6	12.2	73.0	7.9	77.3	7.5	80.2	8.1	88.9	4.1	81.1	5.4	72.7	8.9
5 vs 28	83.6	6.9	83.4	6.8	85.3	6.2	87.5	5.7	90.8	2.9	89.1	3.6	81.7	6.5
5 vs 37.5	74.8	9.4	75.2	8.1	78.5	7.9	81.9	7.2	88.5	4.1	82.6	5.1	75.9	8.1
28 vs 37.5	91.2	2.7	92.3	4.0	92.2	3.6	93.3	4.4	96.2	3.7	94.4	4.5	92.2	4.0

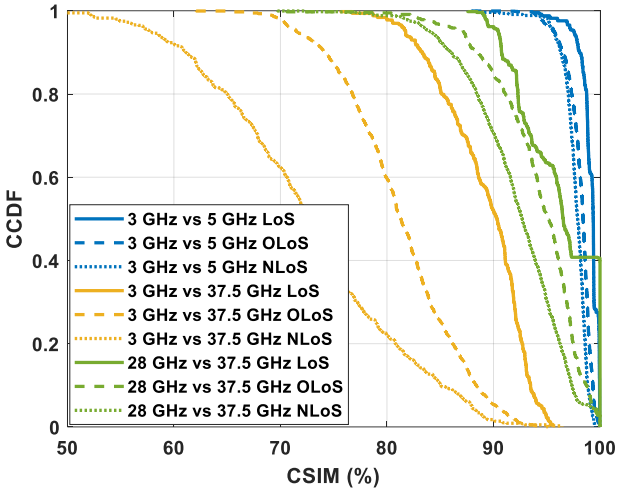

Fig. 6. CCDFs of the AAoA-dimensional CSIM across multiple frequency bands under different propagation scenarios. The three colors blue, yellow, and green represent three groups of frequency band pairs to be compared, i.e., 3 GHz vs. 5 GHz, 3 GHz vs. 37.5 GHz and 28 GHz vs. 37.5 GHz, respectively, while the solid lines, dashed lines, and dotted lines represent the LoS, OLoS, and NLoS scenarios, respectively.

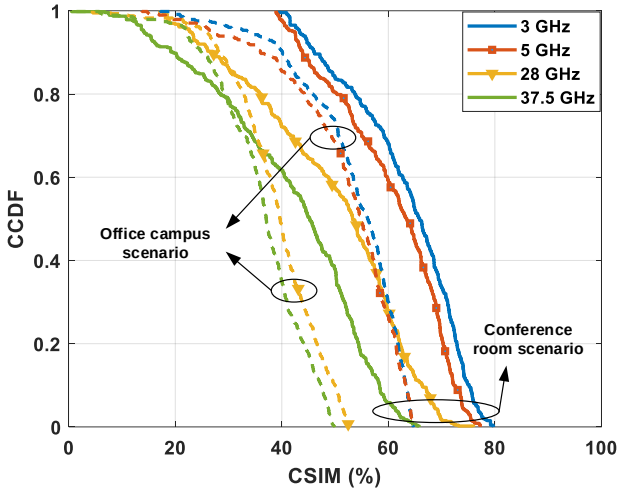

Fig. 7. Simulated CCDFs of the CSIM across different polarizations. The four colors blue, red, yellow, and green represent four frequency bands, i.e., 3 GHz, 5 GHz, 28 GHz, and 37.5 GHz, respectively, whereas the solid lines and dashed lines represent the conference room and the office campus environments, respectively.

bilities of the sub-6 GHz signals. As the frequency increases, the penetration and diffraction of the signals decrease. When two frequency bands differ greatly, such as the 3 GHz and 37.5 GHz, the direct path has a significant influence on the channel similarity. Compared with the LoS cases, the average channel similarities under the OLoS and NLoS scenarios are decreased by 7.8 and 16.2 percentage points, respectively. For two mmWave bands under LoS scenarios, there are several cases with only one direct path, showing a similarity of 100%.

The K factor is the ratio of the power of the direct ray to the sum power of other reflection paths, reflecting the complexity of signal propagation in the channel. In the conference room environment, the mean K factors are -0.4 dB, -0.6 dB, 3.7 dB, and 5.8 dB in the four frequency bands, which are lower than those in the office campus environment, where the mean K factors are greater than 6 dB. The abundance of multipaths in the conference room leads to a complex communication environment. Empirically, the CSIM is negatively correlated with the complexity of the propagation environment. The more complex the propagation environment is, that is, the smaller the K factor is, the lower the site-specific frequency similarity tends to be.

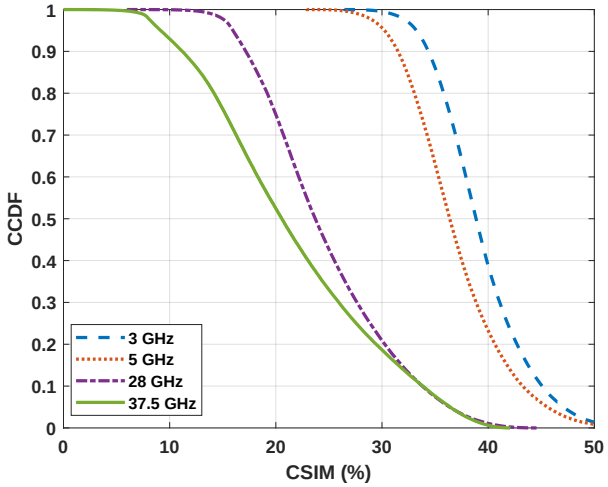

Fig. 8. Simulated CCDFs of the CSIM across different environments.

B. Polarization Similarity Analysis

The channels obtained under different TX-RX antenna polarization configurations are combined to calculate the polarization similarity. The simulated CCDFs of the similarities between the two polarizations are shown in Fig. 7. The

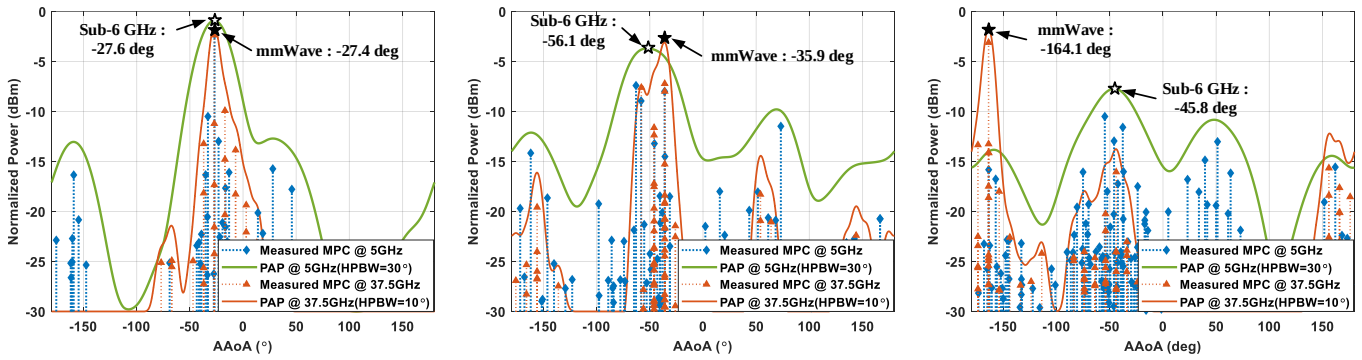

(a) (b) (c)

Fig. 9. Measurement-based analysis of AAoA-dimensional channel similarity between 5 and 37.5 GHz, where the hollow and solid stars represent the optimal beam directions for sub-6 GHz and mmWave channels in the same RX location, respectively. (a) Successful case in the office campus environment; (b) Non-successful case in the conference room environment; (c) Non-successful case in the office campus environment.

similarity between channels with different polarizations is relatively weak. The simulation results reveal that the maximum polarization similarity is less than 80%, and with increasing frequency, the polarization similarity weakens in both the conference room and the office campus environments. There is a significant gap of more than 10 percentage points between the polarization similarity of the mmwave channels and that of the sub-6 GHz channels. In addition, the polarization similarities of all four frequency bands in the indoor scenario are greater than those of the corresponding bands in the outdoor scenario; this is mainly because in the indoor environment, especially at lower frequencies, the abundant multipaths have more opportunities to interact with the scatterers in the propagation environment, which increases the possibility of polarization torsion, and then increases the similarity between the two orthogonal polarizations.

C. Environment Similarity Analysis

Fig. 8 shows the CCDFs of the similarities between two propagation environments based on the channel characteristics. Before calculation, all the channels are aligned based on the strongest path so that the differences in propagation delay due to the relative locations of the transceivers are excluded. Obviously, the similarities between the mmWave channels are less than those between the sub-6 GHz channels. An increase in the carrier frequency weakens the channel similarity. This is due to the multipath sparsity of the mmWave channels, highlighting the importance of the direct path (the strongest path), which can also be explained by the K factor. In higher frequency bands, especially in LoS scenarios, the mismatch of direct paths leads to a sharp decline in the similarity of the two channels, that is, the two channels tend to be orthogonal. The large variances of CSIMs indicate that the mmWave channels are easily affected by the propagation environment and the transceiver locations. The channel similarities obtained at different RX positions are quite different even in the same scenario. However, in the sub-6 GHz bands, the abundant multipath extends the incoming wave direction, which makes the channels have a higher correlation in the spatial domain. In other words, the channel similarity between the two propagation environments is weak at less than 50%. The large differences indicate that signal processing algorithms, such as the beam-searching strategy, need to be designed separately with respect to their environmental characteristics.

D. Feasibility of Out-of-Band Information-Assisted Beam Search

A relationship is established between the proposed CSIM and the beam direction differences across multiple frequency bands to explore the feasibility of out-of-band information-assisted beam search. The sub-6 GHz/mmWave band combinations of 5/37.5 GHz are used for the analysis. The measured discrete MPCs are filtered by the ideal 3GPP beam patterns with different HPBWs according to the carrier frequency. The beam widths are set to 30° and 10°, respectively. If the difference between the optimal beam directions of the two frequency bands is less than $\widetilde{\vartheta}_\mathrm{r}$, the spatial information provided by the out-of-band channel is considered beneficial to the beam search at the target frequency band. In other words, only the $\pm\widetilde{\vartheta}_\mathrm{r}$ range centered on the optimal beam direction of the out-of-band channel needs to be searched to obtain the optimal direction of the target band channel, which greatly reduces the beam training overhead. Fig. 9(a) shows an example in the office campus environment. The optimal beam directions at 5 GHz and 37.5 GHz match well with the 0.2° direction difference, and the corresponding CSIM is 85.4%.

However, the sub-6 GHz channels may provide inaccurate or even incorrect spatial information in some cases. As shown in Figs. 9(b) and 9(c), the AAoA-dimensional CSIMs between the sub-6 GHz channel and the mmWave channel is 77.2%. There are two main reasons for the difference in beam direction. One is the different angular resolutions of the sub-6 GHz/mmWave systems. This type of angle mismatch is more common in indoor environments when the RX is close to the reflector, where two MPCs reach the RX with an angle difference approximately equal to the beam width. As shown in Fig. 9(b), the optimal beam directions formed by two MPCs with similar powers after beam filtering can be obviously distinguished, with a difference of 20.2° slightly greater than $\widetilde{\vartheta}_\mathrm{r}$. Fortunately, the two channels remain highly similar under this condition, and the optimal direction can be obtained with a small extension of the search range. The other type of angle

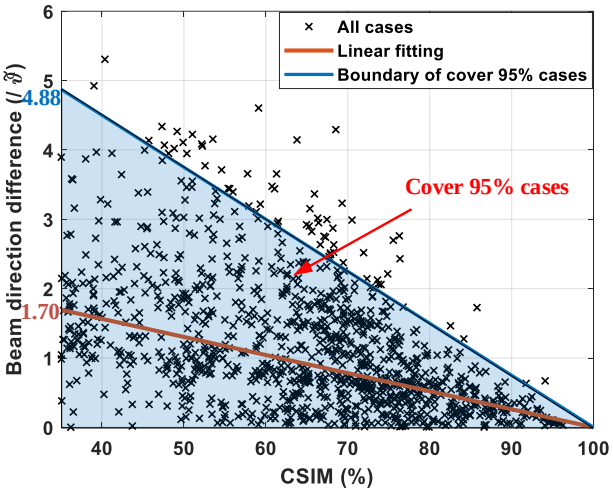

(a)

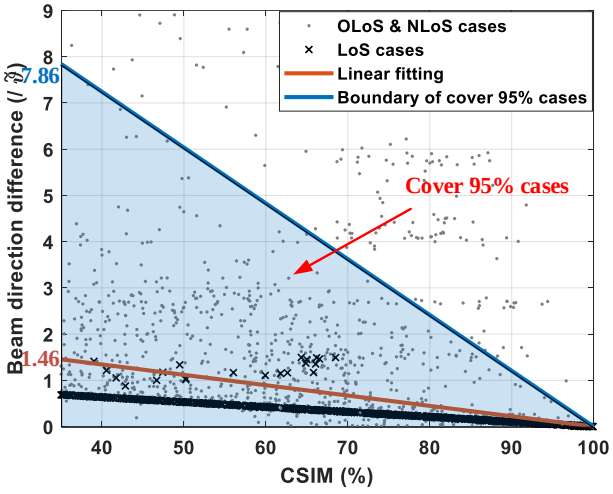

(b)

Fig. 10. Linear fittings of the beam direction difference vs CSIM between 5 and 37.5 GHz in (a) the conference room and (b) the office campus environment, where the black crosses and gray dots represent cases including simulated and measured results, the shaded area contains 95% of the cases, and the red line is a linear fit for all the cases.

mismatch often occurs at low signal-to-noise ratio (SNR) RX locations where the forward link is blocked. The channels shown in Fig. 9(c) were measured on *Route 1* in the office campus environment, and the direct path was obstructed by dense foliage. The sub-6 GHz signals can still pass through the foliage to reach the RX. However, with increasing carrier frequency, vegetation attenuation becomes increasingly severe, resulting in the signal strength of the forward link being lower than that of the backward link from the glass curtain wall. The channel similarity is greatly weakened, and the large difference in the beam direction results in the sub-6 GHz spatial information not contributing to the mmWave beam search, which is the worst-case.

By traversing all channel combinations at 5 GHz and 37.5 GHz in both environments, the relationships between the beam direction differences and the CSIM are shown in Fig. 10. A reasonable beam search range threshold is provided to balance the beam search overhead and minimize the worst cases like

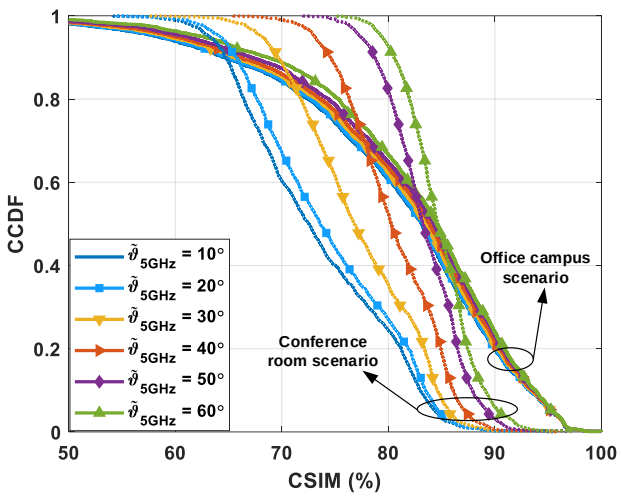

Fig. 11. Simulated CCDFs of the CSIM across 5 GHz and 37.5 GHz channels under different beamwidths of the sub-6 GHz channel, where the beam width of the HF channel is 10°.

Fig. 9(c). The success rate of the out-of-band information-assisted beam search is environmentally dependent. In the indoor conference room, the mean and variance of the beam direction difference decrease with increasing CSIM; that is, the higher the channel frequency similarity is, the smaller the beam range to be searched to find the optimal beam direction. When the CSIMs are maintained above approximately 86%, out-of-band information-assisted beam search can be effectively applied at almost all the RX locations, with the optimal beam direction obtained in the $1 \times \tilde{\vartheta}_{\mathrm{r}}$ range. However, in the outdoor environment, the CSIMs in the LoS and OLoS/NLoS scenarios have different characteristics, as shown in Fig. 10(b). For the LoS scenarios, the beam pointing difference has an obvious linear relationship with the CSIM; this is because the strength of the direct path is much greater than that of the reflected paths in an open environment with no occlusion, and the multiple paths are sparse, resulting in the difference in the direct path determining the CSIM to a large extent. However, when the direct path is attenuated by foliage or completely blocked by buildings, many multipath scattering components with similar strengths easily lead to angle mismatches. Thus, compared with the indoor propagation environment, channel pairs with the same CSIM often need a larger search interval in the outdoor environment to successfully align the beam. Based on above conclusions, and the statistical results of the simulated and measured CSIMs in subsection IV-A, the sub-6 GHz spatial information is useful for mmWave beam training.

In addition, both the CSIM and beam direction are affected by the beam width of the communication system. Fig. 11 shows the simulated CCDFs of the CSIM across the 5 GHz and 37.5 GHz channels under different beam widths (i.e., 10°, 20°, 30°, 40°, 50°, and 60°) of the sub-6 GHz channel, where the beam width of the mmWave channel is 10°. As mentioned above, the narrower the beam width is, the more stringent the similarity conditions for a pair of MPCs since their beams need to be aligned enough to overlap. The effect of the beam width on the channels in the indoor environment is greater than that in the outdoor environment, which is also related to

the channel sparsity in the outdoor environment. The wider the sub-6 GHz channel beam width is, the larger the CSIM that can be derived, thus increasing the success rate of searching for the mmWave optimal beam direction within $\widetilde{\vartheta}_{\mathrm{r}}$; however, the low resolution means that the less information provided by the sub-6 GHz channel, the larger the search range needed for beam alignment.

V. Conclusion

In this paper, a multidimensional CSIM based on structural multipath information has been proposed for the universal evaluation of channel similarities. By accounting for the physical characteristics of the channels, the proposed CSIM provides a clear quantitative evaluation in one or more dimensions rather than a vague visual judgment. Simulated and measured channel data from two typical environments (a conference room environment and an office campus environment) in four frequency bands are used to analyze and verify the performance of the proposed CSIM. The statistical distributions of the CSIM were investigated to explore the similarities across different frequency bands in different environments. The results show that cross-band similarity is related mainly to the frequency interval and environment complexity. In general, large frequency intervals and rich multipaths weaken the channel similarity. In addition, the feasibility of out-of-band information-assisted beam search on the basis of cross-band CSIM is preliminarily investigated. The out-of-band information helps reduce the beam training overhead to some extent, but it is more critical to update the search strategy according to the environmental characteristics. The low similarity between these two environments also illustrates that signal processing algorithms cannot be blindly applied from another unrelated environment.

For future work, using channel similarity is expected to significantly reduce the computational overhead of beam searching. On the one hand, the channel similarity index can be improved by considering more dimensions, such as Doppler, as well as the actual antenna array patterns for dynamic multidimensional channel similarity measures. More statistical performance analyses across multiple frequency bands and multiple environments based on extensive field measurements need to be performed to provide prior knowledge for the creation of highly efficient beam management strategies. On the other hand, developing a portable and highly efficient beam management strategy by fully exploring and utilizing the correlation between propagation environments is also of interest.

References

[1] X. You, C. Wang, J. Huang *et al.*, "Towards 6G wireless communication networks: vision, enabling technologies, and new paradigm shifts," *Sci. China Inf. Sci.*, vol. 64, no. 1, 2021.

[2] C.-X. Wang, X. You, X. Gao *et al.*, "On the road to 6G: Visions, requirements, key technologies, and testbeds," *IEEE Commun. Surv. Tutor.*, vol. 25, no. 2, pp. 905–974, 2023.

[3] T. S. Rappaport, G. R. MacCartney, M. K. Samimi, and S. Sun, "Wideband millimeter-wave propagation measurements and channel models for future wireless communication system design," *IEEE Trans. Commun.*, vol. 63, no. 9, pp. 3029–3056, 2015.

[4] D.Dupleich, R. Muller, M. Landmann, E.-A. Shinwasusin, K. Saito, J.-I. Takada, J. Luo, R. Thoma, and G. Del Galdo, "Multi-band propagation and radio channel characterization in street canyon scenarios for 5G and beyond," *IEEE Access*, vol. 7, pp. 160 385–160 396, 2019.

[5] A. Ali, N. G. Prelcic, and R. W. Heath, "Millimeter wave beam-selection using out-of-band spatial information," *IEEE Trans. Wirel. Commun.*, vol. 17, no. 2, pp. 1038–1052, 2018.

[6] ——, "Spatial covariance estimation for millimeter wave hybrid systems using out-of-band information," *IEEE Trans. Wirel. Commun.*, vol. 18, no. 12, pp. 5471–5485, 2019.

[7] N. G. Prelcic, A. Ali, V. Va, and R. W. Heath, "Millimeter-wave communication with out-of-band information," *IEEE Commun. Mag.*, vol. 55, no. 12, pp. 140–146, 2017.

[8] Y. Xiu, W. Wang, and Z. Zhang, "A message passing approach to acquire mm-Wave channel state information based on out-of-band data," *IEEE Access*, vol. 6, pp. 45 665–45 680, 2018.

[9] J. Huang, C. Wang, H. Chang, J. Sun, and X. Gao, "Multi-frequency multi-scenario millimeter wave MIMO channel measurements and modeling for B5G wireless communication systems," *IEEE J. Sel. Areas Commun.*, vol. 38, no. 9, pp. 2010–2025, 2020.

[10] P. Zhang, J. Li, H. Wang, H. Wang, and W. Hong, "Indoor small-scale spatiotemporal propagation characteristics at multiple millimeter-wave bands," *IEEE Antennas Wirel. Propag. Lett.*, vol. 17, no. 12, pp. 2250–2254, 2018.

[11] P. Zhang, B. Yang, C. Yi, H. Wang, and X. You, "Measurement-based 5G millimeter-wave propagation characterization in vegetated suburban macrocell environments," *IEEE Trans. Antennas Propag.*, vol. 68, no. 7, pp. 5556–5567, 2020.

[12] J. Pascual-Garcia, L. Rubio, V. Rodrigo Penarrocha *et al.*, "Wireless channel analysis between 25 and 40 GHz in an intra-wagon environment for 5G using a ray-tracing tool," *IEEE Trans. Intell. Transp. Syst.*, vol. 23, no. 12, pp. 24 621–24 635, 2022.

[13] D. Dupleich, R. Muller, S. Skoblikov *et al.*, "Multi-band indoor propagation characterization by measurements from 6 to 60 GHz," in *Proc. 13th Eur. Conf. Antennas Propag. (EuCAP)*, 2019, pp. 1–5.

[14] T. Jiang, J. Zhang, M. Shafi, L. Tian, and P. Tang, "The comparative study of S-V model between 3.5 and 28 GHz in indoor and outdoor scenarios," *IEEE Trans. Veh. Technol.*, vol. 69, no. 3, pp. 2351–2364, 2020.

[15] Y. L. C. De Jong, J. A. Pugh, M. Bennai, and P. Bouchard, "2.4 to 61 GHz multiband double-directional propagation measurements in indoor office environments," *IEEE Trans. Antennas Propag.*, vol. 66, no. 9, pp. 4806–4820, 2018.

[16] X. Hong, C. Wang, J. Thompson, B. Allen, W. Q. Malik, and X. Ge, "On space-frequency correlation of UWB MIMO channels," *IEEE Trans. Veh. Technol.*, vol. 59, no. 9, pp. 4201–4213, 2010.

[17] L. Li, X. Su, Y. Zhang, Y. Lin, and Z. Li, "Trend modeling for traffic time series analysis: An integrated study," *IEEE Trans. Intell. Transp. Syst.*, vol. 16, no. 6, pp. 3430–3439, 2015.

[18] A. Gogolou, T. Tsandilas, T. Palpanas, and A. Bezerianos, "Comparing similarity perception in time series visualizations," *IEEE Trans. Vis. Comput. Graphics*, vol. 25, no. 1, pp. 523–533, 2019.

[19] H. Guo, L. Wang, X. Liu, and W. Pedrycz, "Trend-based granular representation of time series and its application in clustering," *IEEE Trans. Cybern.*, vol. 52, no. 9, pp. 9101–9110, 2022.

[20] Z. Wang, A. Bovik, H. Sheikh, and E. Simoncelli, "Image quality assessment: From error visibility to structural similarity," *IEEE Trans. Image Process.*, vol. 13, no. 4, pp. 600–612, 2004.

[21] M. P. Sampat, Z. Wang, S. Gupta, A. C. Bovik, and M. K. Markey, "Complex wavelet structural similarity: A new image similarity index," *IEEE Trans. Image Process.*, vol. 18, no. 11, pp. 2385–2401, 2009.

[22] 3GPP, "Study on channel model for frequencies from 0.5 to 100 GHz," 3rd Generation Partnership Project (3GPP), TR 38.901 V15.0.0, Tech. Rep., June 2018.

[23] N. Czink, P. Cera, J. Salo, E. Bonek, J. p. Nuutinen, and J. Ylitalo, "A framework for automatic clustering of parametric MIMO channel data including path powers," in *Proc. IEEE Vehicular Technol. Conf.*, 2006, pp. 1–5.

[24] ——, "Improving clustering performance by using the multi-path component distance." *IEE Electron. Lett.*, vol. 42, no. 1, pp. 44–45, 2006.

[25] Y. Li, J. Zhang, P. Tang, and L. Tian, "Clustering in the wireless channel with a power weighted statistical mixture model in indoor scenario," *China Commun.*, vol. 16, no. 7, pp. 83–95, 2019.

[26] C. Huang, A. F. Molisch, Y. A. Geng, R. He, B. Ai, and Z. Zhong, "Trajectory-joint clustering algorithm for time-varying channel modeling," *IEEE Trans. Veh. Technol.*, vol. 69, no. 1, pp. 1041–1045, 2020.

[27] C. Yi, P. Zhang, H. Wang, and W. Hong, "Multipath similarity index measure across multiple frequency bands," *IEEE Wirel. Commun. Lett.*, vol. 10, no. 8, pp. 1677–1681, 2021.

[28] P. Zhang, P. Kyosti, K. Haneda, P. Koivumaki, Y. Lyu, and W. Fan, "Out-of-band information aided mmWave/THz beam search: A spatial channel similarity perspective," *IEEE Commun. Mag.*, vol. 00, no. 00, pp. 1–7, 2022, early access.

[29] P. Kyosti, P. Zhang, A. Parssinen, K. Haneda, P. Koivumaki, and W. Fan, "On the feasibility of out-of-band spatial channel information for millimeter-wave beam search," *IEEE Trans. Antennas Propag.*, vol. 71, no. 5, pp. 4433–4443, 2023.

[30] J. Li, P. Zhang, C. Yu, H. Wang, and W. Hong, "High-efficiency wideband millimeter-wave channel sounder system," in *Proc. 13th Eur. Conf. Antennas Propag. (EuCAP)*, 2019, pp. 1–5.

[31] B. H. Fleury, M. Tschudin, R. Heddergott, D. Dahlhaus, and K. Ingeman Pedersen, "Channel parameter estimation in mobile radio environments using the SAGE algorithm," *IEEE J. Sel. Areas Commun.*, vol. 17, no. 3, pp. 434–450, 1999.

[32] X. Yin, C. Ling, and M. Kim, "Experimental multipath-cluster characteristics of 28-GHz propagation channel," *IEEE Access*, vol. 3, pp. 3138–3150, 2015.

[33] ITU, "Effects of building materials and structures on radiowave propagation above about 100 MHz," ITU-R, Rec., Tech. Rep. P.2040-2, Sep. 2021.

[34] C. Yi, W. Chen, Q. Wu, and H. Wang, "Machine learning-assisted calibration for ray-tracing channel simulation at centimeter-wave and millimeter-wave bands," *IEEE Antennas Wireless Propag. Lett.*, vol. 23, no. 5, pp. 1623–1627, 2024.

Response to Comments for AP2310-2417

Reply to the Comments of Track Editor:

Based on the criticsm made by the reviewers and the AE, the paper is not suitable for publication.

Re:

We have revised our manuscript according to the valuable suggestions and comments.

Reply to the Comments of the Associate Editor:

Please use appropriate frequency band classification as it is misleading using LF and HF to refer to the bands used in the paper.

Re:

Thanks for your valuable suggestions. In the revised version of this manuscript, we use sub-6 GHz bands and millimeter wave bands instead of the ambiguous LF and HF for explicit expression and indicate the specific frequency in each special case.

Reply to the Comments of Reviewer #1:

General comments:

The paper aims to propose a new measure for multi-band channel modeling, which is an interesting and well-motivated topic. In general, the authors properly present their work, which results in a solid work. However, there are some comments from the review in terms of motivation, modeling, simulation, and analysis, which are as follows.

Re:

We thank you for your advice on our work. The following are our responses to your suggestions and comments.

Specific comments:

1. The motivation is unclear, and the research problems are not well formulated. First of all, the core problem in wireless channel modeling is to characterize and model the channels in terms of frequency and scenario, thus, the real research problems for multi-band systems are not well formulated. Then, mainly, what is the limitation of the current measures?

Re:

We reorganized the motivation in the revised manuscript. First, to pursue faster communication rates and lower communication delay, multiband communication systems by combining the capabilities of high-frequency and low-frequency systems show great promise for achieving both breadth and depth of coverage compared with traditional single-frequency systems. The multiband channel information needs to be fully utilized to give full play to the advantages of the multiband wireless communication system. Therefore, an evaluation index is needed to establish the connection between the channels of different frequency bands, to evaluate the degree of similarity between the two channels, so as to determine how much channel information is common. On the other hand, the information transmission scheme designed based on channel similarity can effectively reduce the channel estimation cost and improve the channel capacity. This similarity index can provide a reference for this transmission scheme, that is, to what similarity degree the two channels reach, this transmission scheme can operate stably.

Then, several existing measures are also cited. Channel parameters, such as rms delay spread and rms angle spread, represent the characteristics of a particular channel in a particular dimension, but can not directly establish the connection between the two channels. The correlation coefficient is only evaluated from a mathematical perspective, which is easily affected by noise and cannot be measured comprehensively across multiple dimensions. The multipath component distance (MCD) is used to measure the distance between two multipaths. However it does not unify the dimensions in the multiple dimensions, and it needs to be further extended to measure the similarity. Other measures, such as time domain channel similarity index measure, can only be used for similarity assessment in a certain dimension.

2. As the authors mentioned, several existing similarity indexes can be used for time or angular domain. In fact, the amplitude is also included. Moreover, cannot these methods be extended to other domains?

Re:

Existing similarity indexes, such as correlation coefficient, SIM [Yi2021] and spatial channel similarity metrics[Kyosti2023], are described based on the power spectrum, which becomes unintuitive when extended to high dimensions, and will be affected by the noise and the RF front-end performance. Also, there is a lack of a unified metric to balance the importance between the different dimensions. Actually, the measure we propose in this manuscript are extended from the MCD. On the one hand, coherence parameter distances are introduced based on the angular resolution and the delay resolution of the communication system, which also eliminates the dimensional differences in different dimensions, scaling the distance measure to within the range of 0 to 1. The multidimensional MPC parameter distance is extensible and the candidate dimensions include but are not limited to the complex amplitude, delay, AoA and AoD dimensions. On the other hand, the distances of the subpaths are combined to derive the similarity of the entire channels.

[Yi2021] C. Yi, P. Zhang, H. Wang, and W. Hong, “Multipath similarity index measure across multiple frequency bands,” *IEEE Wirel. Commun. Lett.*, vol. 10, no. 8, pp. 1677–1681, 2021.

[Kyosti2023] P. Kyosti, P. Zhang, A. Parssinen, K. Haneda, P. Koivumaki, and W. Fan, “On the feasibility of out-of-band spatial channel information for millimeter-wave beam search,” *IEEE Trans. Antennas Propag.*, vol. 71, no. 5, pp. 4433–4443, 2023.

3. The authors used HF and LF which actually are dedicated to cellular systems, which should be clarified.

Re:

In this work, we mainly investigate the channel similarities across the band of sub-6 GHz and the millimeter wave, so we use the sub-6 GHz frequency band and millimeter wave frequency band instead of the ambiguous LF and HF for explicit expression in the revised version of this manuscript.

4. The statement that the losses caused by reflection or other MPCs weaken the correlation needs to be reconsidered. Not only the loss but also many factors can influence the correlation. Here is just an example, please check the writing.

Re:

Thank you for your advice on our work. We have checked the whole manuscript and corrected these similar errors.

5. For the writing, there are too many uncertain tones, such as to a certain extent, somewhat, please avoid them and make sure what you stated is well verified.

Re:

Thank you for your careful reading. We improve our proposed similarity index and add extensive measurement and simulation results for verification. In addition, we have improved our writing in the revised version and avoid these uncertain tones.

6. It is known that ray-tracing simulation can tune the propagation mechanism, where the authors should mention what kind of propagation they simulated. According to the observation from the authors, C_A containing C_B, is not supersizing when you use ray-tracing, where everything is deterministic. Also, what obtained channel parameters as well as simulation parameters should be mentioned.

Re:

The commercial ray tracing-based simulator Wireless InSite was applied to obtain the CIRs in multiple frequency bands. All simulation configurations are consistent with the measurement settings. The dimensions of the scenarios and the placement of the scatterers were recreated as much as possible in the simulator. The antennas used in the simulations are horn/dipole antennas with the same HPBWs as the measurement antennas used in the corresponding frequency band. The material properties, including relative permittivity and conductivity, were updated with the carrier frequency following the ITU recommendations. Based on previous research on the simulation depth, the orders of three propagation mechanisms, i.e., reflection, transmission, and diffraction, were set to [6, 2, 2] for a trade-off between the accuracy of the simulation results and the time consumption. The detailed simulation configurations are listed in Table II and the channel parameters of C_A, C_B and C_C are provided in Table III.

Table II Multifrequency channel simulation configurations

Parameter	Value
Carrier Frequency (GHz)	3, 5, 28, 37.5
Bandwidth (MHz)	100, 300, 1000
Angular resolution (deg)	1, 10, 20, 30, 40, 50, 60
Polarization	Co- and cross-polarization
Reflection order	6
Transmission order	2
Diffraction order	2

Table III Parameter of the three example channels

Channel	C_A	C_B	C_C
Distance (m)	8.3	8.3	5.1
Frequency (GHz)	3	37.5	37.5
Number of MPCs	24	8	7
Average Delay (ns)	34.3	30.1	18.9
RMS Delay Spread (ns)	8.6	6.6	8.3
Average AAoA (deg)	48.5	54.2	0.6
RMS AAoA Spread (deg)	49.3	44.1	51.2

7. The angular resolution of 10 degrees is a bit too large, the authors can consider using a higher resolution in ray-tracing simulations, to compensate for it.

Re:

Thank you for your advice and we have considered a higher delay/angular resolution in the ray-tracing simulation. The angular resolution of the measured channel is only 10 degrees due to the performance limitations of the test system.

First, we compare the test and simulation channel at this resolution, and make the simulation results consistent with the test results by adjusting the simulation configuration parameters, such as the dielectric constant, conductivity and reflection order of the material, that is, the simulation channel can simulate the real channel under this condition. Then we improve the resolution of the simulation channel and study the change of channel similarity under different resolution. In addition, we added more comparison of simulation frequency and polarization.

8. Can the authors explain more about the maximum operation of \beta_i and \gamma_i? It is a bit difficult to understand now. How to determine the importance of weights?

Re:

We have improved our proposed similarity index and simplified the calculation steps. In the improved index system, some intermediate parameters and the subjective weight parameters are removed to derive a more objective and concise index. The previous maximum operation is replaced by pairwise pairing of the most similar subpaths within the two channels. In addition, the weights is set to equal if there is no special explanation.

9. The authors stated they use structural multipath information, actually, only delay and AAoA are used, in this way, the authors are suggested to compare to existing benchmark measures, such as MCD. Moreover, for MCD, it is also feasible to jointly consider delay and angular information, please double-check it.

Re:

Actually, the measure we propose in this manuscript are extended from the MCD. However, the existing MCD does not unify the measurement in each dimension. It only represents the distance between the subpaths and not the similarity between channels. The multipath parameter distance in this paper is inspired by MCD. On the one hand, coherence parameter distances are introduced based on the angular resolution and the delay resolution of the communication system, which also eliminates the dimensional differences in different dimensions, scaling the distance measure to within the range of 0 to 1. On the other hand, the distances of the subpaths are combined to derive the similarity of the two channels. The multidimensional MPC parameter distance is extensible and the candidate dimensions include but are not limited to the complex amplitude, delay, AoA, and AoD dimensions.

10. It is found that most values of CSIM are larger than 50%, which is because the authors compare the channels in the same environment. For more validation of efficiency, the authors can also compare different channel states in the same frequency.

Re:

Thank you for your advice on our work. The channels obtained in the different propagation environments are compared in subsection III-B. C_A and C_B are simulated channels obtained at the same RX location at 3 GHz and 37.5 GHz, respectively. The TX-RX distance is 8.3 m. C_C is another mmWave channel simulated at a relatively close distance of 5.1m. A comparison of CSIM(C_A, C_B) and CSIM(C_B, C_C) reveals that the channel difference caused by the location change is greater than that caused by the frequency change. Moreover, the environmental similarity is also analyzed in subsection IV-C.

11. The relationship between K factor and CSIM is not clear enough, it is better to illustrate its empirical relation by using figures.

Re:

We have added more descriptions about the relationship between the K factor and CSIM. The K factor is the ratio of the power of the direct ray (or for simplicity, the strongest ray) to the sum power of other reflection paths, reflecting the complexity of signal propagation in the channel. However, since the K factor, like other channel parameters, represents the characteristics of a specific channel, rather than the correlation between the two channels, the K factor measured at a certain frequency band cannot be directly associated with the CSIM. In the conference room environment,

the mean K factors are -0.4 dB, -0.6 dB, 3.7 dB, and 5.8 dB in the four frequency bands, less than those in the office campus environment, where the mean K-factors are greater than 6 dB. In other words, in each frequency band, the K factors in the conference room are greater than those in the office campus. The abundance of multipath in the conference room leads to a complex communication environment, and consequently, the site-specific frequency similarities are weaker, which are consistent with the results in subsection IV-A.

Moreover, we try to describe the relationship between the average K factor between the two frequency bands and their CSIM, as shown in Fig. R1. The x-coordinate represents the average K factor of all channels in the two frequency bands in the LoS/OLoS/NLoS scenario. For a given frequency pair, the statistical mean of the CSIM increases with the average K factor. For NLoS scenarios, the direct path is severely blocked and the multipath effect is obvious, which weakens the channel similarity. However, in the LoS scenarios, the K factor is usually large, and the channel similarities remain at a high level.

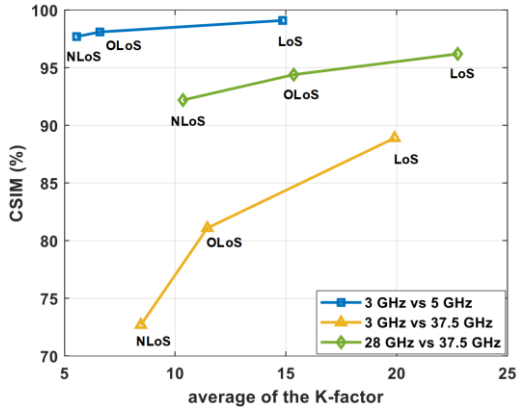

Fig. R1 Comparison of the average of the K-factor with the CSIM.

12. For the optimal beam shown in Fig. 6, does it correspond to the LoS case? For NLoS and OLoS, how to determine the optimal direction, because the peak does not mean the optimal transmission direction, right? It may be a strong reflection that we should avoid.

Re:

The low-resolution angle information provided by the low-frequency wide beam communication system is used to assist the narrow beam selection of the millimeter wave system, to reduce the beam searching cost and improve the communication capacity, which is an important requirement for us to utilize the similarity between different frequency bands.

We present three typical cases of optimal beam selection, including successful cases and two unsuccessful cases. For LoS scenarios, due to the strong similarity between the millimeter wave channels and the low-frequency channels, their strongest beam pointing is consistent, and we can easily find the best beam pointing with little computational overhead. The other two are typical unsuccessful cases. For the case in Fig. R2(b), the optimal beam direction has shifted due to the inconsistent angular resolution of the two communication systems. In this case, we only need to slightly increase the narrow beam search range of the millimeter wave system to find the best beam direction, that is to say, the spatial information provided by the low-frequency channel is still helpful for the beam selection. For the case in Fig. R2(c), which mainly happens in the NLoS or OLoS scenarios, the best beam provided by the low-frequency channel is precisely the strong reflection that needs to be avoided. This is the worst-case scenario, where the out-of-band information provides little or no effective help in beam selection.

We calculated the relationship between the beam search success rate and CSIM in Fig. R3. A reasonable beam search range threshold is provided to balance the beam search overhead and minimize the worst cases like Fig. R2(c).

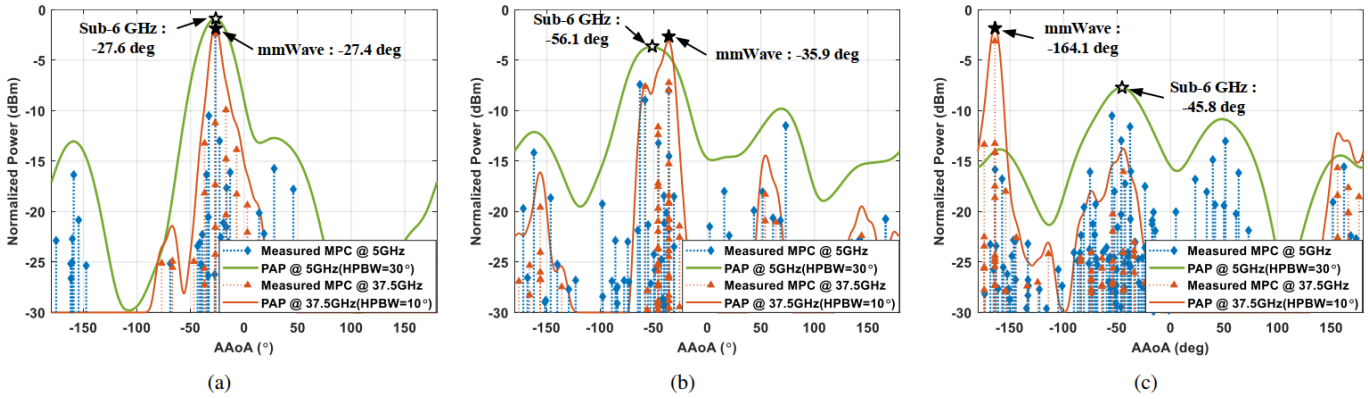

Fig. R2. Measurement-based analysis of AAoA dimensional channel similarity between 5 and 37.5 GHz, where the hollow and solid stars represent the optimal beam directions for sub-6 GHz and mmWave channels in the same RX location, respectively. (a) Successful case in the office campus environment; (b) Nonsuccessful case in the conference room environment; (c) Nonsuccessful case in the office campus environment.

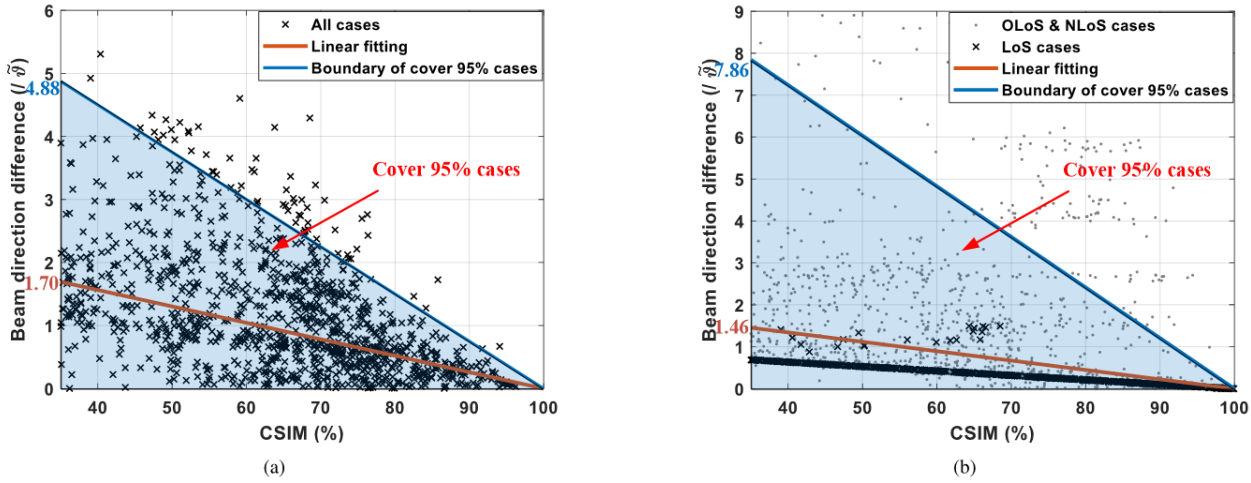

Fig. R3 Linear fittings of the beam direction difference vs CSIM between 5 and 37.5 GHz in (a) the conference room and (b) the office campus environment, where the black crosses and gray dots represent cases including simulated and measured results, the shaded area contains 95% of cases, and the red line is a linear fit for all cases.

13. When the authors consider a fixed angular resolution, the values of AAoA should be discrete? How to obtain continuous values should be clarified. The authors can explain more for the almost same results at 3 and 5 GHz in Fig. 9.

Re:

Due to the limitations of the hardware configuration and the measurement cost, the angular resolution is discretized to 10 degrees. To obtain continuous accurate angle information, there are two main schemes. One is to improve the spatial resolution of the channel sounder, such as rotating smaller angular intervals to collect channel data. In addition, super-resolution parameter estimation algorithms, such as SAGE, are used to estimate accurate angle information. However, this method will inevitably increase the measurement cost and parameter estimation complexity greatly. The second solution is to use simulation to compensate for the lack of the resolution in the measurement. The commercial ray tracing-based simulator Wireless InSite was applied in this paper to obtain the CIRs in multiple frequency bands. All simulation configurations are consistent with the measurement settings. The dimensions of the scenarios and the placement of the scatterers were recreated as much as possible in the simulator. In addition, the

machine learning-assisted calibration method was introduced to further fine-tune the simulation parameters to make the simulation channels more consistent with the measured channels.

Fig. R4 shows the CCDFs of the similarities between two propagation environments based on the channel characteristics. We not only improve our proposed index but also preprocess the channel data before calculation. All the channels are aligned based on the strongest path so that the differences in propagation delay due to the relative locations of the transceivers are excluded. Moreover, more sample combinations are added to the calculation to ensure that the results traverse all cases. We have added more descriptions of the results. "*Obviously, the similarities between the mmWave channels are less than those between the sub-6 GHz channels. An increase in the carrier frequency weakens the channel similarity. This is due to the multipath sparsity of the mmWave channels, highlighting the importance of the direct path (the strongest path), which can also be explained by the K factor. In higher frequency bands, especially in LoS scenarios, the mismatch of direct paths leads to a sharp decline in the similarity of the two channels, that is, the two channels tend to be orthogonal. The large variances of CSIMs indicate that the mmWave channels are easily affected by the propagation environment and the transceiver locations. The channel similarities obtained at different RX positions are quite different even in the same scenario. However, in the sub-6 GHz bands, the abundant multipath extends the incoming wave direction, which makes the channels have a higher correlation in the spatial domain. In other words, the channel similarity between the two propagation environments is weak at less than 50%.*"

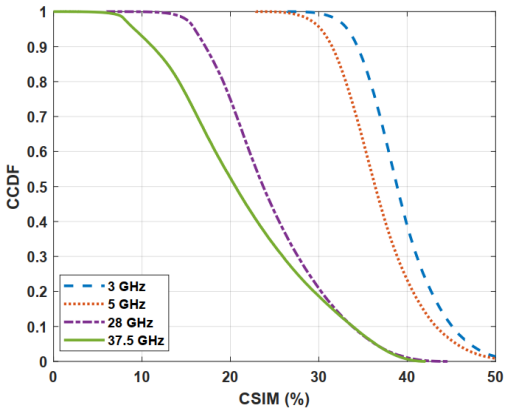

Fig. R4. Simulated CCDFs of the CSIM across different environments.

Reply to the Comments of Reviewer #2:

Comments:

1. The comparison between frequency bands should be performed in similar conditions of bandwidth and polarization. it is not understandable to me the use of horizontally polarized configuration during the mmWave channel measurements. The bandwidth used in the sounder should also would be similar or proportional to the frequency band. So, for lower frequencies, according to the bandwidth required to detect the multipath contributions, I would expect a bandwidth larger than 100 MHz.

Re:

Thanks for your comment. First, unfortunately, there is no bandwidth of more than 100 MHz available to us for the channel measurements. In the actual measurement environment, there are always interference signals in the low-frequency bands, including the cellular signals, the WiFi signals, or other experimental signals, so we need to find a clean spectrum near the target frequency band, which is often less than 100 MHz.

Second, we performed the comparison in the conditions of the same bandwidth. Due to the limitation of the actual bandwidth of the low-frequency channels, we extract the high-frequency signals to the uniform bandwidth of 100 MHz. This method ensures a fair comparison, but it also inevitably compromises the resolution in the multipath detection. On the one hand, the super-resolution parameter estimation algorithms, such as SAGE, were used to extract the effective paths; On the other hand, we set different and higher resolutions through ray tracing simulation to compensate for the limitation of the measured data. We also compare the distribution of the channel similarity under different resolutions.

Then, we performed the comparison in the conditions of the same polarization. The reason for using the horizontal polarization configuration in the millimeter wave measurements is that the pattern of the millimeter wave antenna is irregular. The H-plane beam width is more than 90 degrees, and more than that in the E-plane. When the TX antenna is placed horizontally polarized, the beam has a wider coverage on the horizontal plane and its coverage is comparable to that of the dipole antenna used for low-frequency measurement. Note that during the millimeter wave channel measurements, the RX antenna is also placed with horizontal polarization. Therefore, the measured channels are all co-polarized channels, which is consistent with the low-frequency measurement polarization configuration. In addition, we supplement the simulation of two polarized channels. The results show that the channel obtained is almost the same regardless of the polarization of the TX antenna, as long as the polarization configuration of the TX and RX antennas are the same.

2. Please, verify that with the sounder resolutions you can detect correctly both the LoS and the multipath contributions.

Re:

First, the channel measurements were conducted in multiple frequency bands by changing the corresponding radio frequency (RF) device using a commercial off-the-shelf (COTS) instrument-based flexible channel sounder. The details on the channel sounder can be found in [Li2019], [Zhang2021]. At the TX side, a high-performance vector signal generator (R&S SMW200A) is used to continuously transmit a binary periodic complementary Golay pair of length 4096. Compared with the widely used pseudonoise (PN) sequence, this Golay pair exhibits perfect complementary auto-correlation properties with more than 3 dB gain. At the RX side, a vector signal analyzer (R&S FSW50) is utilized for raw data acquisition. In addition, power amplifiers and low-noise amplifiers for all concerned bands are employed to extend the dynamic range of the channel sounder. During the measurements, two separate Rubidium (Rb) standard references are used at TX and RX for frequency synchronization with 10 MHz reference sources, as well as triggering data reception with 1 pulse per second (1PPS) signals. The calibration measurements connect transceiver RF front ends to calculate the system impulse responses, which have the advantage of minimizing the impact of the channel sounder on PDP analysis.

Then, the peak detection algorithm is used to estimate MPCs [Zhang2021], [Zhang2019]. A sliding window with a specific duration (usually 30 ns) is designed to compute the ratio of effective multipath components to all received paths from the end of PDP above the detection threshold. Moreover, the super-resolution parameter estimation algorithms, such as SAGE, were used to extract the effective paths.

Finally, ray tracing simulation was used to compensate for the lack of the high resolution in the measurement. The commercial ray tracing-based simulator Wireless InSite was applied in this paper to obtain the CIRs in multiple frequency bands. All simulation configurations are consistent with the measurement settings. The dimensions of the scenarios and the placement of the scatterers were recreated as much as possible in the simulator. In addition, the machine learning-assisted calibration method was introduced to further fine-tune the simulation parameters to make the simulation channels more consistent with the measured channels [Yi2024].

[Li2019] J. Li, P. Zhang, H. Wang, C. Yu, and W. Hong, “High-efficiency millimeter-wave wideband channel measurement system,” in *Proc. Eur. Conf. Antennas Propag. (EuCAP)*, Krakow, Poland, Apr. 2019, pp. 1–5.

[Zhang2021] P. Zhang, H. Wang, and W. Hong, “Radio propagation measurements and cluster-based analysis for 5G millimeter-wave cellular systems in dense urban environments,” *Front. Inf. Technol. Electron. Eng.*, vol. 22, pp. 1–16, July 2021.

[Zhang2020] P. Zhang, B. Yang, C. Yi, H. Wang, and X. You, “Measurement-based 5G millimeter-wave propagation characterization in vegetated suburban macrocell environments,” *IEEE Trans. Antennas Propag.*, vol. 68, no. 7, pp. 5556–5567, 2020.

[Zhang2019] P. Zhang, J. Li, H. Wang and X. You, "Millimeter-Wave Space-Time Propagation Characteristics in Urban Macrocell Scenarios," in *Proc. ICC 2019 - 2019 IEEE International Conf. Commun. (ICC)*, Shanghai, China, 2019, pp. 1-6, doi: 10.1109/ICC.2019.8761087.

[Yi2024] C. Yi, W. Chen, Q. Wu and H. Wang, "Machine Learning-Assisted Calibration for Ray-Tracing Channel Simulation at Centimeter-Wave and Millimeter-Wave Bands," *IEEE Antennas Wireless Propag. Lett.*, vol. 23, no. 5, pp. 1623-1627, May 2024, doi: 10.1109/LAWP.2024.3364243.

3. Also ellaborate on the polarization configurations and how the channels can be comparable even with different polarization configurations.

Re:

In the low-frequency channel measurements, the TX and RX antennas are vertically polarized, while in the millimeter wave channel measurements, the TX and RX antennas are horizontally polarized for wider coverage. Therefore, all the measured channels are co-polarized channels. In the channel simulation, to investigate the channel characteristics under different polarization conditions, we supplement the channel simulation under two polarization configurations, namely co-polarization and cross-polarization.

For the investigation of the channel frequency similarity, only the co-polarized channel data is used. For the comparison of cross-polarized channel similarity, we put these two polarized channels together and compare the parameters of the corresponding multipaths, mainly the amplitude, and finally obtain the similarity of the cross-polarized channel. The simulated CCDFs of the similarities between the two polarizations are shown in Fig. R5. The similarity between channels with different polarizations is relatively weak. The simulation results show that the maximum polarization similarity is less than 80%, and with the increase in frequency, the polarization similarity weakens both in the conference room and the office campus environment.

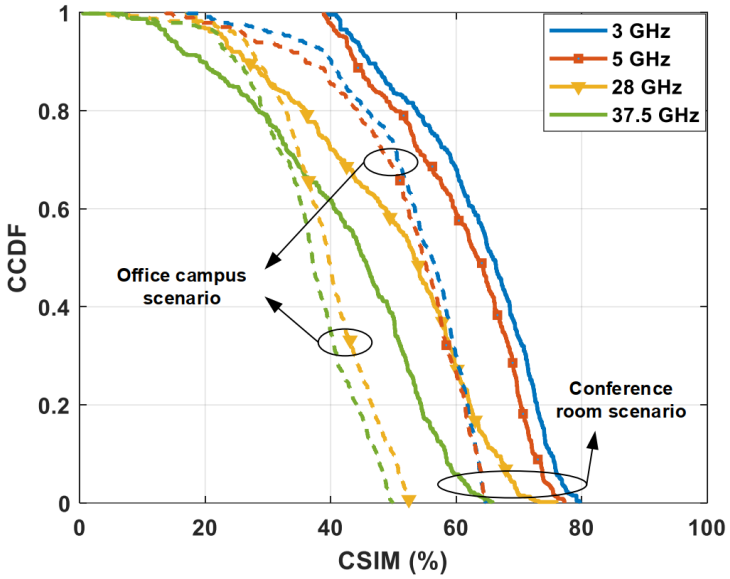

Fig. R5. Simulated CCDFs of the CSIM across different polarizations.

~~Multi-Frequency and Multi-Scenario Channel~~ Cross-Channel Similarity ~~Characterization~~ Analysis and Application Using a Multidimensional Structural ~~Multipath Information~~Measure

Cheng Yi, *Graduate Student Member, IEEE*, Peize Zhang, *Member, IEEE*, Haiming Wang, *Member, IEEE*, Cheng-Xiang Wang, *Fellow, IEEE*, and Xiaohu You, *Fellow, IEEE*

***Abstract*—To meet the ~~ever-increasing demands for coverage and data rate in~~ required full coverage and ultrahigh data rate demands of next-generation mobile communications, the coexistence of multiple radio frequency systems operating in well-separated frequency bands in precisely identified scenarios ~~will be exploitedin the long term~~must be exploited. In this context, ~~it is necessary to investigate~~ an investigation of frequency-dependent and environment-dependent channel characteristics by exploring the spatial and temporal correlations of multipath channels across ~~scenarios. A~~ different frequency bands and different environments is imperative. In this paper, a structural channel similarity index measure (CSIM) is proposed, which comprehensively considers ~~multidimensional~~ several multipath parameters of two different channels, including amplitude, phase, delay, angle of arrival (AoA), and angle of departure (AoD). Based on extensive ~~ray tracing simulations and~~ field measurement campaigns and ray tracing simulations conducted across both ~~the centimeter-wave and millimeter-wave~~ centimeter wave (cmWave) and millimeter wave (mmWave) bands in typical indoor and outdoor scenarios, the proposed CSIM is proven to effectively measure similarity ~~in specific dimensions , while its statistical distributionsrepresent~~ from specific dimensions as well as the statistical distributions, and the similarities between channels across different frequencies and different environments are presented. Moreover, the ~~cross-band CSIM can be applied to evaluate the feasibility of an~~ feasibility of out-of-band information-assisted beam search based on cross-band channel similarity is also validated.

***Index Terms*—Channel ~~characteristics, channel~~ similarity index measure (CSIM), channel ~~measurements~~characteristics, channel simulations ~~, centimeter-wave, millimeter-wave,~~ and measurements, multiband and multi-environment, beam search

Manuscript received ; revised ; accepted . Date of publication ; date of current . This work was supported in part by the National Natural Science Foundation of China under Grants 62271133 and 61960206006 and the Fundamental Research Funds for the Central Universities of China under Grant 2242022k60006. *(Corresponding author: Haiming Wang.)*

Cheng Yi and Haiming Wang are with the State Key Laboratory of Millimeter Waves, Southeast University, Nanjing 211189, China, and with the Pervasive Communication Research Center, Purple Mountain Laboratories, Nanjing 211111, China (e-mail: chengyi@seu.edu.cn, hmwang@seu.edu.cn).

Peize Zhang was with the State Key Laboratory of Millimeter Waves, Southeast University, Nanjing 211189, China, and is now with the Centre for Wireless Communications, University of Oulu, 90570 Oulu, Finland (e-mail: peize.zhang@oulu.fi).

Cheng-Xiang Wang and Xiaohu You are with the National Mobile Communications Research Laboratory, Southeast University, Nanjing 211189, China, and with the Pervasive Communication Research Center, Purple Mountain Laboratories, Nanjing 211111, China (e-mail: chxwang@seu.edu.cn, xhyu@seu.edu.cn).

Color versions of one or more of the figures in this paper are available online at http://ieeexplore.ieee.org.

Digital Object Identifier

I. Introduction

THE saturation of the spectrum in sub-6 GHz ~~frequency bands~~ band has made it impossible to meet the exploding demands for communication capacity and high transmission rates ~~[1]~~ [1], [2]. The development and utilization of higher frequency bands is considered ~~to be~~ an effective solution to this dilemma. The abundant unplanned spectrum resources in millimeter wave (mmWave) bands have attracted the enthusiastic attention of researchers worldwide [3]. On the one hand, by combining the capabilities of high-frequency and low-frequency systems, multiband communication systems show great promise for achieving both a breadth and depth of coverage compared with traditional single-frequency systems [4]. The wide range of frequencies spanned leads to different propagation mechanisms and gives rise to differences in channel characteristics. Radio waves in sub-6 GHz ~~frequency bands~~ band can achieve wider coverage ~~due to~~ because of their high diffraction and penetration performance, ~~while~~ whereas mmWave signals suffer from more serious path loss and blockage and can only be used for short-range coverage. Large-scale antenna arrays have thus been introduced to focus the energy in the desired directions, although ~~this approach greatly increases the system~~they greatly increase the system's hardware complexity as well as the computational overhead of signal processing. ~~On the one hand, by combining the capabilities of high-frequency (HF) and low-frequency (LF) systems, multiband communication systems show great promise for achieving both breadth and depth of coverage compared with traditional single-frequency systems [4]~~To reduce the training overhead of angle of arrival (AoA) estimation, several algorithms have been proposed that explore sub-6 GHz channel state information (CSI) to assist mmWave spatial correlation matrix estimation [5]–[8]. On the other

hand, the design of wireless communication systems and their wireless communication system design and coverage performance are strongly related to their deployment environments. The characteristics of mmWave channels mmWave channel characteristics are sensitive to the propagation environment, necessitating which requires accurate scenario recognition to meet the particular communication demands of dedicated communication demands in specific propagation environments. Therefore, we need to fully understand must fully clarify how the propagation characteristics change with the carrier frequency in the different propagation environments.

The radio propagation characteristics in the sub-6 GHz bands band have been extensively studied, and corresponding technologies are the corresponding systems have been widely used in the current commercial communication systems. At present, many studies have focused on the channel characteristics of the popular mmWave frequency bands, and many accurate or universal channel models have been proposed based on on the basis of both measured and simulated data [9]. Based on extensive measured channel data from typical indoor and outdoor scenarios in the bands of 28 GHz and 39 GHz bands, the frequency dependence of the path loss and the root mean square (RMS) angular spread was were discussed in [10] and [11]. In [3], a measurement-based mmWave propagation channel model for the range from 28 GHz to 73 GHz was presented. The propagation characteristics were modeled in multiple dimensions, including which included directional and omnidirectional channel models, temporal and spatial channel models, and outage probabilities. In addition, side-by-side comparisons of the propagation characteristics over a wide range of mmWave bands were provided. Many works have focused on channel simulations and measurements across multiple frequency bands and environments. However, the channel correlations in these works have been derived only they have derived channel correlations based on visual observation observations or statistical comparisons of the channel parameters [12], [13]. For example, in [14], channel measurements were conducted in the bands of 3.5 GHz and 28 GHz bands in indoor and outdoor scenarios to study the channel property differences between the microwave band and the mmWave band [14]. The Saleh–Valenzuela (S-V) model was chosen to analyze the statistical parameters of the clusters, such as the number of clusters, the intercluster interval, and the ray decay factor. The effects of the frequency and bandwidth on the decay factor were are discussed in detail. In [15], the authors carried out channel measurements in an indoor cubicle office and a conference room, using seven frequency bands ranging from 2.4to 61 –61 GHz. Based on the multipath parameter estimation results, frequency-dependent modeling of the path loss, shadow fading, the cross-polarization ratio, delay spread and angular spread was presented. However, these channel parameters can represent only the characteristics of a certain dimension of a particular channel but cannot establish a connection between two channels.

Intuitively, the similarity between HF and LF channels can be observed when the propagation environment and the transceiver configurations are the same. Based on similar channel information, a variety of cross-band cooperative transmission strategies have been proposed to reduce the training overhead of configuring the optimal links. In the frequency division duplexing (FDD) communication system, the spatial reciprocity of uplink and downlink channels in different frequency bands is used to assist the acquisition of downlink channel state information (CSI) according to the easily obtained uplink CSI [?], [?]. According to the measured results in [?], the uplink channels (1935 MHz) and the downlink channels (2125 MHz) have a high degree of spatial consistency, and the angular power spectrums (PASs) of the main path of the uplink and downlink channels are with a strong correlation, showing that such spatial parameters are independent of frequency. As the training time multiplies to align the narrower beams formed by the large-scale antenna arrays, using out-of-band information extracted from a high level of channel similarity between the mmWave and sub-6 GHz band channels has been proposed to help establish a mmWave link [5], [7]. The authors transformed the compressed beam-selection into a weighted sparse signal recovery problem, and proposed a customized structured precoder/combiner design based on the weighting information obtained from sub-6 GHz channels . In [6], an can be observed when the environment and the transceiver configurations are the same. Therefore, the question arises of exactly how similar they are, and to what degree of similarity can we use out-of-band covariance translation approach and an out-of-band aided compressed covariance estimation approach were proposed to predict the mmWave covariance and compress covariance estimation.

However, coarse out-of-band information may not necessarily contribute to CSI prediction, or even cause the opposite consequences. An imperfect estimate of the covariance will lead to the loss in the signal-to-noise ratio (SNR) [6]. Measurement analysis of failed cases where the LF beam information provides an adequate basis for the HF beam directions suggests that out-of-band information cannot be relied on blindly [16]. As the frequency increases, free space path loss, as well as the losses caused by reflection, penetration and diffraction increase frequency-dependently, weakening the correlation across different frequency bands. Moreover, the estimation algorithms show significantly different performance in different scenarios. Accurate scenario identification and classification play an important role in improving communication system efficiency and reliability [?], [?]. Thanks to the machine learning methods, a variety of channel characteristics can be extracted and synthesized to realize scenario identification [?], [?], [?], which is a subtle and complex approach. The dynamic propagation environments also increase the channel unpredictability.

In a word, channel similarity is a prerequisite for cross-band cooperative transmission algorithms. The questions arise of how to use the channel cross-band similarity as prior knowledge to guide the design of an out-of-band spatial information-assisted training strategy and at what level of channel similarity the cooperative algorithm can achieve stable prediction performance. The relationship between channel similarity and the availability of out-of-band information needs to be explored, as well as the influence of various factors, such

~~as the antenna array pattern, the complexity of the propagation environment, and whether the direct path is obstructed.~~

~~Therefore, a~~ . A specific index is needed to measure this similarity. The correlation coefficient, which reflects the degree of linear correlation between two variables, is a common index for evaluating the correlation between signals received at adjacent antenna units in MIMO systems [17]. However, the correlation coefficient is ~~evaluated only~~ only evaluated from a mathematical perspective, which is easily affected by noise, and cannot be measured comprehensively across multiple dimensions. Power profiles with similar correlation coefficients do not necessarily show similar differences. ~~Accordingly, more~~ The same deficiency is found in similarity evaluations of time series or images. When measuring the correlation of two time series, the trend of the series is introduced to compensate for the information lost by judging only by the Euclidean distance [18]–[20]. Compared with the mean square error (MSE) and the peak signal-to-noise ratio (PSNR), the structural similarity (SSIM) calculated based on the brightness and contrast of local patterns can better reflect the similarity between images from the structural perspective, which is more in line with the human perception of images [21], [22]. Consequently, inspired by this structural similarity, more physical characteristics of the propagation channels should also be considered ~~to evaluate~~ when evaluating two power profiles. The clustered delay line (CDL) channel model of the 3rd Generation Partnership Project (3GPP) [23], which is mainly used for link-level channel simulations, specifies a series of parameters, including the delays of clusters, the angles of departure (AoDs), the AoAs, the phases, and the amplitudes. These parameters determine the propagation characteristics with respect to the transceiver. The multipath component distance (MCD) [24] is ~~an index that is~~ one of the indices widely used in automatic multipath clustering algorithms [24]–[27] to quantify the separation between multipath components (MPCs). Furthermore, a channel similarity index measure was proposed in [28], in which the power delay profile is regarded as a time series~~and the propertiesof clusters~~, and cluster properties, such as the arrival time and decay rate, are ~~taken into account~~considered. Two spatial channel similarity metrics ~~were proposed in [16], [29] to explore~~ focused on exploring the feasibility of using ~~LF~~ sub-6 GHz channel information for coarse estimation of ~~HF beam directions~~ mmWave beam directions were proposed in [16], [29]. However, these metrics can ~~only be used~~ be used only for channel similarity ~~measurement~~ measurements in either the time domain or ~~the~~ angular domain, ~~not in~~ and not for all dimensions.

~~In this work, extensive channel simulation and measurement have been conducted across both the centimeter-wave and millimeter-wave (mmWave) bands in conference room and office campus scenarios. A~~ More importantly, how can channel cross-band similarity be used as prior knowledge to guide the design of the out-of-band spatial information-assisted beam search strategy, and at what level of channel similarity can the beam search algorithm obtain a stable prediction performance? The relationship between channel similarity and the availability of out-of-band information needs to be explored, as well as the influence of various factors, such as the antenna array pattern, the propagation environment complexity, and whether the direct path is obstructed.

In this work, a structural channel similarity index measure (CSIM) is proposed ~~based on~~ on the basis of multidimensional structural information. Not only can ~~this measure~~ it be used to compare the similarity between two specific channels, but its statistical characteristics can also reflect the similarity between different frequency bands and different propagation environments. Based on the proposed CSIM, the feasibility of out-of-band information-assisted beam search is also investigated~~from the propagation analysis perspective~~. The main contributions of this work are summarized as follows.

1) To ~~investigate frequency and environment-dependent channel characteristics, a large amount of multi-frequency and multi-scenario channel data have been collected. The transmitter (TX) and receiver (RX) locations are set the same in a certain scenario for a fair comparison. Ray-tracing based channel simulation is applied to assist in obtaining large amounts of full-dimensional channel data due to the huge cost of conducting extensive field measurements. Measured data obtained at four frequency bands from two scenarios are used to analyze the temporal and spatial channel characteristics in the actual communication environment.~~
2) ~~An objective CSIM is proposed to~~ reasonably and effectively evaluate the similarities of different channels in the form of numerical values, an objective CSIM is proposed, which accounts for the multidimensional structural information of the effective rays, including the complex amplitude, delay, AoA~~and AoD, as well as~~ , and AoD. The proposed structural CSIM can evaluate channel similarity from one or more dimensions.
3) The CSIM can be used to measure channel similarity under different transceiver configurations, considering the effects of delay resolution and angular resolution~~under different transceiver configurations~~. Its statistical characteristics can reflect ~~the similarity between channels across different frequency bands and different~~ channel similarity across different bands or environments.
4) Channel similarity is related to beam direction differences ~~for an investigation of~~ to investigate the feasibility of out-of-band information-assisted beam search strategies. The availability of out-of-band information depends on the complexity of the propagation environment, which is related to the ~~Rician~~ K factor.

The remainder of this paper is organized as follows. Section II presents extensive channel ~~simulations and measurements conducted in~~ measurements and simulations conducted at multiple bands in two ~~scenarios to collect~~ environments that collected a large amount of channel data ~~for use in~~ to use for analyzing the channel similarity. The proposed multidimensional CSIM is introduced in ~~section III. In section~~ Section II. In Section IV, the statistical distributions of the CSIM across multiple frequency bands and two ~~scenarios~~ environments are presented, as well as the feasibility of ~~an~~ out-of-band information-assisted beam search. Finally, ~~section~~ Section V

concludes the paper.

II. Channel ~~Simulation and~~ Measurement and Simulation Campaigns

Channel ~~simulations and measurements~~ measurements and simulations were conducted in multiple frequency bands in typical indoor and outdoor scenarios, i.e., a conference room and an office campus. The test frequencies ranged from the microwave band to the mmWave band, including 3 GHz, 5 GHz, 28 GHz, and 37.5 GHz. A large amount of channel data was obtained ~~through both simulations and measurements~~ from the measurements and simulations for channel similarity analyses. In this section, the propagation environments and the measurement and simulation configurations are described in detail, followed by ~~the parameter~~ data preprocessing and a channel characteristic analysis.

A. *Channel Measurements*

Using a commercial off-the-shelf (COTS) instrument-based flexible channel sounder [30], channel measurements were conducted in multiple frequency bands by changing the corresponding radio frequency (RF) device. Considering the limitations of the hardware configuration and the ~~methods of data preprocessing.~~ measurement cost, only channel state information (CSI) in the time domain and the AoA domain was detected and analyzed. For the mmWave channel measurements, high-gain horn antennas were used to receive spatial MPCs by rotating in the azimuth and elevation planes. The angle resolution was 10°, which is related to the half-power beam width (HPBW) of the receiving antennas and the rotary step size of the rotator. An open-ended waveguide antenna with an HPBW greater than 80° was employed for wide coverage on the transmitter (TX) side. For the sub-6 GHz channel measurements, dipole antennas were used on both the TX and receiver (RX) sides. To obtain the AoA, a virtual planar array of 8×8 elements was used by translating the dipole antenna at the RX. The TX and RX antennas were placed in both vertically and horizontally polarized configurations during the channel measurements. The detailed specifications can be found in Table III. GPS-disciplined rubidium standard references were used for precise clock synchronization. Before the measurements, the system impulse response was calculated by physically connecting the RF ports of the TX and RX.

B. ~~*Channel Simulations*~~

~~Simulated PDPs and PAPs. PDPs; PAPs. Here, $\mathcal{C}_{\mathrm{A}}$ and $\mathcal{C}_{\mathrm{B}}$ were obtained from the same RX location in different frequency bands, and $\mathcal{C}_{\mathrm{B}}$ and $\mathcal{C}_{\mathrm{C}}$ were obtained from different RX locations, both at 37.5 GHz.~~

~~The commercial ray tracing-based simulator Wireless InSite was applied to obtain the channel impulse responses (CIRs) in multiple frequency bands. As shown in~~ Fig. 1 ~~,~~ depicts the layouts of the TX and RX locations in the typical indoor and outdoor scenarios~~were considered~~. The dimensions of the conference room are $11.7 \times 9.0 \times 3.0$ m^3. In the conference room, there are several pieces of typical office furniture, such as metal cabinets, wooden desks, and leather chairs. The height of the desks is approximately 0.8 m. On the desktops, there are some office supplies and experimental equipment. The walls are made of concrete, glass, and wood. The metal cabinets and ~~the~~ railings next to the floor-to-ceiling windows are the main ~~reflectors. The dimensions of the conference room and the placement of the office furniture were recreated as much as possible in the simulator. The TXs were placed in the same location, close to the door in the northwest corner and~~ scatterers. In this scenario, the TXs were fixed in the northwest corner of the conference room at a height of 2.6 m~~, in the multifrequency channel simulations. The RXs, a total of 2240, were distributed uniformly over a rectangular area with a spacing of 0.2 m to simulate the channel conditions throughout the space. The RX height was~~ . Twenty-nine RX locations were selected, with fixed spacings of 1 m and 1.3 m. The height of the RX antennas was set to 1.8 m, ~~slightly higher~~ which is slightly greater than the desktop height, ~~in keeping with the height of the channel sounder used in the field measurements~~so all the measured TX–RX location pairs corresponded to the line-of-sight (LoS) scenario. The outdoor scenario is a typical office campus surrounded by buildings ~~of~~ 9–18 m in height. The roads on the office campus are lined with evergreen camphor trees with thick branches and leaves. The average tree height is approximately 8 m. There are ~~some~~ several winding paths and bushes in the roadside flower beds. ~~The~~ In this scenario, the TX antennas were deployed on ~~top of the lower building to the south~~ the roof of the building at a height of 12.3 m, with ~~a downtilt of 15°. Three sets of RXs~~ the beam pointing into the middle of the canyon. Dozens of typical RX locations were selected along the three routes, including 8 LoS TX–RX pairs, 45 obstacle-LoS (OLoS) TX–RX pairs obstructed by foliage, and 6 non-LoS (NLoS) TX–RX pairs blocked by the building. The TX–RX separation distances varied from 20 m to 85 m, and the spacing of the RX locations along each route was 2 m.

Measurements were carried out at the 3 GHz, 5 GHz (specifically, 5.4 GHz in the indoor scenario and 4.8 GHz in the outdoor scenario due to the interference signals encountered during the measurements), 28 GHz and 37.5 GHz

TABLE I
Multifrequency Channel Measurement Specifications

Parameter		Value			
Carrier Frequency (GHz)		3	5	28	37.5
Bandwidth (MHz)		100		100	300
TX Antenna	Gain (dBi)	2.0		6.0	6.5
	E-plane HPBW (°)	60		102	80
	H-plane HPBW (°)	360		63	55
RX Antenna	Gain (dBi)	2.0		26.2	27.5
	E-plane HPBW (°)	60		10	
	H-plane HPBW (°)	360		10	
RX Rotation Range in Azimuth (°)		/		0 ∼ 350	
RX Rotation Range in Elevation (°)		/		50 ∼ 120	
RX Rotation Step (°)		/		10	

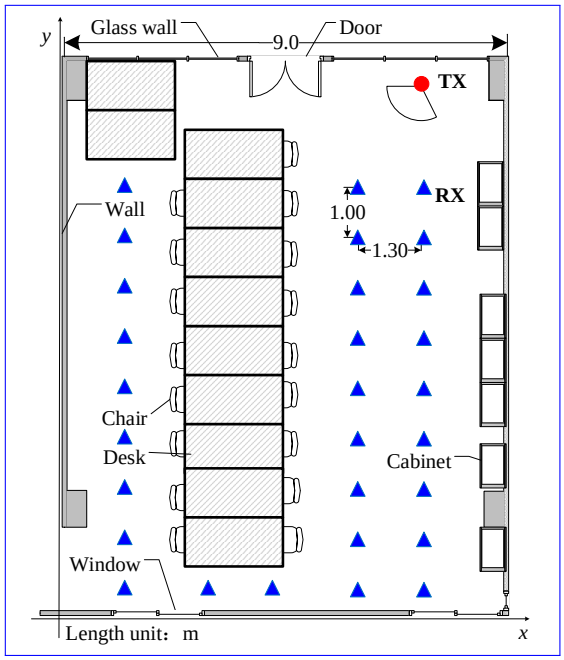

(a)

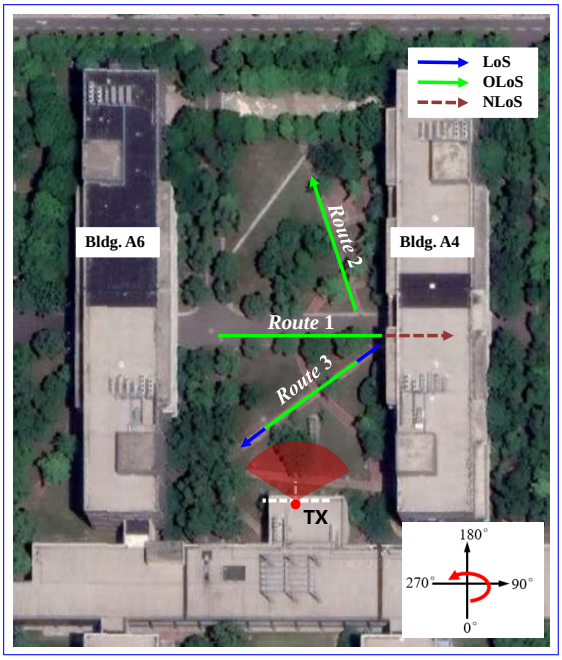

(b)

Fig. 1. Layouts of (a) the conference room scenario and (b) the outdoor office campus scenario.

bands. A simplified peak detection algorithm [11] is proposed here to estimate MPCs. For the direction-scan measurement method, the angular power spectrum (APS) can be obtained in accordance with the received power of the directional channel. For simplicity, the angular resolution of the MPCs is considered 10° since standard gain horn antennas with an HPBW of 10° were adopted. For the sub-6 GHz channel measurements, the SAGE algorithm [31], [32] is used to accurately estimate the MPCs.

B. Channel Simulations

To compensate for the resolution limitations in the channel measurements, the commercial ray-tracing-based simulator Wireless InSite was applied to obtain higher-resolution CIRs in multiple frequency bands. All the simulation configurations are consistent with the measurement settings. The dimensions of the scenarios, and the placement of the scatterers, were recreated as much as possible in the simulator. In the conference room, the TXs were placed in the same location in the northwest corner in the multifrequency channel simulations at a height of 2.6 m. A total of 2240 RXs were distributed uniformly over a rectangular area with a spacing of 0.2 m to simulate the channel conditions throughout the space. The RX height was 1.8 m, which is consistent with the height of the channel sounder used in the field measurements. In the office campus, the TX antenna was deployed on top of the southern building. Three RX sets along the roads (*Route 1*, *Route 2* and *Route 3*) were selected, ~~comprising~~ including 3168 RX locations with a spacing of 0.5 m. Due to ~~shading by~~ the shading of the vegetation, most communication links are ~~obstructed LoS (OLoS)~~ OLoS links, which are ~~mainly distributed~~ distributed mainly along *Route 1* and *Route 2* and in the middle of *Route 3*. The remaining links are LoS links at both ends of *Route 3* and ~~non-LoS (NLoS)~~ NLoS links along *Route 1* extending to the corridor in the building.

~~Simulations were carried out in the 3 GHz, 5 GHz (specifically, 5.4 GHz for the indoor scenario and 4.8 GHz for the outdoor scenario), 28 GHz and 37.5 GHz bands. Because of the interference signals encountered during LF channel measurements, it was necessary to select suitable candidate frequency bands for the two scenarios individually.~~ The antennas used in the simulations ~~were directional~~are horn/~~omnidirectional~~ dipole antennas with the same ~~half-power beamwidths (HPBWs)~~ HPBWs as the measurement antennas used in the corresponding frequency ~~bands~~band. Note that the material properties, including the relative permittivity and conductivity, were updated with the carrier frequency in accordance with the ITU recommendations [33]. The transmit power was uniformly set to 0 dBm~~. The~~ , and the receiver sensitivity was set to -250 dBm to ensure that sufficient paths could be received. Based on previous research on the simulation depth, the orders of ~~the~~ three propagation mechanisms, i.e., reflection, transmission, and diffraction, were set to $[6, 2, 2]$ ~~to achieve a suitable~~ for a trade-off between the accuracy of the simulation results and the time consumption. ~~Using the ray-tracing-based simulator, the detailed parameters of each ray could~~ In addition, the machine learning-assisted calibration method was introduced to further fine-tune the simulation parameters to make the simulation channels more consistent with the measured channels [34] . Using the ray-tracing-based simulator, more simulation results at multiple frequency bands, different delay/angular resolutions, and polarization configurations can be obtained directly ~~.~~

~~The normalized power delay profiles (PDPs)and power angle profiles (PAPs)of three simulated channels in the conference room scenario are presented in Fig. 3. $\mathcal{C}_{\mathrm{A}}$ and $\mathcal{C}_{\mathrm{B}}$~~

TABLE II
MULTIFREQUENCY CHANNEL SIMULATION CONFIGURATIONS

Parameter	Value
Carrier Frequency (GHz)	3, 5, 28, 37.5
Bandwidth (MHz)	100, 300, 1000
Angular resolution (°)	1, 10, 20, 30, 40, 50, 60
Polarization	co- and cross-polarization
Reflection order	6
Transmission order	2
Diffraction order	2

~~are simulated channels obtained from the same RX location at~~ for more in-depth comparative investigations. The detailed simulation configurations are listed in Table II.

C. *Channel Characteristic Analysis*

The RMS delay spread and RMS angular spread are channel characteristic parameters used to measure the dispersion of the ~~sub-6 GHz channel in both the time domain and the spatial domain, with the number of MPCs being approximately one-third of that of the sub-6 GHz channel, and there are fewer subpaths in the clusters. However, the~~ signal in the time domain or the angle domain. The RMS delay spread and RMS angular spread measured at the specific RX position across multiple frequency bands are depicted in Fig. 2. An obvious trend is that the channel dispersion characteristics decrease with increasing carrier frequency. A comparison of the results of these two scenarios reveals that the RMS delay spread measured in the conference room scenario is smaller than that measured in the office campus scenario, but the conclusion of the RMS angular spread is the opposite. This is mainly due to the distinctive propagation environments. In the conference room scenario, the signals pass through the surrounding walls or internal objects to reach the receiver. The incoming directions of the ~~reflected rays are still abundant in the indoor scenario. In a comparison between $\mathcal{C}_{\mathrm{A}}$ and $\mathcal{C}_{\mathrm{B}}$, whose propagation environments are exactly the same, almost all of the rays in $\mathcal{C}_{\mathrm{B}}$ are found to have corresponding rays in $\mathcal{C}_{\mathrm{A}}$, except for differences in the normalized power. In other words, $\mathcal{C}_{\mathrm{A}}$ almost 'contains' $\mathcal{C}_{\mathrm{B}}$.~~

D. ~~*Channel Measurements*~~

~~Using a commercial off-the-shelf (COTS) instrument-based flexible channel sounder [30], channel measurements were conducted in multiple frequency bands by changing the corresponding radio frequency (RF) device. Considering the limitations of the hardware configuration and the measurement cost,~~ scattering paths are rich, and their powers are relatively strong, so the signal energy is concentrated in the time domain and dispersed in the ~~CSI was detected and analyzed only in~~ angle domain. In addition, these dispersion parameters do not vary dramatically because of the similar propagation environments in the conference room scenario. The office campus scenario is wide open, and the internal environment varies, showing different channel characteristics at different RX positions. The scattering paths take longer to travel to the RXs, and they tend to be weaker in power. The channels are relatively sparse both in the time domain and the ~~azimuth AoA (AAoA)~~ angle domain. For the ~~mmWave channel measurements, high-gain horn antennas were used to receive spatial MPCs by rotating in the azimuth and elevation planes. The angular resolution was 10°, which is related to the HPBW of the receiving antennas and the rotary step size of the rotator. An open-ended waveguide antenna with an E-plane HPBW greater than 80° was employed for wide coverage on the TX side. The TX and RX antennas were placed in a horizontally polarized configuration during the mmWave channel measurements.~~ LoS channels, the RMS delay spread and RMS angular spread are small, but the RMS delay spread is still larger than that in the conference room scenarios. Owing to the blockage effect, the degree of dispersion in both the time domain and the angle domain also increases. For the ~~sub-6 GHz channel measurements, dipole antennas were used on both the TX and RX sides. To obtain the AAoA, a virtual planar array of 8×8 elements was constructed by translating the dipole antenna at the RX. The detailed specifications can be found in Table III. GPS-disciplined rubidium standard references were used for precise clock synchronization. Before the measurements, the system impulse response was calculated by physically connecting the RF ports of the TX and RX~~channels measured along *Route 2*, the strong reflection paths from the backward glass curtain wall result in a greater delay and angular spread.

TABLE III
MULTIFREQUENCY CHANNEL MEASUREMENT SPECIFICATIONS

Parameter		Value			
Carrier Frequency (GHz)		3	5	28	37.5
Bandwidth (MHz)		100		100 300	
TX Antenna	Gain (dBi)	2.0		6.0	6.5
	E-plane HPBW (°)	60		102	80
	H-plane HPBW (°)	360		63	55
RX Antenna	Gain (dBi)	2.0		26.2	27.5
	E-plane HPBW (°)	60		10	
	H-plane HPBW (°)	360		10	
RX Rotation Range in Azimuth (°)		/		$0 \sim 350$	
RX Rotation Range in Elevation (°)		/		$50 \sim 120$	
RX Rotation Step (°)		/		10	

~~Fig. 1 depicts the layouts of the TX and RX locations, with red dots representing the TXs. In the conference room scenario, the TXs were fixed in the northwest corner of the conference room at a height of 2.6 m, consistent with the simulation setup. Twenty-nine RX locations (represented by blue triangles in Fig. 1(a)) were selected, with fixed spacings of 1 m and 1.3 m. The height of the RX antennas was set to 1.8 m; as a result, all measured TX–RX location pairs~~

However, channel parameters characterize the characteristics of a particular channel rather than the connection between two channels. On the one hand, these parameters only show the frequency dependence of the propagation characteristics, and we still cannot explore

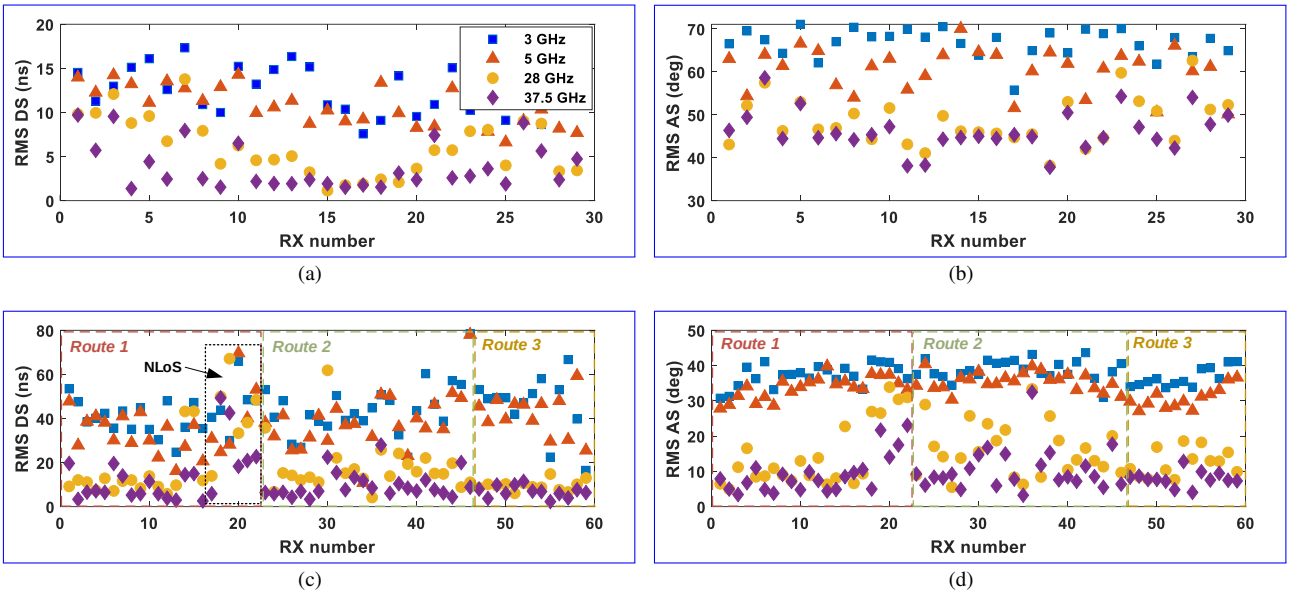

Fig. 2. Measured (a) RMS delay spread and (b) RMS AAoA spread in the conference room scenario and measured (c) RMS delay spread and (d) RMS AAoA spread in the office campus scenario.

the detailed characteristics of the channels across different frequencies on the basis of these parameters alone. On the other hand, channels in different propagation environments may have similar channel parameters, and more parameters are needed to characterize and distinguish them. For example, the normalized power delay profiles (PDPs) and power angle profiles (PAPs) of three simulated channels in the conference room ~~corresponded to the LoS scenario~~ scenario are presented in Fig. 3, as are the channel parameters listed in Table **??**. $\mathcal{C}_{\rm A}$ and $\mathcal{C}_{\rm B}$ are simulated channels obtained at the same RX location at 3 GHz and 37.5 GHz, respectively. The TX-RX distance is 8.3 m. ~~In the outdoor office campus scenario,~~ $\mathcal{C}_{\rm C}$ is another mmWave channel simulated at a relatively close distance of 5.1 m. The MPCs of the mmWave channels are sparser than those of the sub-6 GHz channel in both the time domain and the spatial domain, with the number of MPCs being approximately one-third of that of the ~~TX antennas were deployed on the roof of the building, with the beam pointing into the middle of the canyon. Dozens of typical RX locations were selected along the three routes, including 8 LoS TX–RX pairs, 45 OLoS TX–RX pairs obstructed by foliage, and 6 NLoS TX–RX pairs blocked by the building. The TX–RX separation distances varied from 20 mto 85 m, and the spacing of the RX locations along each route was 2 m.~~

~~A simplified peak detection algorithm [11] is adopted here to estimate the MPCs . With the direction-scan measurement method, the angular power spectrum (APS) can be obtained in accordance with the received power of each directional channel. For simplicity, the angular resolution of the MPCs is considered to be 10° since standard gain horn antennas with an HPBW of 10° were adopted. For the~~ sub-6 GHz channel~~measurements, the SAGE algorithm [31], [32] is used to accurately estimate the MPCs~~ , and there are fewer MPCs in the clusters. However, ~~due to the limitations of the virtual planar arrays used at the RXs and~~ the ~~E-plane HPBW of 60° of the dipole antennas,~~ incoming directions of the reflected rays are still abundant in the indoor scenario. Note that $\mathcal{C}_{\rm A}$ and $\mathcal{C}_{\rm C}$ have similar delay/angular spreads, but they do have obvious differences. Thus, more parameters, such as the average delay and average AoA, are needed for further characterization. In a comparison between $\mathcal{C}_{\rm A}$ and $\mathcal{C}_{\rm B}$, whose propagation environments are exactly the same, almost all of the ~~angular resolution is very low on the elevation plane, and only the AAoA is considered in the angular domain.~~ rays in $\mathcal{C}_{\rm B}$ can be found to have corresponding rays in $\mathcal{C}_{\rm A}$, except they have a difference in the normalized power. However, these channel parameters do not intuitively reflect this similarity.

III. Channel Similarity Analysis

Based on the analysis in subsection II-C, a single channel parameter is not enough to represent a specific channel, let alone reflect the connection between two channels. Therefore, if one wants to use the known channel information to infer an unknown channel, a novel measure is needed to associate these two channels. In this section, a channel similarity index named the CSIM is proposed ~~on the basis of an~~ according to the improved multipath parameter distance. The similarity of any two channels in one or more dimensions can be measured by a numerical value, and the time/angular resolutions are also accounted for.

A. Channel Similarity Index Measure (CSIM)

~~When a radio wave travels through a variety of scatterers on multiple paths to reach the RX, the CIR~~ The channel similarity can be decomposed into the similarities of several MPC pairs, which are defined in terms of the parameter distance in different dimensions. The CIR $h(t)$ can be represented as a multidimensional function of the channel parameters, including the complex amplitude ~~(amplitude α and phase ϕ)~~, the delay τ, the ~~AAoA $\varphi_{\rm r}$, the elevation~~ AoA ~~(EAoA)$\theta_{\rm r}$, the~~

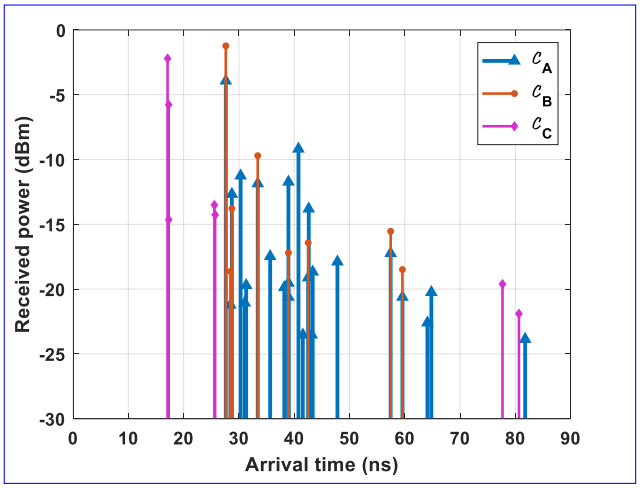

(a)

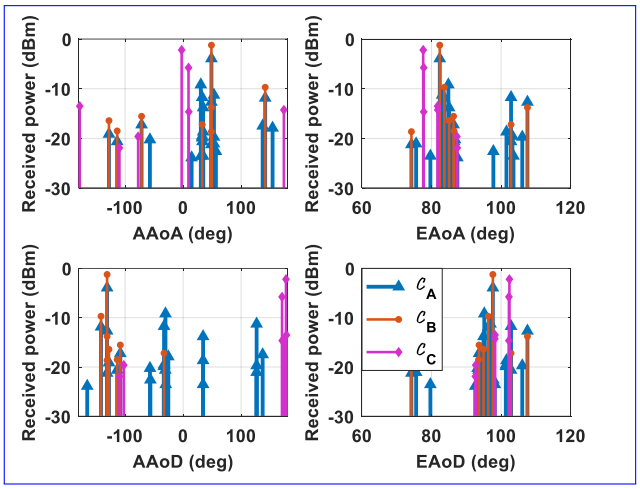

(b)

Fig. 3. Simulated PDPs and PAPs. (a) PDPs; (b) PAPs. Here, $\mathcal{C}_A$ and $\mathcal{C}_B$ are obtained from the same RX location in different frequency bands, and $\mathcal{C}_B$ and $\mathcal{C}_C$ are obtained from different RX locations at 37.5 GHz.

~~azimuth AoD (AAoD) φ_t~~Φ_R (including the azimuth AoA φ_R and the elevation AoA θ_R), and the AoD Φ_T (including the azimuth AoD φ_T and the elevation AoD ~~(EAoD)θ_t~~: θ_T):

$$h(t) = \sum_{i}^{L} \alpha_i \delta(\tau - \tau_i)\delta(\Phi_R - \Phi_{R,i})\delta(\Phi_T - \Phi_{T,i}), \quad (1)$$

where L is the number of MPCs. These parameters set each specific MPC apart from the others and eventually give rise to a unique channel. The parametric multipath channel can be represented by $\mathcal{C} = \{\Theta_1, ..., \Theta_L\}$, where ~~$\Theta_i = \{\alpha_i, \phi_i, \tau_i, \varphi_{r,i}, \theta_{r,i}, \varphi_{t,i}, \theta_{t,i}\}$~~ $\Theta_i = \{\alpha_i, \tau_i, \Phi_{R,i}, \Phi_{T,i}\}$ ($1 \le i \le L$ ~~,~~and where $i \in \mathbb{Z}$) represents the parameters of the ith MPC.

~~To design an index that can measure the degree of subpath structural similarity between two channels~~ Suppose that $\mathcal{C}_X$ and $\mathcal{C}_Y$ are two channels to be compared, with the detected MPCs of L_X and L_Y, respectively. $\Theta_{i,X}$ and $\Theta_{j,Y}$ represent the parameter sets of the ith MPC in $\mathcal{C}_X$ and the jth MPC in $\mathcal{C}_Y$. The multidimensional MPC parameter distance $d(\Theta_{i,X}, \Theta_{j,Y})$ can be synthesized as a Euclidean distance on the candidate dimensions as follows:

$$d(\Theta_{i,X}, \Theta_{j,Y}) = \sqrt{\frac{1}{N}({d_{\alpha_{ij}}}^2 + {d_{\tau_{ij}}}^2 + {d_{\Phi_{R},ij}}^2 + {d_{\Phi_{T},ij}}^2 + \ldots)}, \quad (2)$$

where N is the number of selected dimensions. The multidimensional MPC parameter distance is extensible, and the candidate dimensions include, but are not limited to, the complex amplitude, delay, AoA, and AoD dimensions, corresponding to distances $d_{\alpha_{ij}}$, ~~all of these parameters need to be considered, not only numerically but also physically. Before the comparisoncan be performed~~$d_{\tau_{ij}}$, $d_{\Phi_{R},ij}$ and $d_{\Phi_{T},ij}$.

Before comparison, power normalization and a unified coordinate system are ~~needed~~ required to exclude the ~~influence of the~~ system gain and facilitate fair comparisons. To simplify the calculation, a reasonable threshold should be set to extract only MPCs with power levels greater than this threshold while ignoring small signals. Then, the total power of all effective MPCs is normalized to 0 dBm.

~~Suppose that $\mathcal{C}_X$ and $\mathcal{C}_Y$ are two channels to be compared. $\Theta_{i,X}$ $(1 \le i \le L_X,\ i \in \mathbb{Z})$ and $\Theta_{j,Y}$ $(1 \le j \le L_Y,\ j \in \mathbb{Z})$ represent the parameter sets of the ith MPC in $\mathcal{C}_X$ and the jth MPC in $\mathcal{C}_Y$, respectively. L_X and L_Y are the numbers of MPCs in $\mathcal{C}_X$ and $\mathcal{C}_Y$, respectively.~~ An improved MCD is proposed to calculate the multidimensional channel parameter distances. ~~Coherent~~ Coherence parameter distances are introduced ~~based on the~~ on the basis of the angular resolution and the delay resolution of the communication system, ~~thereby eliminating~~ which also eliminate the dimensional differences in different dimensions~~and~~ , scaling the distance measure to within the range of 0 to 1. Specifically, the distances ~~$d_{\tau_{ij}}$, $d_{\Phi_{r,ij}}$ and $d_{\Phi_{t,ij}}$ in the time, AoA and AoD dimensions, respectively,~~ $d_{\alpha_{ij}}$, $d_{\tau_{ij}}$ and $d_{\Phi_{R(T),ij}}$ are defined as~~follows:~~ :

$$d_{\tau_{ij}\alpha_{ij}} = \frac{1}{2}\left\|\alpha_i - \alpha_j\right\|_2, \quad (3)$$

$$d_{\Phi_{r,ij}\tau_{ij}} = \begin{cases} \frac{|\tau_i - \tau_j|}{\widetilde{\tau}}, & |\tau_i - \tau_j| \le \widetilde{\tau}, \\ 1, & \text{otherwise}, \end{cases} \quad (4)$$

$$d_{\Phi_{t,ij}\Phi_{R(T),ij}} = \begin{cases} \frac{\Delta_{R(T)}}{\min(\widetilde{\vartheta}_{R(T)}, \pi)}, & \Delta_{R(T)} \le \min\left(\widetilde{\vartheta}_{R(T)}, \pi\right), \\ 1, & \text{otherwise}, \end{cases} \quad (5)$$

where ~~$\tau_{i(j)}$ represents the arrival time of the corresponding MPC in $\mathcal{C}_{X(Y)}$ and $\Phi_{r,i(j)}$ and $\Phi_{t,i(j)}$ are the steering vectors formed by the AoA and AoD, respectively. $\langle \Phi_{r(t),i}, \Phi_{r(t),j} \rangle$ is the spatial angle between the vectors $\Phi_{r(t),i}$ and $\Phi_{r(t),j}$, calculated as $\langle \Phi_{r(t),i}, \Phi_{r(t),j} \rangle = \arccos\left(\frac{\Phi_{r(t),i}\Phi_{r(t),j}}{\|\Phi_{r(t),i}\|\|\Phi_{r(t),j}\|}\right)$.~~ $\|\cdot\|_2$ represents the Euclidean norm and $\Delta_{R(T)} = \langle \Phi_{R(T),i}, \Phi_{R(T),j} \rangle$ is the space angle formed by $\Phi_{R(T),i}$ and $\Phi_{R(T),j}$. $\widetilde{\tau}$ represents the ~~value of the~~ least distinguishable delay, which is related to the signal bandwidth~~and is equal~~ , and is set to the average delay resolution of the channels to be compared~~, and $\widetilde{\vartheta}_{r(t)}$~~.

$\widetilde{\vartheta}_{\mathrm{R(T)}}$ is the average angular resolution on the RX~~(TX)~~/TX side, representing the least distinguishable angle. ~~It can be intuitively understood that~~ Intuitively, under a unified coordinate system, two MPCs are considered ~~to be~~ similar if the beams formed by them overlap in ~~space and time, and their~~ the space-time range, and the degree of similarity is linearly related to the parameter distance.

~~Once the power levels of the MPCs have been normalized, the normalized amplitudes are between 0 and 1. Then, the distance $d_{\alpha_{ij}}$ in the complex amplitude dimension can be defined as the modulus of the difference between the vectors corresponding to the two complex amplitudes:~~

$$d_{\alpha_{ij}} = \frac{1}{2}\left\|\Omega_i - \Omega_j\right\|_2,$$

~~where $\Omega_{i(j)} = [\alpha_{i(j)}\cos\phi_{i(j)}, \alpha_{i(j)}\sin\phi_{i(j)}]^{\mathrm{T}}$. More often than not, we tend to focus on the absolute value of the amplitude or power, ignoring its phase. Therefore, the phase can be set to a fixed value; then, the actual range of $d_{\alpha_{ij}}$ will be from 0 to 0.5. This is reasonable because we impose consistency in one dimension, thereby narrowing the distance between the two MPCs. Accordingly, based on the different levels of importance of the dimensions of concern, the multidimensional channel parameter distance between the ith MPC in $\mathcal{C}_{\mathrm{X}}$ and the jth MPC in $\mathcal{C}_{\mathrm{Y}}$ can be synthesized as a weighted Euclidean distance as follows:~~

$$d(\Theta_{i,\mathrm{X}}, \Theta_{j,\mathrm{Y}}) = \sqrt{w_\alpha d_{\alpha_{ij}}^2 + w_\tau d_{\tau_{ij}}^2 + w_{\Phi_\mathrm{r}} d_{\Phi_\mathrm{r},ij}^2 + w_{\Phi_\mathrm{t}} d_{\Phi_\mathrm{t},ij}^2}, \quad (6)$$

~~where w_α, w_τ, w_{Φ_r} and w_{Φ_t} represent the weights for the dimensions of the normalized complex amplitude, arrival time, AoA and AoD, respectively, and satisfy $w_\alpha + w_\tau + w_{\Phi_\mathrm{r}} + w_{\Phi_\mathrm{t}} = 1$. In general, we set the weights for the nontarget dimensions to 0 and then set the weights for the other dimensions to be equal.~~ The smaller the value of ~~d_{ij}~~ $d(\Theta_{i,\mathrm{X}}, \Theta_{j,\mathrm{Y}})$ is, the more similar the two ~~rays~~ MPCs are. The value of ~~d_{ij}~~ $d(\Theta_{i,\mathrm{X}}, \Theta_{j,\mathrm{Y}})$ is equal to 0 only if the two MPCs are exactly the same ~~in~~ on the target dimensions. Conversely, the ~~subpath~~ MPC similarity is defined as~~follows:~~ :

$$s_{ij} = 1 - d(\Theta_{i,\mathrm{X}}, \Theta_{j,\mathrm{Y}}) \in [0, 1]. \quad (7)$$

~~For the jth MPC in $\mathcal{C}_{\mathrm{Y}}$, we traverse all~~ According to the maximum s_{ij}, the MPCs in $\mathcal{C}_{\mathrm{X}}$ ~~to find that with the smallest parameter distance as the most similar MPC . Then, the similarity of~~ and $\mathcal{C}_{\mathrm{Y}}$ ~~with respect to $\mathcal{C}_{\mathrm{X}}$ is defined~~ are pairwise matched into L_{match} pairs, which form a set $\mathbb{M}$. Considering the contribution of the MPC power to the total channel power, the channel similarity CSIM is finally derived as the power-weighted average similarity, that is,~~:~~

$$s_{\mathrm{Y}\to\mathrm{X}} = \sum_{j=1}^{L_\mathrm{Y}} |\alpha_j|^2 \max(\beta_j), \quad (8)$$

$$\mathrm{CSIM}(\mathcal{C}_\mathrm{X}, \mathcal{C}_\mathrm{Y}) = \frac{1}{2}(s_{\mathrm{Y}\to\mathrm{X}} + s_{\mathrm{X}\to\mathrm{Y}}) = \frac{1}{2}\left(\sum_{j=1}^{L_\mathrm{Y}} |\alpha_j|^2 \max(\beta_j) + \sum_{i=1}^{L_\mathrm{X}} |\alpha_i|^2 \max(\gamma_i)\right) \times 100\%. \quad (9)$$

~~where $\beta_j = [s_{1j}, s_{2j}, \cdots, s_{L_\mathrm{X}j}]$ represents the set of subpath similarities between the jth MPC in $\mathcal{C}_\mathrm{Y}$ and each MPC in $\mathcal{C}_\mathrm{X}$. $|\alpha_j|^2$ is~~

B. Cross-Channel Similarity Assessment

Based on the proposed CSIM in subsection III-A, the CSIMs between the example channels are summarized in Table **??**. The CSIM is site-specific since the frame of reference is unified in all the comparisons. Channels under the same propagation environment have strong similarity. The similarity between $\mathcal{C}_\mathrm{A}$ and $\mathcal{C}_\mathrm{B}$ is more than 70% in any dimension, which is significantly greater than the similarities of the ~~power of~~ channels under different propagation environments. A comparison of $\mathrm{CSIM}(\mathcal{C}_\mathrm{A}, \mathcal{C}_\mathrm{B})$ and $\mathrm{CSIM}(\mathcal{C}_\mathrm{B}, \mathcal{C}_\mathrm{C})$ reveals that the channel difference caused by the location change is greater than that caused by the frequency change. The differences between the site-specific channel characteristics are caused mainly by the propagation mechanism changing with increasing carrier frequency, since the propagation environment is relatively static. The frequency-dependent electrical parameters of the ~~jth MPC; the greater~~ scatterers affect the multipath powers, which further results in a difference in the MPC distribution. The full-dimensional CSIMs are generally smaller than the single-dimensional CSIMs because the differences in more dimensions are taken into account. Unlike the conventional channel parameters, the ~~proportional power of an MPC is, the greater its contribution to the channel similarity. In the same way, the similarity of $\mathcal{C}_\mathrm{X}$ with respect to $\mathcal{C}_\mathrm{Y}$ can be calculated as~~

$$s_{\mathrm{X}\to\mathrm{Y}} = \sum_{i=1}^{L_\mathrm{X}} |\alpha_i|^2 \max(\gamma_i),$$

~~where $\gamma_i = [s_{i1}, s_{i2}, \cdots, s_{iL_\mathrm{Y}}]$ represents the set of subpath similarities between the ith MPC in $\mathcal{C}_\mathrm{X}$ and each MPC in $\mathcal{C}_\mathrm{Y}$.~~ proposed CSIM can effectively evaluate the degree of the similarity between MPCs in various dimensions.

~~Notably, $s_{\mathrm{Y}\to\mathrm{X}}$ does not necessarily equal $s_{\mathrm{X}\to\mathrm{Y}}$ because the most similar paths that match each other in the two calculations are not necessarily the same. Suppose that $\mathcal{C}_\mathrm{Y}$ is a channel that contains only a certain subpath of $\mathcal{C}_\mathrm{X}$; then, $s_{\mathrm{Y}\to\mathrm{X}} > s_{\mathrm{X}\to\mathrm{Y}}$. This is because the matching MPC can be found in $\mathcal{C}_\mathrm{X}$ for any MPC in $\mathcal{C}_\mathrm{Y}$, but the same is not true for the MPCs in $\mathcal{C}_\mathrm{X}$. In other words, if $\mathcal{C}_\mathrm{X}$ 'contains' $\mathcal{C}_\mathrm{Y}$, $\mathcal{C}_\mathrm{Y}$~~

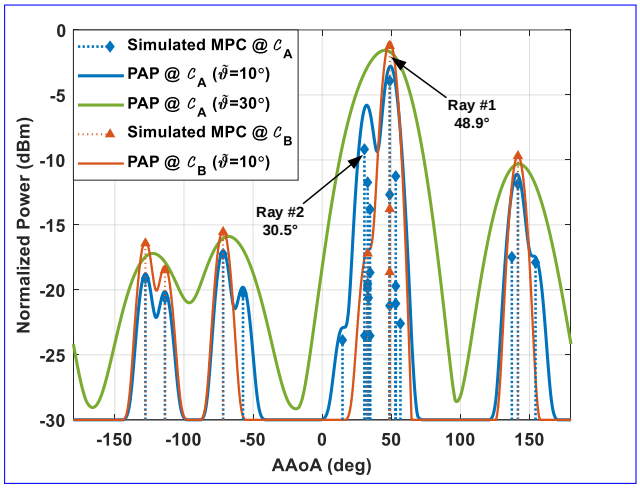

Fig. 4. Angular power spectra filtered with standard beam patterns.

~~will always be highly similar to $\mathcal{C}_X$. Finally, the mean channel similarity, i.e., the CSIM, is derived as follows:~~

$$\begin{aligned}\mathrm{CSIM}(\mathcal{C}_X,\mathcal{C}_Y) &= \frac{1}{2}(s_{Y\to X}+s_{X\to Y})\\ &= \frac{1}{2}\left(\sum_{j=1}^{L_Y}|\alpha_j|^2\max(\beta_j)+\sum_{i=1}^{L_X}|\alpha_i|^2\max(\gamma_i)\right)\times 100\%.\end{aligned} \tag{10}$$

C. ~~Channel Similarity Assessment Using the CSIM~~

~~Reconstructed~~ The reconstructed power spectra can be computed ~~based on the discrete MPCs,~~ on the basis of the discrete MPCs and with the antenna pattern and system responses embedded [16], [32]. In Fig. 4, the continuous power spectra filtered with standard beam patterns of certain ~~beamwidths~~ beam widths in different frequency bands are shown in the time domain and the angular domain. Taking the angular power spectrum as an example, an MPC with a larger ~~beamwidth~~ beam width will have an impact on a wider range of the power spectrum. Ray #1 and Ray #2 are the direct path and the primary reflection path of $\mathcal{C}_A$, respectively, with their ~~AAoAs~~ AAoA values being 18.4° apart. These two MPCs ~~will~~ do not interfere with each other if the ~~LF~~ sub-6 GHz system has an angular resolution of 10° because the two reconstructed beams are separated, whereas ~~these same two beams will~~ the two beams overlap if the angular resolution is 30°.

We assume that the bandwidth of ~~HF channels ,~~ the mmWave channels B_{HF} ~~,~~ is 300 MHz, and that the ~~corresponding~~ angular resolution $\widetilde{\vartheta}_{\mathrm{HF}}$ is 10° due to the generally greater bandwidth and better beam pointing accuracy of ~~HF systems, whereas the bandwidth and angular resolution of LF channels~~ mmWave systems, and those of the sub-6 GHz channel are set to B_{LF}=100 MHz and $\widetilde{\vartheta}_{\mathrm{LF}}$=30°~~by default. Based on the CSIM index proposed in subsection III-A, the CSIMs between the previously introduced example channels are summarized in Table ??, where the bold values are those calculated under the default configuration. The CSIM is site-specific since the frame of reference is unified in all comparisons. As seen by comparing $\mathrm{CSIM}(\mathcal{C}_A,\mathcal{C}_B)$ and $\mathrm{CSIM}(\mathcal{C}_B,\mathcal{C}_C)$, the channel difference caused by the location change is greater than that caused by the frequency change. The differences between the site-specific channel characteristics are mainly caused by how the propagation mechanism changes with increasing carrier frequency since the propagation environment is relatively static. The frequency-dependent electrical parameters of the scatterers affect the multipath power levels, further resulting in a difference in the MPC distributions. The full-dimensional CSIMs are generally smaller than single-dimensional CSIMs because the former account for differences in more dimensions~~. To explore the effects of delay resolution and angular resolution on channel similarity, CSIMs with different resolutions of the sub-6 GHz system are also calculated for comparison. The delay and AAoA dimensional similarity between $\mathcal{C}_A$ and $\mathcal{C}_B$ are 85.8% and 87.2%, respectively, which are slightly greater than those without considering delay or angular resolution. With increasing delay resolution or angular resolution, the similarity between the channels decreases. This is because in the CSIM evaluation system, beam overlap is regarded as a prerequisite for similarity between two MPCs. Consequently, a higher resolution increases the requirements for channel similarity.

~~In addition, it is worth noting that $\mathrm{CSIM}(\mathcal{C}_X,\mathcal{C}_Y)$ consists of two unidirectional measures $s_{X\to Y}$ and $s_{Y\to X}$, which are not necessarily equal. In particular, the two unidirectional CSIMs between an HF channel and an LF channel tend to differ significantly. For example, $s_{B\to A}=95.3\%$ and $s_{A\to B}=73.0\%$. This is because an LF channel will usually contain the corresponding MPCs of an HF channel at the same location as well as MPCs that the HF channel does not have, which is consistent with the results in Fig. 3. A larger $s_{\mathrm{HF}\to\mathrm{LF}}$ value indicates that the beams of the HF channel are more likely to be found in the beam range of the LF channel, thus providing a reference for a beam search in an HF system assisted by LF information.~~

~~To explore the effects of the delay resolution and angular resolution on the channel similarity, CSIMs for LF systems with different resolutions are also calculated for comparison. The AAoA-dimensional similarity between $\mathcal{C}_A$ and $\mathcal{C}_B$ is 90.3% when the bandwidth of $\mathcal{C}_A$ is 100 MHz and is 87.2% when its bandwidth is 300 MHz, intuitively corresponding to the similarities between the green and red curves and between the blue and red curves in Fig. 4, respectively. With an increase in the delay resolution or angular resolution, the similarity between the channels decreases. This is because in the CSIM evaluation system, beam overlap is regarded as a prerequisite for similarity between two MPCs. Consequently, a higher resolution raises the requirements for channel similarity.~~

IV. Results and Discussion

Based on the large amount of multiband channel data ~~simulated and measured~~ measured and simulated in the two typical ~~scenarios~~environments, the channel similarities across frequency bands ~~and across~~ or environments are presented, as ~~well as the influence of blockage on this similarity~~are the

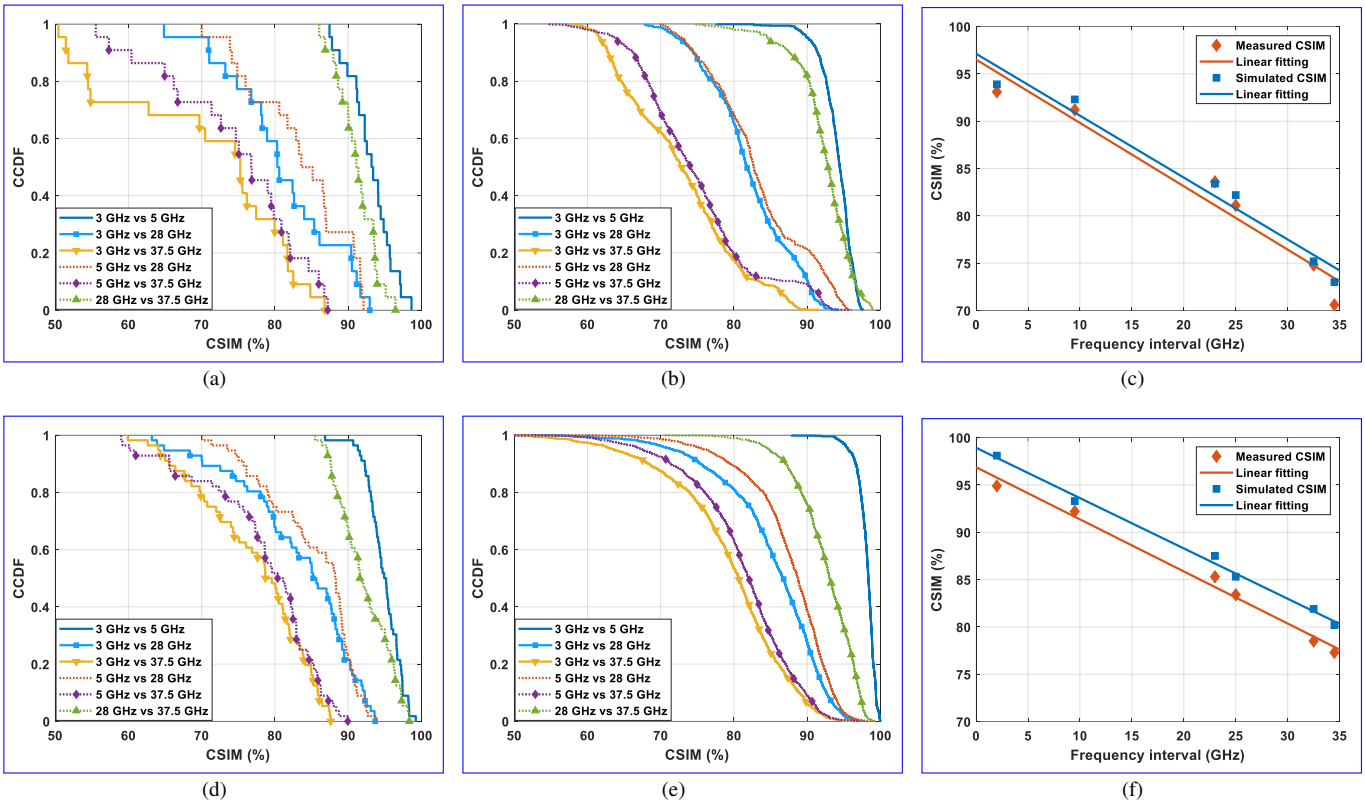

Fig. 5. Simulated and measured CCDFs of the CSIM across different frequency bands. ~~Simulated full-dimensional CSIM in the conference room scenario; Simulated AAoA-dimensional CSIM in the conference room scenario;~~ (a) Measured ~~AAoA-dimensional CSIM~~ and (b) simulated CSIMs in the conference room scenario~~; Simulated full-dimensional CSIM in~~ , and (c) linear fitting of the ~~outdoor office campus scenario; Simulated AAoA-dimensional~~ CSIM ~~in the outdoor office campus scenario~~with frequency interval; (d) Measured ~~AAoA-dimensional CSIM~~ and (e) simulated CSIMs in the ~~outdoor~~ office campus scenario, and (f) linear fitting of the CSIM with frequency interval.

influences of the blockage and polarization configurations. Moreover, as an application example, the feasibility of ~~an~~ out-of-band information-assisted beam search by using the CSIM as prior knowledge is ~~discussed~~also presented.

A. ~~Multifrequency~~ Frequency Similarity Analysis

The similarities of channels across multiple frequency bands obtained at the same location ~~have been calculatedto provide~~ are calculated, which provides a comparison of the site-specific channel characteristics across different frequencies. The complementary cumulative distribution functions (CCDFs) of the CSIM are depicted in Fig. 5, and ~~the associated~~ their statistics are provided in Table IV. Figs. ~~?? and ??~~ 5(a) and 5(d) show the empirical CCDFs of the ~~full-dimensional CSIM simulated~~ CSIM measured in the conference room ~~scenario~~ environment and the office campus ~~scenario, which account for the channel characteristics in each dimension~~environment. Obviously, there is a clear distinction in the similarities between cross-band channels. The similarities between mmWave channels and between sub-6 GHz channels both tend to be high, up to ~~approximately 95% in 50% of cases. Hence, the conditions for similarity between mmWave channels are more stringent because more accurate beam alignment is needed~~an average of more than 90%. The similarities between well-separated frequency bands seem to be related to ~~both~~ the frequency interval and the frequency ratio between the ~~higher frequency and the lower frequency, but more important are~~ mmWave bands and the sub-6 GHz bands; however, the complexity of the propagation environment and the characteristics of the scatterers are more important. In general, the smaller the frequency ~~interval and~~ span and the frequency ratio are, the ~~higher~~ greater the similarity. ~~As seen by comparing Fig. ??~~ A comparison of Fig. 5(a) and Fig. ~~??,~~ 5(d) reveals that the cross-band similarities in the office campus ~~scenario are slightly larger~~ environment are slightly greater than those in the conference room ~~scenario~~environment, and the corresponding similarities between ~~HF and LF channels are more than 8% larger~~the mmWave channels and sub-6 GHz channels are approximately 5% greater. According to the distributions of the ~~simulated~~ measured MPCs, there are more strong reflection/scattering MPCs in the indoor environment, ~~while there are usually only a few reflection MPCs and~~ whereas there is usually only one direct path~~MPC~~ , and few reflection/scattering MPCs in the outdoor environment; thus, the indoor propagation environment is more complex ~~,~~ with more strong ~~reflections~~multipaths, weakening the similarity between the channels.

The ~~consistency of the angular-domain channel characteristics across multiple frequency bands has received more attention in research on cross-band cooperative transmissions~~simulation results provide extensive channel data with higher delay/angular resolution and include more candidate dimensions. The CCDFs of the ~~AAoA-dimensional~~ multidimensional CSIM are shown in Figs. ~~?? and ??. Due~~

TABLE IV
CSIM STATISTICS ACROSS MULTIPLE FREQUENCIES

Freq. (GHz)	Conference Room				Office Campus									
	meas.		simu.		meas.		simu.		simu. (LoS)		simu. (OLoS)		simu. (NLoS)	
	mean	std	mean	std	mean	std	mean	std	mean	std	mean	std	mean	std
3 vs 5	93.1	3.0	93.9	2.3	94.9	2.3	98.1	1.2	99.1	0.9	98.1	1.3	97.7	1.1
3 vs 28	81.1	7.6	82.2	5.7	83.4	7.9	85.3	6.9	90.8	3.1	87.0	4.6	78.4	7.6
3 vs 37.5	70.6	12.2	73.0	7.9	77.3	7.5	80.2	8.1	88.9	4.1	81.1	5.4	72.7	8.9
5 vs 28	83.6	6.9	83.4	6.8	85.3	6.2	87.5	5.7	90.8	2.9	89.1	3.6	81.7	6.5
5 vs 37.5	74.8	9.4	75.2	8.1	78.5	7.9	81.9	7.2	88.5	4.1	82.6	5.1	75.9	8.1
28 vs 37.5	91.2	2.7	92.3	4.0	92.2	3.6	93.3	4.4	96.2	3.7	94.4	4.5	92.2	4.0

~~to the exclusion of the differences in other dimensions, the channel similarities in the angular domain are higher than those in the full-dimensional case. Because~~ 5(b) and 5(e). The statistical distributions of the simulated CSIMs are consistent with the trends of the measured results. Since the MPCs are relatively sparse in the angular domain in the office campus ~~scenario~~environment, the degrees of channel similarity among all frequency bands are high~~and~~, and are greater than those in the conference room ~~scenario~~environment, which is consistent with the previous conclusion. ~~Note that some of the similarity values between mmWave channels are 100% at some RX locations, where only one MPC can be received.~~ Figs. 5(c) and 5(f) present the linear fitting of the mean CSIMs with the frequency interval between the two frequency bands. As the frequency interval increases, the mean CSIM decrease with slopes of -0.65 and -0.55 in the conference room environment and the office campus environment, respectively. The simulation results have the same variation trend as the measured results, with a slight overestimation of 1–2 percentage points.

~~These simulation results may tend to be optimistic~~ Note that the simulated results are slightly larger than the corresponding measured results; this is because of the ~~ideal static propagation environment. Due to dynamic~~ changes in the ~~measurement environment and~~ real measurement environment, and the differences in the measurement system configuration, which weaken the measured channel similarities~~are somewhat lower than the simulated ones, but they are representative of the real channel similarity in an actual complex environment. As shown in Figs. ?? and ??, the measured channel similarities are usually 3 to 8 percentage points lower than the simulated values, and those between HF and LF channels in the outdoor environment are up to 10 percentage points lower.~~. The different measurement schemes applied for the mmWave channel measurements and ~~the~~ sub-6 GHz channel measurements ~~have inevitably affected~~ inevitably affect the extraction of effective paths. ~~In the mmWave bands, the similarities are high due to the strong tolerance of the scanning-based measurement method to environmental changes. In contrast, the virtual array-based measurement method relies on phase differences to estimate the angular information in the LF bands, which requires a strictly static propagation environment. Thus, the similarities of the actually measured LF bands are smaller. In addition, the~~ The interference signals that often appear during ~~LF~~ the sub-6 GHz channel measurements are an important cause of angle estimation deviation. There will always be interference in a practical application environment, especially ~~outdoors. Thus,~~ in an outdoor environment. Nevertheless, the simulation results match the actual channels well. In addition, when attempting to use ~~LF~~ out-of-band angle information to assist in ~~an HF beam search based on~~ beam search on the basis of channel similarity, a sufficient error margin must be considered.

B. ~~*Effects of Blockage*~~

~~Going one step further~~Furthermore, the channel similarity ~~in~~ under different propagation scenarios (i.e., the LoS, OLoS and NLoS scenarios) is discussed based on the channel data from the office campus ~~scenario~~environment. As shown in Fig. 6, the channel similarity between any two frequency bands ~~in~~ under the LoS scenario is greater than that ~~in~~ under the OLoS/NLoS ~~scenarios~~scenario. When a direct path is missing, the signals must ~~either~~ penetrate or bypass the scatterers in the environment or reflect off their surfaces to reach the ~~receiver~~RX, resulting in lower received power levels. The electromagnetic properties of the scatterers in different frequency bands increase the uncertainty of the reflected rays, and thus reduce the degree of channel similarity. The similarity gain increases with ~~an~~ increasing frequency difference. For ~~LF~~ the sub-6 GHz channels, the statistical results for the channel similarity ~~in~~ under the OLoS and NLoS scenarios are almost the same ~~due to~~ because of the strong penetration and diffraction capabilities of ~~LF signals. However, as~~ the sub-6 GHz signals. As the frequency increases, the penetration and diffraction of the signals ~~also~~ decrease. When two frequency bands differ greatly, such as the 3 GHz and 37.5 GHz, the ~~presence of a~~ direct path has a significant influence on the channel similarity. Compared with the LoS ~~scenario, the channel similarities in~~ cases, the average channel similarities under the OLoS and NLoS scenarios are decreased by ~~1.0 and 2.5~~ 7.8 and 16.2 percentage points, respectively~~, in 50% of cases~~. For two mmWave bands ~~in the LoS scenario~~under LoS scenarios, there are ~~quite a few cases (approximately 20%)~~ several cases with only one direct path, ~~resulting in~~ showing a similarity of 100%.

~~Measurement-based analysis of the AAoA-dimensional channel similarity between the 5 and 37.5 GHz bands, where the hollow and solid stars represent the optimal beam~~

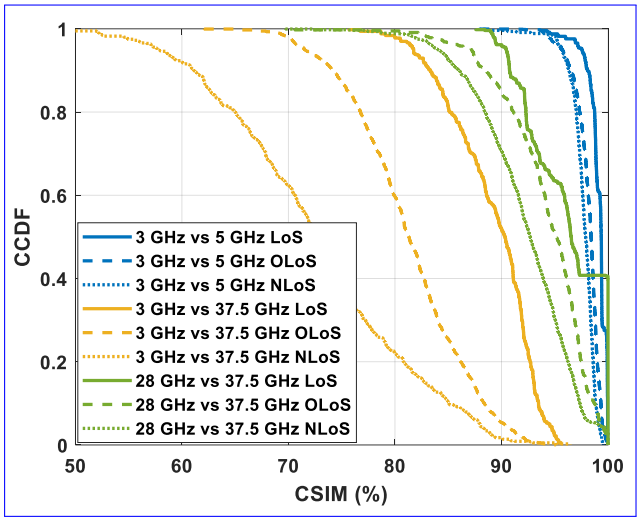

Fig. 6. CCDFs of the AAoA-dimensional CSIM across multiple frequency bands ~~in~~ under different propagation scenarios. The three colors blue, yellow, and green represent three ~~pairs~~ groups of frequency ~~bands~~ band pairs to be compared, i.e., 3 GHz vs. ~~4.8~~ 5 GHz, 3 GHz vs. 37.5 GHz and 28 GHz vs. 37.5 GHz, respectively, while the solid lines, ~~dotted~~ dashed lines, and dotted lines ~~with squares~~ represent the LoS, OLoS, and NLoS scenarios, respectively.

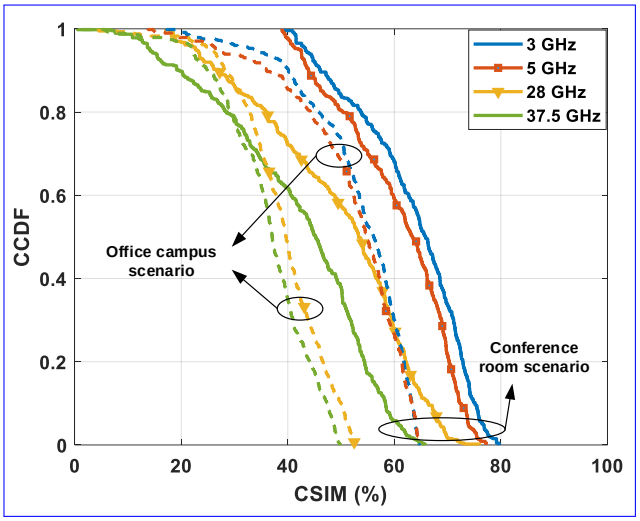

Fig. 7. Simulated CCDFs of the CSIM across different polarizations. The four colors blue, red, yellow, and green represent four frequency bands, i.e., 3 GHz, 5 GHz, 28 GHz, and 37.5 GHz, respectively, whereas the solid lines and dashed lines represent the conference room and the office campus environments, respectively.

~~directions for LF and HF channels, respectively, in the same RX location. Successful case in the office campus scenario; Failed case in the conference room scenario; Failed case in the office campus scenario. The Rician K factor , which reflects the complexity of propagation environment to a certain extent, can be calculated roughly as the~~

The K factor is the ratio of the power of the direct ~~path~~ ray to the sum power of other ~~indirect paths [?]~~reflection paths, reflecting the complexity of signal propagation in the channel. In the conference room ~~scenario~~environment, the mean K factors ~~in the four frequency bands~~ are -0.4 dB, -0.6 dB, 3.7 dB, and 5.8 dB ~~; these values are less~~ in the four frequency bands, which are lower than those in the office campus ~~scenario~~environment, where the mean K factors are ~~all~~ greater than 6 dB~~in LoS cases~~. The abundance of ~~multiple paths~~ multipaths in the conference room leads to a complex communication environment. Empirically, the CSIM is negatively correlated with the complexity of the propagation environment. The more complex the propagation environment is, that is, the smaller the K factor is, the lower the site-specific frequency similarity tends to be.

B. ~~Feasibility of an Out-of-Band Information-Assisted Beam Search~~Polarization Similarity Analysis

The channels obtained under different TX-RX antenna polarization configurations are combined to calculate the polarization similarity. The simulated CCDFs of the similarities between the two polarizations are shown in Fig. 7. The similarity between channels with different polarizations is relatively weak. The simulation results reveal that the maximum polarization similarity is less than 80%, and with increasing frequency, the polarization similarity weakens in both the conference room and the office campus environments. There is a significant gap of more than 10 percentage points between the polarization similarity of the mmwave

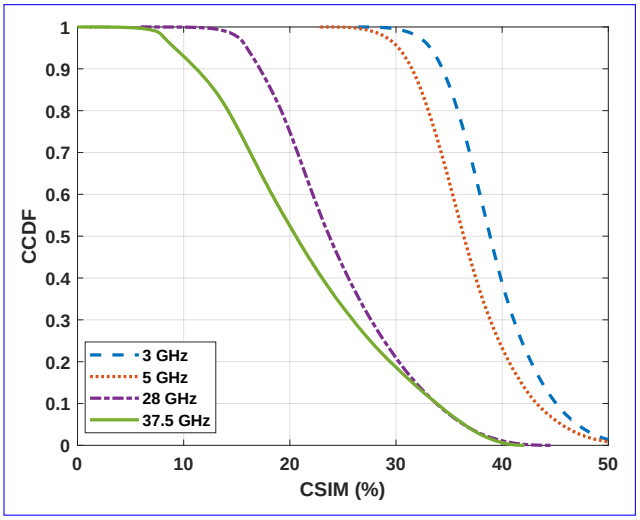

Fig. 8. Simulated CCDFs of the CSIM across different environments.

channels and that of the sub-6 GHz channels. In addition, the polarization similarities of all four frequency bands in the indoor scenario are greater than those of the corresponding bands in the outdoor scenario; this is mainly because in the indoor environment, especially at lower frequencies, the abundant multipaths have more opportunities to interact with the scatterers in the propagation environment, which increases the possibility of polarization torsion, and then increases the similarity between the two orthogonal polarizations.

~~We attempt to establish the relationship~~

C. Environment Similarity Analysis

Fig. 8 shows the CCDFs of the similarities between two propagation environments based on the channel characteristics. Before calculation, all the channels are aligned based on the strongest path so that the differences in propagation delay due to the relative locations of the transceivers are excluded. Obviously, the similarities between the mmWave channels are

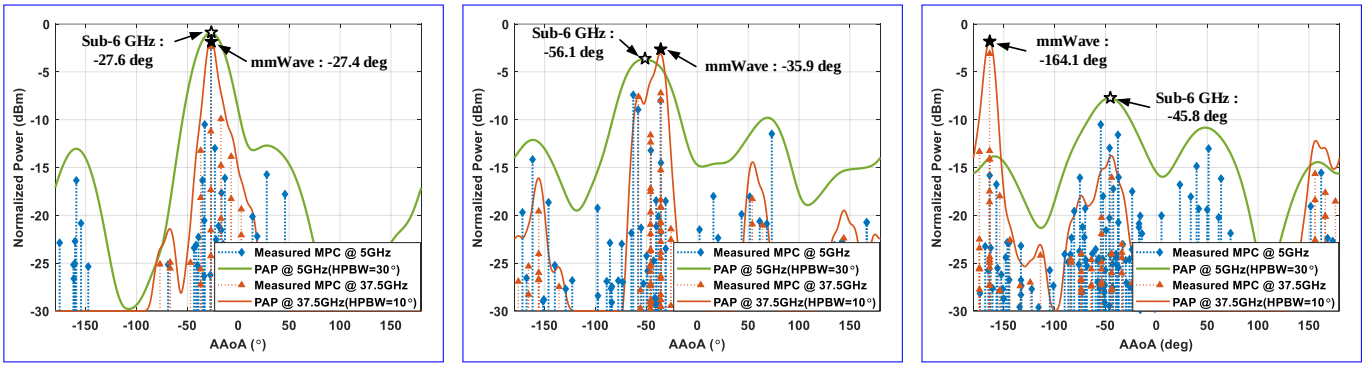

(a) (b) (c)

Fig. 9. Measurement-based analysis of AAoA-dimensional channel similarity between 5 and 37.5 GHz, where the hollow and solid stars represent the optimal beam directions for sub-6 GHz and mmWave channels in the same RX location, respectively. (a) Successful case in the office campus environment; (b) Non-successful case in the conference room environment; (c) Non-successful case in the office campus environment.

less than those between the sub-6 GHz channels. An increase in the carrier frequency weakens the channel similarity. This is due to the multipath sparsity of the mmWave channels, highlighting the importance of the direct path (the strongest path), which can also be explained by the K factor. In higher frequency bands, especially in LoS scenarios, the mismatch of direct paths leads to a sharp decline in the similarity of the two channels, that is, the two channels tend to be orthogonal. The large variances of CSIMs indicate that the mmWave channels are easily affected by the propagation environment and the transceiver locations. The channel similarities obtained at different RX positions are quite different even in the same scenario. However, in the sub-6 GHz bands, the abundant multipath extends the incoming wave direction, which makes the channels have a higher correlation in the spatial domain. In other words, the channel similarity between the two propagation environments is weak at less than 50%. The large differences indicate that signal processing algorithms, such as the beam-searching strategy, need to be designed separately with respect to their environmental characteristics.

D. Feasibility of Out-of-Band Information-Assisted Beam Search

A relationship is established between the proposed CSIM and the beam direction differences across multiple frequency bands to explore the feasibility of ~~an~~ out-of-band information-assisted beam search. The ~~LF~~sub-6 GHz/~~HF combination~~ mmWave band combinations of 5/37.5 GHz ~~is chosen~~ are used for the analysis. The measured discrete MPCs are filtered by the ideal 3GPP beam patterns with different HPBWs ~~in accordance with~~ according to the carrier frequency. The ~~beamwidths~~ beam widths are set to 30° and 10°, respectively~~; thus, the average angular resolution is $\widetilde{\vartheta}_{\mathrm{r}} = 20°$ here~~. If the difference between the optimal beam directions ~~for~~ of the two frequency bands is less than $\widetilde{\vartheta}_{\mathrm{r}}$, ~~it is considered that~~ the spatial information provided by the out-of-band channel is ~~beneficial for a beam search in~~ considered beneficial to the beam search at the target frequency band. In other words, only the $\pm\widetilde{\vartheta}_{\mathrm{r}}$ range centered on the optimal beam direction ~~for~~ of the out-of-band channel needs to be searched to ~~find~~ obtain the optimal direction ~~for the target band~~ of the target band channel, which ~~will greatly reduce~~ greatly reduces the beam training overhead. Fig. 9(a) shows an example in the office campus ~~scenario. It can be observed that the~~ environment. The optimal beam directions at ~~4.8 GHz and at~~ 5 GHz and 37.5 GHz ~~are well matched, with a~~ match well with the 0.2° direction difference, and the corresponding CSIM is ~~96.0~~85.4%.

However, ~~LF~~ the sub-6 GHz channels may provide inaccurate or even incorrect spatial information in some cases. ~~In~~ As shown in Figs. 9(b) and 9(c), the AAoA-dimensional CSIMs between the ~~LF and HF channels are 93.2%and 83.6%, respectively~~sub-6 GHz channel and the mmWave channel is 77.2%. There are two main reasons for ~~such a~~ the difference in beam direction. One is the different angular resolutions of the ~~LF~~sub-6 GHz/~~HF~~ mmWave systems. This type of angle mismatch is more common in indoor environments when the RX is close to ~~a reflector, in which case two MPCs may~~ the reflector, where two MPCs reach the RX with an angle difference approximately equal to the ~~beamwidth~~beam width. As shown in Fig. 9(b), the optimal beam directions formed by two MPCs with similar ~~power levels~~ powers after beam filtering can be ~~clearly~~ obviously distinguished, with a difference of 20.2° ~~,~~slightly greater than $\widetilde{\vartheta}_{\mathrm{r}}$. Fortunately, the two channels remain highly similar under this condition, and the optimal direction can ~~still~~ be obtained with ~~only~~ a small extension of the search range. The other type of angle mismatch often occurs ~~in low SNR~~ at low signal-to-noise ratio (SNR) RX locations where the forward link is blocked. The channels shown in Fig. 9(c) were measured ~~along~~ on *Route 1* in the office campus ~~scenario, where~~ environment, and the direct path ~~is obstructed by the~~ was obstructed by dense foliage. The ~~LF~~ sub-6 GHz signals can still pass through the foliage to reach the RX. However, with ~~an increase in the~~ increasing carrier frequency, ~~the vegetation-induced~~ vegetation attenuation becomes increasingly ~~strong~~severe, resulting in the signal strength of the forward link being lower than that of the backward link from the glass curtain wall. ~~Hence, the~~ The channel similarity is greatly weakened, and the large difference in ~~beam direction means that the LF spatial information can make no meaningful contribution to the HF beam search~~the beam direction results in the sub-6 GHz spatial information not contributing to the mmWave beam search, which is the

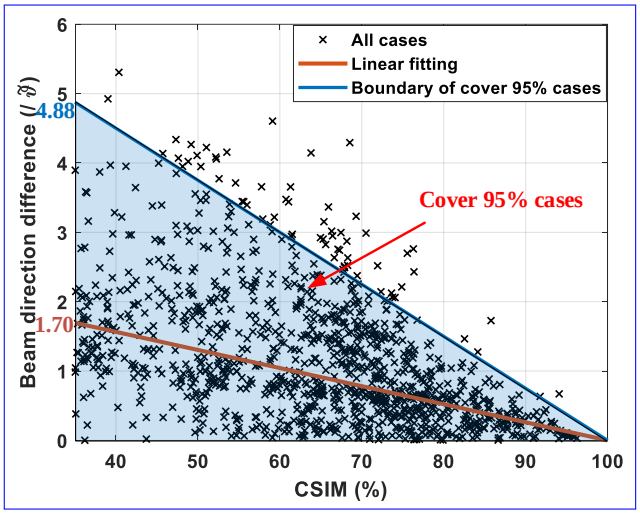

(a)

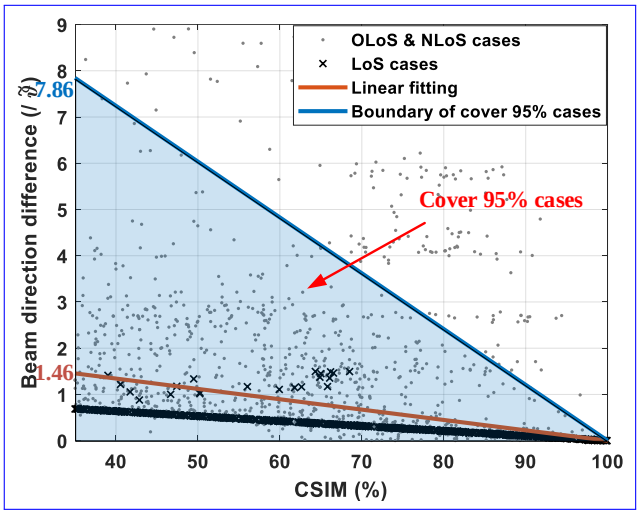

(b)

Fig. 10. Linear fittings of the beam direction difference vs CSIM between 5 and 37.5 GHz in (a) the conference room and (b) the office campus environment, where the black crosses and gray dots represent cases including simulated and measured results, the shaded area contains 95% of the cases, and the red line is a linear fit for all the cases.

worst-case.

~~Linear fits of the beam direction difference vs. the CSIM between the 5 and 37.5 GHz bands in the conference room and the office campus scenario, where the black crosses and gray dots represent cases including simulated and measured results, respectively; the shaded area contains 95% of cases; and the red line is a linear fit for all cases.~~

~~The relationships between beam direction differences (divided by $\tilde{\vartheta}_{\mathrm{r}}$) and the CSIM found by~~ By traversing all channel combinations at 5 GHz and 37.5 GHz in both ~~scenarios~~ environments, the relationships between the beam direction differences and the CSIM are shown in Fig. 10. ~~It is obvious that the~~ A reasonable beam search range threshold is provided to balance the beam search overhead and minimize the worst cases like Fig. 9(c). The success rate of ~~an~~ the out-of-band information-assisted beam search ~~depends on the environment~~is environmentally dependent. In the indoor conference room, the mean and variance of the

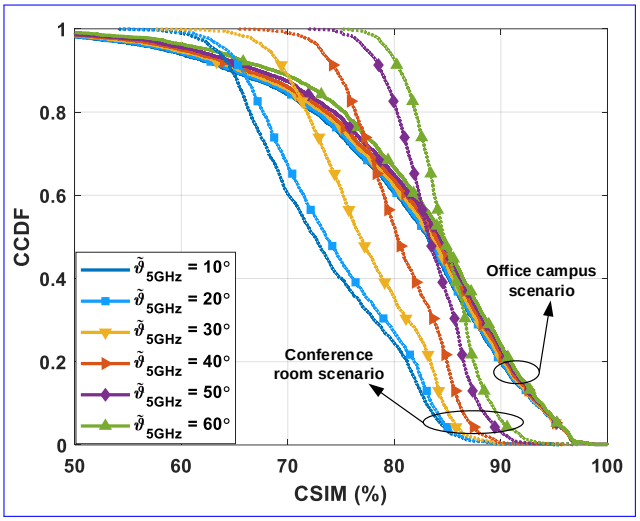

Fig. 11. Simulated CCDFs of the CSIM across 5 GHz and 37.5 GHz channels under different beamwidths of the sub-6 GHz channel, where the beam width of the HF channel is 10°.

beam direction difference decrease ~~as the CSIMincreaseswith~~ increasing CSIM; that is, the higher the channel frequency similarity is, the smaller the beam range ~~that needs~~ to be searched to find the optimal beam direction. When the ~~CSIM is~~ CSIMs are maintained above approximately 86%, ~~an~~ out-of-band information-assisted beam search can be ~~well~~ effectively applied at almost all the RX locations, ~~as~~ with the optimal beam direction ~~indeed lies~~ obtained in the $1 \times \tilde{\vartheta}_{\mathrm{r}}$ range. However, in the outdoor environment, the CSIMs in the LoS and OLoS/NLoS scenarios ~~exhibit~~ have different characteristics, as shown in Fig. 10(b). For the LoS ~~scenario, the beampointing~~ scenarios, the beam pointing difference has an obvious linear relationship with the CSIM~~. This is because in an open environment with no occlusion,~~ ; this is because the strength of the direct path is much greater than ~~those~~ that of the reflected paths in an open environment with no occlusion, and the multiple paths are sparse, resulting in the difference ~~from~~ in the direct path determining the CSIM to a large extent. However, when the direct path is attenuated by foliage or completely blocked by buildings, ~~the presence of many MPCs~~ many multipath scattering components with similar strengths ~~can~~ easily lead to ~~an angle mismatch~~angle mismatches. Thus, compared with the indoor propagation environment, ~~a larger search interval is often needed for~~ channel pairs with the same CSIM often need a larger search interval in the outdoor environment to successfully align the beam~~in the outdoor environment~~. Based on ~~the above conclusions~~above conclusions, and the statistical results ~~for~~ of the simulated and measured CSIMs ~~reported~~ in subsection IV-A, ~~LF~~ the sub-6 GHz spatial information is useful for ~~HF~~ mmWave beam training.

~~Simulated CCDFs of the CSIM across 5 GHz and 37.5 GHz channels under different LF channel beamwidths, where the beamwidth of the HF channel is 10°. Simulated CCDFs of the CSIM across different scenarios.~~

In addition, both the CSIM and ~~the~~ beam direction are affected by the ~~beamwidth~~ beam width of the communication

system. Fig. 11 shows the simulated CCDFs of the CSIM across the 5 GHz and 37.5 GHz channels under different ~~LF channel beamwidths~~ beam widths (i.e., 10°, 20°, 30°, 40°, 50°, and 60°) of the sub-6 GHz channel, where the ~~beamwidth of the HF~~ beam width of the mmWave channel is 10°. As mentioned above, the narrower the ~~beamwidth~~ beam width is, the more stringent the similarity conditions for a pair of MPCs since their beams need to be aligned enough to overlap. The effect of the ~~beamwidth on the channel overlap~~ beam width on the channels in the indoor environment is greater than that in the outdoor environment, which is also related to the channel sparsity in the outdoor environment. The wider the ~~LF channel beamwidth~~ sub-6 GHz channel beam width is, the larger the CSIM that ~~is derived, and thus , the greater the~~ can be derived, thus increasing the success rate of searching for the ~~optimal HF~~ mmWave optimal beam direction within $\widetilde{\vartheta}_{\mathrm{r}}$; however, ~~a lower~~ the low resolution means that ~~less information is~~ the less information provided by the ~~LF channel, necessitating a larger search range~~ sub-6 GHz channel, the larger the search range needed for beam alignment.

E. ~~*Multienvironment Similarity Analysis*~~

~~Fig. 8 shows the CCDFs of the similarities between the two propagation environments based on the channel characteristics. Before the calculation, all channels were aligned based on the strongest path to exclude the influence of differences in the propagation delay and average AoA due to the relative locations of the transceivers. Because of the precise delay and angular resolutions, the similarities between mmWave channels are lower than those between sub-6 GHz channels. When the resolutions are set the same, an increase in the carrier frequency leads to stronger channel similarity. This is due to the multipath sparsity of the mmWave channels, highlighting the importance of the direct path (or the strongest path), which is also reflected by the K factor. The frequency inconsistency between the two environments, i.e., the use of 4.8 GHz in the office campus and 5.4 GHz in the conference room, weakens the similarity. Although the absolute frequency interval is small, the relative frequency ratio is nonnegligible in the LF bands. In other words, the channel similarity between the two propagation environments is weak, less than 50%. The large differences indicate that relevant signal processing algorithms, including the beam search strategy mentioned above, need to be designed separately for the different environmental characteristics.~~

V. ~~Conclusions~~

~~A~~

V. Conclusion

In this paper, a multidimensional CSIM based on structural multipath information ~~is~~ has been proposed for the universal evaluation of channel similarities. By accounting for the physical characteristics of the channels, the proposed CSIM ~~can provide~~ provides a clear quantitative evaluation in one or more dimensions rather than ~~merely~~ a vague visual judgment. Simulated and measured channel data from two typical ~~scenarios~~ environments (a conference room ~~scenario~~ environment and an office campus ~~scenario~~environment) in four frequency bands are used to analyze and verify the performance of the proposed CSIM. The statistical distributions of the CSIM ~~can be~~ were investigated to explore the similarities across different frequency bands in different environments. The results show that ~~the~~ cross-band similarity is ~~mainly related~~ related mainly to the frequency interval and ~~the environmental~~ environment complexity. In general, ~~larger~~ large frequency intervals and ~~richer multipath conditions will~~ rich multipaths weaken the channel similarity. In addition, the feasibility of ~~an~~ out-of-band information-assisted beam search ~~based on the~~ on the basis of cross-band CSIM is preliminarily investigated. ~~It is found that~~ The out-of-band information ~~can help~~ helps reduce the beam training overhead to some extent, but it is more critical to update the search strategy ~~in accordance with~~ according to the environmental characteristics. The low similarity between these two ~~scenarios~~ environments also illustrates that signal processing algorithms ~~designed for one scenario~~ cannot be blindly applied ~~in another , unrelated scenario~~from another unrelated environment.

~~In~~ For future work, using ~~the similarity between channels~~ channel similarity is expected to significantly reduce the computational overhead of beam searching. On the one hand, the channel similarity index can be improved by considering more dimensions, such as ~~the polarization and Dopplerdimensions~~Doppler, as well as the actual antenna array patterns ~~as a basis for developing~~ for dynamic multidimensional channel similarity measures. More statistical performance analyses across multiple frequency bands and multiple ~~scenarios~~ environments based on extensive field measurements ~~will also~~ need to be ~~pursued~~ performed to provide prior knowledge for the creation of highly efficient beam management strategies. On the other hand, developing a portable and highly efficient beam management strategy by fully exploring and utilizing the ~~correlations~~ correlation between propagation environments ~~may also be~~ is also of interest.

References

[1] X. You, C. Wang, J. Huang *et al.*, "Towards 6G wireless communication networks: vision, enabling technologies, and new paradigm shifts," *Sci. China Inf. Sci.*, vol. 64, no. 1, 2021.

[2] C.-X. Wang, X. You, X. Gao *et al.*, "On the road to 6G: Visions, requirements, key technologies, and testbeds," *IEEE Commun. Surv. Tutor.*, vol. 25, no. 2, pp. 905–974, 2023.

[3] T. S. Rappaport, G. R. MacCartney, M. K. Samimi, and S. Sun, "Wideband millimeter-wave propagation measurements and channel models for future wireless communication system design," *IEEE Trans. Commun.*, vol. 63, no. 9, pp. 3029–3056, 2015.

[4] D.Dupleich, R. Muller, M. Landmann, E.-A. Shinwasusin, K. Saito, J.-I. Takada, J. Luo, R. Thoma, and G. Del Galdo, "Multi-band propagation and radio channel characterization in street canyon scenarios for 5G and beyond," *IEEE Access*, vol. 7, pp. 160 385–160 396, 2019.

[5] A. Ali, N. G. Prelcic, and R. W. Heath, "Millimeter wave beam-selection using out-of-band spatial information," *IEEE Trans. Wirel. Commun.*, vol. 17, no. 2, pp. 1038–1052, 2018.

[6] ——, "Spatial covariance estimation for millimeter wave hybrid systems using out-of-band information," *IEEE Trans. Wirel. Commun.*, vol. 18, no. 12, pp. 5471–5485, 2019.

[7] N. G. Prelcic, A. Ali, V. Va, and R. W. Heath, "Millimeter-wave communication with out-of-band information," *IEEE Commun. Mag.*, vol. 55, no. 12, pp. 140–146, 2017.

[8] Y. Xiu, W. Wang, and Z. Zhang, "A message passing approach to acquire mm-Wave channel state information based on out-of-band data," *IEEE Access*, vol. 6, pp. 45 665–45 680, 2018.
[9] J. Huang, C. Wang, H. Chang, J. Sun, and X. Gao, "Multi-frequency multi-scenario millimeter wave MIMO channel measurements and modeling for B5G wireless communication systems," *IEEE J. Sel. Areas Commun.*, vol. 38, no. 9, pp. 2010–2025, 2020.
[10] P. Zhang, J. Li, H. Wang, H. Wang, and W. Hong, "Indoor small-scale spatiotemporal propagation characteristics at multiple millimeter-wave bands," *IEEE Antennas Wirel. Propag. Lett.*, vol. 17, no. 12, pp. 2250–2254, 2018.
[11] P. Zhang, B. Yang, C. Yi, H. Wang, and X. You, "Measurement-based 5G millimeter-wave propagation characterization in vegetated suburban macrocell environments," *IEEE Trans. Antennas Propag.*, vol. 68, no. 7, pp. 5556–5567, 2020.
[12] J. Pascual-Garcia, L. Rubio, V. Rodrigo Penarrocha *et al.*, "Wireless channel analysis between 25 and 40 GHz in an intra-wagon environment for 5G using a ray-tracing tool," *IEEE Trans. Intell. Transp. Syst.*, vol. 23, no. 12, pp. 24 621–24 635, 2022.
[13] D. Dupleich, R. Muller, S. Skoblikov *et al.*, "Multi-band indoor propagation characterization by measurements from 6 to 60 GHz," in *Proc. 13th Eur. Conf. Antennas Propag. (EuCAP)*, 2019, pp. 1–5.
[14] T. Jiang, J. Zhang, M. Shafi, L. Tian, and P. Tang, "The comparative study of S-V model between 3.5 and 28 GHz in indoor and outdoor scenarios," *IEEE Trans. Veh. Technol.*, vol. 69, no. 3, pp. 2351–2364, 2020.
[15] Y. L. C. De Jong, J. A. Pugh, M. Bennai, and P. Bouchard, "2.4 to 61 GHz multiband double-directional propagation measurements in indoor office environments," *IEEE Trans. Antennas Propag.*, vol. 66, no. 9, pp. 4806–4820, 2018.
[16] P. Kyosti, P. Zhang, A. Parssinen, K. Haneda, P. Koivumaki, and W. Fan, "On the feasibility of out-of-band spatial channel information for millimeter-wave beam search," *IEEE Trans. Antennas Propag.*, vol. 71, no. 5, pp. 4433–4443, 2023.
[17] X. Hong, C. Wang, J. Thompson, B. Allen, W. Q. Malik, and X. Ge, "On space-frequency correlation of UWB MIMO channels," *IEEE Trans. Veh. Technol.*, vol. 59, no. 9, pp. 4201–4213, 2010.
[18] L. Li, X. Su, Y. Zhang, Y. Lin, and Z. Li, "Trend modeling for traffic time series analysis: An integrated study," *IEEE Trans. Intell. Transp. Syst.*, vol. 16, no. 6, pp. 3430–3439, 2015.
[19] A. Gogolou, T. Tsandilas, T. Palpanas, and A. Bezerianos, "Comparing similarity perception in time series visualizations," *IEEE Trans. Vis. Comput. Graphics*, vol. 25, no. 1, pp. 523–533, 2019.
[20] H. Guo, L. Wang, X. Liu, and W. Pedrycz, "Trend-based granular representation of time series and its application in clustering," *IEEE Trans. Cybern.*, vol. 52, no. 9, pp. 9101–9110, 2022.
[21] Z. Wang, A. Bovik, H. Sheikh, and E. Simoncelli, "Image quality assessment: From error visibility to structural similarity," *IEEE Trans. Image Process.*, vol. 13, no. 4, pp. 600–612, 2004.
[22] M. P. Sampat, Z. Wang, S. Gupta, A. C. Bovik, and M. K. Markey, "Complex wavelet structural similarity: A new image similarity index," *IEEE Trans. Image Process.*, vol. 18, no. 11, pp. 2385–2401, 2009.
[23] 3GPP, "Study on channel model for frequencies from 0.5 to 100 GHz," 3rd Generation Partnership Project (3GPP), TR 38.901 V15.0.0, Tech. Rep., June 2018.
[24] N. Czink, P. Cera, J. Salo, E. Bonek, J. p. Nuutinen, and J. Ylitalo, "A framework for automatic clustering of parametric MIMO channel data including path powers," in *Proc. IEEE Vehicular Technol. Conf.*, 2006, pp. 1–5.
[25] ——, "Improving clustering performance by using the multi-path component distance." *IEE Electron. Lett.*, vol. 42, no. 1, pp. 44–45, 2006.
[26] Y. Li, J. Zhang, P. Tang, and L. Tian, "Clustering in the wireless channel with a power weighted statistical mixture model in indoor scenario," *China Commun.*, vol. 16, no. 7, pp. 83–95, 2019.
[27] C. Huang, A. F. Molisch, Y. A. Geng, R. He, B. Ai, and Z. Zhong, "Trajectory-joint clustering algorithm for time-varying channel modeling," *IEEE Trans. Veh. Technol.*, vol. 69, no. 1, pp. 1041–1045, 2020.
[28] C. Yi, P. Zhang, H. Wang, and W. Hong, "Multipath similarity index measure across multiple frequency bands," *IEEE Wirel. Commun. Lett.*, vol. 10, no. 8, pp. 1677–1681, 2021.
[29] P. Zhang, P. Kyosti, K. Haneda, P. Koivumaki, Y. Lyu, and W. Fan, "Out-of-band information aided mmWave/THz beam search: A spatial channel similarity perspective," *IEEE Commun. Mag.*, vol. 00, no. 00, pp. 1–7, 2022, early access.
[30] J. Li, P. Zhang, C. Yu, H. Wang, and W. Hong, "High-efficiency wideband millimeter-wave channel sounder system," in *Proc. 13th Eur. Conf. Antennas Propag. (EuCAP)*, 2019, pp. 1–5.
[31] B. H. Fleury, M. Tschudin, R. Heddergott, D. Dahlhaus, and K. Ingeman Pedersen, "Channel parameter estimation in mobile radio environments using the SAGE algorithm," *IEEE J. Sel. Areas Commun.*, vol. 17, no. 3, pp. 434–450, 1999.
[32] X. Yin, C. Ling, and M. Kim, "Experimental multipath-cluster characteristics of 28-GHz propagation channel," *IEEE Access*, vol. 3, pp. 3138–3150, 2015.
[33] ITU, "Effects of building materials and structures on radiowave propagation above about 100 MHz," ITU-R, Rec., Tech. Rep. P.2040-2, Sep. 2021.
[34] C. Yi, W. Chen, Q. Wu, and H. Wang, "Machine learning-assisted calibration for ray-tracing channel simulation at centimeter-wave and millimeter-wave bands," *IEEE Antennas Wireless Propag. Lett.*, vol. 23, no. 5, pp. 1623–1627, 2024.